

1N-44587

NASA Contractor Report 179492

113P

(NASA-CR-179492) THE MEASUREMENT OF
BOUNDARY LAYERS ON A COMPRESSOR BLADE IN
CASCADE AT HIGH POSITIVE INCIDENCE ANGLE. 2:
DATA REPORT Interim Report (Pennsylvania
State Univ.) 113 p

N87-13442

Unclassified
CSCL 21E G3/07 43672

The Measurement of Boundary Layers on a Compressor Blade in Cascade at High Positive Incidence Angle

II—Data Report

Steve Deutsch and William C. Zierke

*Pennsylvania State University
State College, Pennsylvania*

August 1986

Prepared for
Lewis Research Center
Under Grant NSG-3264



National Aeronautics and
Space Administration

Table of Contents

	<u>Page No.</u>
Introduction	1
Flow Field	1
Raw Data	2
Normal Pressure Gradient	3
Spline Fit	5
Boundary Layer Integral Parameters	6
Similarity Solutions for Laminar Boundary Layers	8
Wall-Wake Velocity Profile for Turbulent Boundary Layers	10
Skin Friction Coefficient of a Turbulent Boundary Layer.	14
Transition	14
Wakes.	15
Analysis of Current Data	16
Conclusions.	17
Nomenclature	18
References	22
Tables	37
Figures.	25

INTRODUCTION

In this two part study, we report detailed boundary layer and wake measurements of the flow field about a double circular arc compressor blade in cascade. The measurements were made at an incidence angle of 5 degrees and a chord Reynolds number of 500,000. The study provides a well documented flow field of some complexity which can be used to develop or test future generations of computational codes.

In the first part of this study, we described the test facility and experimental methods and provided an analysis of the data. This analysis involves the presentation of the boundary layer and wake flow data in standard graphical formats rather than in listings of raw data. We recognize that this presentation, although best for studying the physics of the flow field, may not be adequate for computational comparisons.

In this second part of the study, we make the data accessible to computational comparison by presenting the raw data in tabulated form. We also give, through example, a detailed description of our analysis procedure. Data developed with this analysis procedure are also presented in tabulated form. A computer tape containing the data is available.

FLOW FIELD

The flow field through the cascade of double circular arc compressor blades was established at a chord Reynolds number of 500,000. Figure 1 shows the blade geometry as well as the results of the inlet and outlet flow measurements. The incidence angle of 5 degrees leads to the blade static-pressure distribution shown in Figure 2 and tabulated in Tables 1

and 2. The reference static and total pressures used in defining the pressure coefficients are $p_1 = -414.3$ Pa and $P_{T_1} = 246.1$ Pa. Boundary layers measured on a blade with this static-pressure distribution can include layers that are laminar, transitional, turbulent, or separated depending on the location of the measurement. These measurements are first treated statistically and then analyzed to determine the boundary layer characteristics. The techniques by which we chose to analyze the boundary layer data is described in the following sections.

RAW DATA

The raw data is given in Tables 3 through 27. In general, we present mean velocity, local turbulence intensity, skewness, kurtosis, and percent backflow (reverse flow) as a function of position from the blade surface. For positions from 2.6% chord to 53.6% chord on the suction surface, the measurements were made using a laser Doppler velocimeter (LDV) with no frequency shifting; and hence, no percent backflow could be measured. Neither the skewness nor the kurtosis were calculated for these same positions. The remaining boundary layer and near-wake measurements were made using a frequency shift of 5 MHz. The far-wake measurements of Table 27 were made with a five-hole probe rather than a LDV. Each data point in Tables 3 through 27 is averaged over several (usually 6) experiments. The tables include these average values and deviations based on 95% confidence bands as determined by Student's t test. Mean and turbulence quantities are calculated in the usual manner; that is

$$u = \frac{1}{N} \sum_{n=1}^N u_n$$

and

$$u'^2 = \frac{1}{N} \sum_{n=1}^N (u_n - u)^2$$

while

$$S = \frac{1}{N} u^{1/3} \sum_{n=1}^N (u_n - u)^3$$

and

$$K = \frac{1}{N} u^{1/4} \sum_{n=1}^N (u_n - u)^4$$

Local turbulence intensity is taken as u'/u and turbulence intensity is taken as u'/U_e , where U_e is the boundary layer edge velocity.

NORMAL PRESSURE GRADIENT

Surface curvature, blowing, or suction may induce significant streamline curvature in a flow. Streamline curvature in turn causes a normal pressure gradient which results in a cross streamline gradient in the inviscid velocity profile. As shown in Figures 3 and 4, the freestream velocity does not reach a constant value (the edge velocity, U_e). Boundary layer analyses, however, assume that the location of the boundary layer edge is known and that a constant freestream velocity exists outside the boundary layer. To use or formulate a boundary layer analysis, the procedure must account for the effect of the normal pressure gradient.

Mellor and Wood [1971] and Ball, Reid, and Schmidt [1983] outlined one method which accounts for these effects. The method assumes that the measured velocity profiles represent composite profiles. This implies that each of the profiles has a region where the viscous effects predominate, a region in which viscous effects are negligible, and an intermediate region in which the viscous-inviscid results match. Mathematically, the measured composite profile is the sum of a boundary layer profile and an inviscid profile, less what appears in both. The last quantity is commonly called the boundary layer edge velocity, U_e . That is

$$u_{\text{meas}} = u_{\text{bl}} + u_{\text{inv}} - U_e$$

Clearly, both the boundary layer velocity u_b and the measured velocity

u_{meas} must go to zero at the wall, so that

$$U_e = (u_{\text{inv}})_{\text{wall}}$$

and the scheme reduces to finding the value of the edge velocity.

The validity of applying this procedure to velocity data is difficult to establish. However, it does allow for a consistent method to analyze measured velocity profiles provided that the inviscid region can be properly identified from the data. There does not appear to be a rigorous way to do this, so that as in the prior reported study (Deutsch and Zierke [1984]), a consistent method which produces plausible results is adopted.

A least-squares technique is used to fit a polynomial to the inviscid velocity profile. Since the inviscid profiles may have significant curvature, the analysis provides an option of fitting the inviscid profile with a linear, quadratic, or cubic polynomial. The difficulty lies in choosing the data points to be included in the least-squares analysis. To minimize this problem, the number of data points used in the polynomial fit was varied. First, the maximum number of points, N_{max} , which could possibly be within the inviscid region was determined. For $\partial p / \partial y > 0$ (as an example see Figure 3), N_{max} is taken to be the number of points between the point furthest from the wall and the point of maximum velocity. For $\partial p / \partial y < 0$ (as an example see Figure 4), the data point at which the profile slope changes by at least 50% is used instead of the point of maximum velocity. For the data in Figure 3, N_{max} was determined to be 19, while N_{max} was found to be 24 for the data of Figure 4. Many applications have shown that for the region of $0.55 N_{\text{max}} \leq N_{\text{inv}} \leq 0.95 N_{\text{max}}$, the value of U_e is relatively independent of the number of points in the fit. This is clearly shown for the data of Figures 3 and 4 in Table 28. Each polynomial was extrapolated to the wall to obtain U_e and a mean and a standard deviation of all values of U_e were determined. The degree of the polynomial was chosen to minimize the standard deviation of U_e . These

standard deviations have been observed to be quite small (~ 0.5%). A u profile was calculated using the mean value of U_e and a polynomial fit of u_{inv} . We used, $N_{inv} = 0.75 N_{max}$ as the number of data points in the fit to determine U_e as the U_e found in this way was consistently close to the average U_e . A smoothed spline fit of the boundary layer velocity profile was used to calculate the boundary layer thickness, δ . δ is taken at the position at which

$$u = 0.99 U_e .$$

Figures 5 and 6 show the reconstructed boundary layer profiles (triangles) corresponding to Figures 3 and 4. As might be anticipated, the effect of the normal pressure gradient does not penetrate far into the boundary layer.

Deutsch and Zierke [1984] discuss the plausibility of this approach by comparing plots of the shape of the resulting turbulence intensity versus normalized distance from the wall (y/δ) against classical measurements. They conclude that the technique does indeed give reasonable results. It should be noted that Klock [1983] developed an alternate method of accounting for the effects of the normal pressure gradient using the equations for the boundary layer parameters. That technique was found here, however, to be too difficult to employ.

SPLINE FIT

Comparisons between boundary layers are often made in terms of simple integral thicknesses or their ratios (shape factors).

In order to calculate the boundary layer integral parameters, the analysis must fit the velocity data points with a mathematical curve. A parametric cubic spline was used for the curve fit. This curve parametrically develops the u and y ordered pairs as independent functions of the overall

arc length of the curve. Even this curve fit tends to oscillate when a cusp appears in the profile. Therefore, a smoothing routine was added to the spline fit. Near the wall, a parametric cubic spline was fit between the data point nearest to the wall and the zero velocity point that would occur at the wall. For boundary layer profiles not well resolved in the near-wall region, this latter fit represents the largest potential error in the calculation of the integral parameters. Figures 7 and 8 show the calculated spline fits to the boundary layer profiles of Figures 5 and 6.

BOUNDARY LAYER INTEGRAL PARAMETERS

The most common of the parameters which characterize the boundary layer are integral thicknesses based on the conservation of mass, momentum, and energy. In effect, the boundary layer acts to displace the streamlines in the flow outside the boundary layer away from the wall. A displacement thickness, δ^* , can be defined as the distance by which the solid surface would have to be displaced to maintain the same mass flowrate in a hypothetical inviscid flow. For steady, incompressible flow, δ^* can be defined as

$$\delta^* = \int_0^\infty (1 - \frac{u}{U_e}) dy .$$

δ^* is probably the most fundamental integral thickness and is commonly used as a normalizing factor in presenting data since the alternative, the boundary layer thickness, is difficult to measure. A momentum thickness, θ , can be determined from the steady, incompressible momentum equation as

$$\theta = \int_0^\infty \frac{u}{U_e} (1 - \frac{u}{U_e}) dy .$$

The momentum thickness represents the momentum loss due to the presence of the boundary layer and is proportional to the drag when no streamwise pressure

gradient exists. Many empirical correlations use the momentum thickness.

Finally, a steady, incompressible energy thickness can be defined as

$$\delta_3 = \int_0^{\infty} \frac{u}{U_e} [1 - (\frac{u}{U_e})^2] dy .$$

Reynolds numbers can be formed based on all three of these integral thicknesses using the boundary layer edge velocity. They are especially useful in describing the boundary layers just before, during, and just after transition.

Some parameters describe the shape of the velocity profile. The first and second shape factors of the velocity profile are defined as

$$H_{12} = \frac{\delta^*}{\theta}$$

and

$$H_{32} = \frac{\delta_3}{\theta} .$$

Note that the definitions require that both shape factors be greater than unity. For laminar boundary layers, the first shape factor lies between 3.5 and 2.3. Transition brings about a considerable drop in H_{12} giving a turbulent boundary layer in which H_{12} lies between 1.3 and 2.2. Laminar separation takes place at a value of H_{12} near 3.5 while turbulent separation takes place at a value of H_{12} near 2.2.

In the current study, the integral parameters and shape factors were found by integrating the spline fit using a trapezoidal rule with very fine spacing. Values of these parameters and the associated Reynolds numbers are given in Table 29 for each of the profiles shown in Figures 7 and 8. Based on the work of Purtell, Klebanoff, and Buckley [1981] and Murlis, Tsai, and Bradshaw [1982], one would anticipate that the Re_θ for the profile of Figure 8 is too low to support turbulence.

SIMILARITY SOLUTIONS FOR LAMINAR BOUNDARY LAYERS

For a constant streamwise pressure gradient, laminar boundary layers can be plotted in such a way as to collapse them all to the same curve. Such laminar boundary layers are said to be self-similar and solutions to the boundary layer momentum equations may be solved using a similarity solution. A similarity solution reduces the number of variables in the equation by using a coordinate transformation. The boundary layer momentum equation for steady flow can be written as

$$u \frac{\partial u}{\partial x} + v \frac{\partial u}{\partial y} = - \frac{1}{\rho} \frac{dp_e}{dx} + \nu \frac{\partial^2 u}{\partial y^2}$$

Several different coordinate transformations have been used for similarity solutions. One such transformation is the Levy-Lees transformation (see Cebeci and Smith [1974]) which is given as

$$\xi = \int_0^{x/\ell} \left(\frac{U_e}{U_{ref}} \right) d \frac{x}{\ell}$$

and

$$\eta = \frac{1}{\sqrt{2\xi}} \left(\frac{U_e}{U_{ref}} \right) \left(\frac{y}{\ell} \right) \sqrt{\frac{R_e}{2}}$$

where

$$Re = \frac{\ell U_{ref}}{\nu}$$

These transformation variables are for an incompressible flow with a constant value of viscosity. The variables U_{ref} and ℓ refer to a reference velocity and a reference length, respectively. A similarity function, f , can then be defined from the streamfunction, ψ , as

$$\psi(x, y) = \sqrt{2\xi} f(\xi, \eta)$$

where

$$u = \frac{\partial \psi}{\partial y}$$

and

$$v = - \frac{\partial \psi}{\partial x}$$

The boundary layer momentum equation for steady, incompressible flow can now be transformed into the following differential equation

$$f''' + ff'' + \beta(1 - f'^2) = 2\xi(f'f_\xi' - f_\xi f'')$$

$$\beta = \frac{2\xi}{U_e} \frac{dU_e}{d\xi}$$

β is a streamwise pressure gradient parameter and must be determined from the measured streamwise static-pressure distribution. These measurements are also required to determine the values of ξ . When f has a prime for a superscript, it refers to a derivative with respect to η . A derivative with respect to ξ is noted by a subscript ξ .

Falkner and Skan [1931] developed a similarity solution for laminar boundary layers flowing over wedges with constant streamwise pressure gradients. In terms of the Levy-Lees coordinates, the Falkner-Skan solution involves no changes in the ξ direction. Thus all derivatives with respect to ξ (of f) are zero and the boundary layer momentum equation for steady, incompressible flow reduces to the following ordinary differential equation.

$$f''' + ff'' + \beta(1 - f'^2) = 0$$

The present boundary layer analysis solves this equation using the solution scheme of Hoffman [1983]. The Falkner-Skan solution represents a very good approximation of the laminar boundary layer solution in two cases: first, when the streamwise pressure gradient changes only slowly in the streamwise direction, and second, near the leading edge of the boundary layer surface

(since ξ is very small and the Levy-Lees transformed equation is approximated quite well by the Falkner-Skan equation). In the previous equation when β is equal to zero, the Falkner-Skan solution reduces to the original similarity solution of Blasius [1908] for laminar boundary layers with no streamwise pressure gradient. Separation of the laminar boundary layer will occur for a β with a value of -0.199.

Figure 9 compares the profile of Figure 8 with a Falkner-Skan profile at an equivalent β . Although the streamwise pressure gradient is not constant here, the comparison is quite good. The profile of Figure 8 (via Figures 4 and 6) is laminar. Integral parameters and skin friction values can be computed from the Falkner-Skan solution. These are presented in Table 29; where appropriate they are compared to the values calculated from the spline fit.

WALL-WAKE VELOCITY PROFILE FOR TURBULENT BOUNDARY LAYERS

Turbulent boundary layers are commonly divided into different regions. The innermost region is dominated by viscous shear and is self-similar for all turbulent boundary layers. This region is called the viscous sublayer and is described by

$$\frac{u}{u_\tau} = \frac{yu_\tau}{\nu}$$

or

$$u^+ = y^+$$

where u^+ and y^+ are called inner variables. u_τ is called the shear or friction velocity. Outside of the sublayer but still very close to the wall, the velocity is logarithmic with distance as

$$u^+ \sim \frac{1}{\kappa} \ln(y^+) + C$$

The viscous sublayer and logarithmic region overlap in a region called the buffer layer. Collectively the sublayer, buffer layer, and logarithmic layer are called the "law of the wall." Streamwise pressure gradients have essentially no effect on this region. Outside of this wall region, the streamwise pressure gradients are important and the velocity profile exhibits a wake-like form. Coles [1956] developed an equation for the wake region called the "law of the wake." His composite equation included a wake-like function added to the logarithmic equation. This wall-wake equation can be written as

$$u^+ = \frac{1}{\kappa} \ln(y^+) + C + \frac{\Pi}{\kappa} W(\frac{y}{\delta})$$

where

$$W(\frac{y}{\delta}) = 2 \sin^2(\frac{\pi y}{2\delta}) = 1 - \cos(\frac{\pi y}{\delta})$$

W is called Cole's universal wake function and is normalized to be zero at the wall and to be two at $y = \delta$. Coles' wake parameter Π brings in the effect of the streamwise pressure gradient and has a value of approximately 0.5 for a zero pressure gradient flow. Coles and Hirst [1968] later examined the data from a number of turbulent boundary layer experiments and determined that the von Karman mixing length parameter, κ , should be 0.41 and the law-of-the-wall constant, C , should be 5.0.

The analysis of turbulent boundary layers should include a fit of the data to the wall-wake equation. A least-squares fit of the data to the equation was chosen with u_r and Π as the variables to be determined and δ considered to be a known quantity.* The error between each data point and the wall-wake equation is

* An attempt to use all three variables (u_r , Π , and δ) in a least squares scheme produced inconsistent results.

$$E_i = \frac{u_r}{\kappa} \ln\left(\frac{y_i u_r}{\nu}\right) + u_r C + \frac{u_r \Pi}{\kappa} [1 - \cos(\frac{\pi y_i}{\delta})] - u_i .$$

Now the minimum error squared of all the data points must be found with respect to both u_r and Π . Taking the partial derivative of the error squared for each data point with respect to u_r and Π yields

$$\frac{\partial E_i^2}{\partial u_r} = 2E_i \left(\frac{1}{\kappa} \ln\left(\frac{y_i u_r}{\nu}\right) + \frac{1}{\kappa} + C + \frac{\Pi}{\kappa} [1 - \cos(\frac{\pi y_i}{\delta})] \right)$$

and

$$\frac{\partial E_i^2}{\partial \Pi} = 2E_i \left(\frac{u_r}{\kappa} [1 - \cos(\frac{\pi y_i}{\delta})] \right) .$$

Summing for all the data points and setting the two expressions equal to zero gives two equations

$$\frac{\partial E_i^2}{\partial u_r} = 0$$

and

$$\frac{\partial E_i^2}{\partial \Pi} = 0$$

which can be solved simultaneously for u_r and Π to give the minimum squared error. A secant method is used to solve the simultaneous non-linear equations. Sun and Childs [1976] presented a similar method for compressible turbulent boundary layers using the velocity transformation of van Driest [1951].

In order to use the fit of the wall-wake equation, the range of data points to be used in the fit must be considered. White [1974] states that the logarithmic region does not hold for $y^+ < 35$ (corresponding roughly to $y/\delta < 0.02$). For a large wake component, Coles and Hirst [1968] state that the region being fit should not include $y/\delta > 0.9$. They suggest that this number should be reduced to 0.75 for a zero streamwise pressure gradient and 0.6 for a vanishing wake component. Here the region $0.05 \leq y/\delta \leq 0.75$ was used: Sensitivity to the specific range of data points was not large.

Figure 10 shows the data of Figures 7 (via Figures 3 and 5) in inner variables. Parameters determined from the wall-wake fit are given in Table 29.

Streamwise pressure gradients can have a strong effect on the outer region of a turbulent boundary layer. Typical profiles at an Re_θ of 5,000 for values of Π of -0.5, 0.5, 0.5, 2.0, and 5.0 are shown in Figure 11(a) for illustration. We should note that the value of Re_θ controls the size of the logarithmic region. Shown in Figure 11(b) are profiles for Re_θ of 500, 1,000, 5,000, and 10,000 and a Π of 0.5. Note the difficulty in discerning a logarithmic region for a Re_θ of 500.

Most analyses, short of direct computation, consider boundary layers in which the pressure gradient is constant, so that the profiles are self-similar with downstream distance--so called equilibrium layers. Clauser [1954, 1955] conceived of a parameter

$$\beta_c = \frac{\delta^*}{\tau_w} \frac{dp_e}{dx}$$

to characterize equilibrium. Here τ_w is the wall shear stress. A turbulent boundary layer with a constant β_c has outer region similarity and is called an equilibrium turbulent boundary layer. All of the gross properties of that boundary layer can be described with a single parameter. Clauser [1954, 1955] chose the parameter G , where

$$G = \frac{1}{\Delta} \int_0^\infty \left(\frac{U_e - u}{u_r} \right)^2 dy$$

and

$$\Delta = \int_0^\infty \left(\frac{U_e - u}{u_r} \right)^2 dy .$$

G is called Clauser's shape factor and Δ is termed the defect thickness.

Values of G and Δ for the profile of Figure 7 are

$$G = 19.47$$

and

$$\Delta = 142.1 \text{ mm}$$

The turbulent boundary layer profiles on the cascade blade are non-equilibrium. In practice, one expects non-equilibrium to be the rule rather than the exception.

SKIN FRICTION COEFFICIENT OF A TURBULENT BOUNDARY LAYER

Ludweig and Tillman [1949] developed an empirical expression for the skin friction coefficient of a turbulent boundary layer. The curve-fit expression from their experimental data is

$$C_f \approx 0.246 Re_\theta^{-0.268} 10^{-0.678 H_{12}}$$

Skin friction coefficient (C_f), wall shear stress (τ_w) and friction velocity (u_τ) can be related by

$$C_f = \frac{\tau_w}{\rho U_e^2 / 2}$$

and

$$u_\tau = \sqrt{\frac{\tau_w}{\rho}}$$

The friction velocity calculated from the Ludweig-Tillman expression agrees well with that calculated from the wall-wake fit for all the non-separated turbulent profiles measured.

TRANSITION

Transition represents the region in which a laminar boundary layer becomes turbulent. The length of the transition region depends strongly on, among other parameters, the streamwise pressure gradient and the freestream turbulence intensity. The incomplete transition of the pressure surface profiles is shown in Figure 12. Here the transition is termed incomplete as

the profile at 97.8% chord does not contain a logarithmic region. Also, Re_θ is below that believed capable of sustaining full turbulence. Note the comparison with the Falkner-Skan profiles, particularly the thickening of the profile in the near-wall region.

WAKES

Initially, the analysis of the wake profiles proceeds in the same manner as the analysis of the boundary layer profiles. Since the static pressure is normally constant across the wake, the analysis does not have to account for a normal pressure gradient. A spline is used to curve fit the data points from the point of minimum velocity to the last point in the freestream on one side of the wake. Integral parameters can then be calculated for this side of the wake. The analysis is repeated on the other side of the wake. The integral parameters for the entire wake can be found simply by summing the parameters for each side of the wake. One would expect H_{12} to decay asymptotically to 1.0 as the wake mixes out.

Wake similarity requires different length scales on the pressure side, L_p , and the suction side, L_s , of the wake. L_p and L_s are the distances on the pressure and suction sides of the wake centerline from the point of minimum velocity to a point where the velocity defect is $(U_e - u_{CL})/2$. Lakshminarayana and Davino [1979] suggested a Gaussian distribution to correlate the wake data,

$$\frac{U_e - u}{U_e - u_{CL}} = e^{-0.693\eta}$$

where η is the distance across the wake normalized by the appropriate length scale. One would expect that only far wakes would show similarity with this type of correlation.

ANALYSIS OF CURRENT DATA

The analysis that has just been described was carried out on the raw data of Tables 3 through 27. After accounting for the normal pressure gradient, we computed the boundary layer edge velocity and the boundary layer thickness for the boundary layers on the pressure surface. Table 30 shows these values along with their standard deviations. The computed value of δ at 2.7% chord is doubtful. The measured velocity profiles were then reconstructed to obtain the boundary layer velocity profiles as shown in Tables 31 through 41. These tables also include the profiles of turbulence intensity which were obtained using the values of U_e given in Table 30.

The reconstructed boundary layer profiles on the pressure surface were spline fit and integrated to obtain the various boundary layer parameters. Table 42 shows these parameters. We note here that throughout this analysis, the value of ρ was taken as 1.205 kg/m^3 and the value of ν was taken as $0.150 \text{ cm}^2/\text{sec}$. The boundary layers at 2.7%, 5.9%, and 14.4% chord were so small that the integrations to find θ and δ_3 are questionable. The Ludweig-Tillman equation was only evaluated at 97.9% chord since this was the only chord position where the boundary layer is nearly fully turbulent. Table 43 shows the boundary layer parameters for the pressure surface as obtained from the Falkner-Skan solution.

We analyzed the suction surface boundary layers in a similar manner. Table 44 shows the values of U_e and δ (and their standard derivations) while Tables 45 through 55 show the reconstructed boundary layers. Table 56 shows the boundary layer parameters obtained using the spline fit of the data while Table 57 shows the parameters obtained using the least-squares fit of the data to the wall-wake equation. The wall-wake equation is not valid for the detached layers at 84.2% and 94.9% chord. Table 57 also shows values of C_f

obtained from direct measurements within the viscous sublayer. In Part 1 of this report, we discussed the similarity defect law for turbulent boundary layers developed by Perry and Schofield [1973]. The length and velocity scales of this similarity law are given in Table 58 for the boundary layers on the suction surface.

Tables 59 and 60 show the velocity and turbulence intensity profiles in the near wakes. The far wake, shown in Table 61, has no turbulence intensity values since we measured this wake with a slow response five-hole pressure probe. After spline fitting each side of these wakes, we determined the boundary layer integral parameters and the similarity length scales. Table 62 shows these parameters for the pressure side of the wakes while Table 63 shows these parameters for the suction side of the wakes.

CONCLUSIONS

We have presented a two-part report which describes measurements of the flow field about a double circular arc compressor blade in cascade at an incidence angle of 5 degrees and a chord Reynolds number of 500,000. Part 1 of the report describes the facility, the measurement techniques, and the physics of the flow field. In this, Part 2 of the study, both the raw and analyzed data are presented in a tabulated form with the hope of encouraging computational comparisons. Also in Part 2, we include the details of the procedure which allowed us to analyze the raw data. Other analysis techniques are possible and their results might usefully be compared with what we have given here.

We have placed this tabulated data on a computer tape and the tape is available to other researchers. We should also note that similar measurements at additional incidence angles are currently being completed.

Nomenclature

AR	aspect ratio
B	integral layer thickness in the Perry and Schofield [1973] theory
c	blade chord length
C	law-of-the-wall constant ($= 5.0$)
C_f	skin friction coefficient $= \tau_w / (\rho U_e^2 / 2)$
C_p	static-pressure coefficient $= (p - p_1) / (\rho v_1^2 / 2)$
E	error between the data and wall-wake equation
f	similarity function
G	Clauser's shape factor
H_{12}	first shape factor $= \delta^*/\theta$
H_{32}	second shape factor $= \delta_3/\theta$
i	incidence angle $= \beta_1 - \kappa_1$
K	kurtosis
	reference length
L_p, L_s	pressure and suction surface length scales from the point of minimum velocity to a point where the velocity defect is $(U_e - u_{CL})^2$
LDV	laser Doppler velocimeter
n	data point index
N	number of data points
N_{inv}	number of data points in the inviscid region
N_{max}	maximum number of data points that could possibly be in the inviscid region
p	static pressure
p_e	static pressure at the boundary layer edge
P_T	total or stagnation pressure
r	radius

Nomenclature (Continued)

Re	reference Reynolds number = $\ell U_{ref}/\nu$
Re_c	blade chord Reynolds number = cV_1/ν
Re_θ	momentum thickness Reynolds number = $\theta U_e/\nu$
s	blade spacing
S	skewness
u	streamwise velocity
u'	root mean square value of the turbulent velocity fluctuation
u^+	dimensionless velocity in the inner boundary layer = u/u_τ
u_{bl}	boundary layer velocity
u_τ	shear of friction = $\sqrt{\tau_w/p}$
u_{inv}	inviscid velocity
u_{meas}	measured composite velocity
U_e	velocity at the boundary layer or wake edge
U_s	velocity scale for the Perry and Schofield [1973] defect law
U_{ref}	reference velocity
v	normal velocity
V	velocity
$W(\)$	Coles' universal wake function = $2 \sin^2(\) + 1 - \cos(\)$
x	streamwise coordinate
y	coordinate normal to the blade surface
y^+	dimensionless coordinate normal to the blade surface in inner boundary layer variables
β	Falkner-Skan streamwise pressure gradient parameter; flow angle measured from the axial direction
β_c	Clauser's equilibrium parameter
γ	stagger angle
δ	boundary layer thickness (where $u \approx 0.99 U_e$)
δ^*	displacement thickness

Nomenclature (Continued)

d_3	energy thickness
δ_D	deviation angle = $\beta_2 - \kappa_2$
Δ	defect thickness
g	normalized distance across the wake; dimensionless normal similarity variable
θ	momentum thickness
κ	Von Karman's mixing length parameter (~ 0.41); blade metal angle
ν	kinematic viscosity (0.150 cm ² /sec for air)
ξ	dimensionless streamwise similarity variable
Π	Coles' wake parameter
ρ	fluid density (1.205 kg/m ³ for air)
σ	blade solidity = c/s
τ_w	wall or surface shear stress
ϕ	camber angle = $\kappa_1 - \kappa_2$
ψ	streamfunction
ω	total-pressure loss coefficient = $(P_{T_1} - P_{T_2}) / (\rho v_1^2/2)$

Subscripts

CL	at the wake centerline
i	the i th data point
inv	inviscid
LE	leading edge
m	mean flow
meas	measured
n	data point index
p	pressure

Nomenclature (Continued)

s	suction surface
TE	trailing edge
x	axial direction
wall	at the wall
ξ	derivative with respect to ξ
1	inlet (upstream five-hole probe measurement station)
2	outlet (downstream five-hole probe measurement station)

Superscript

'	derivative with respect to η
—	average over the blade passage

REFERENCES

1. Ball, C. L., Reid, L., and Schmidt, J. F., "End-Wall Boundary Layer Measurements in a Two Stage Fan," NASA TM 83409, June 1983.
2. Blasius, H., "Grenzschichten in Flüssigkeiten mit kleiner Reibung," Z. Angew. Math. Phys., Vol. 56, No. 1, pp. 1-37, 1908. (English Translation, NACA TM No. 1256.)
3. Cebeci, T. and Smith, A. M. O., Analysis of Turbulent Boundary Layers, Academic Press, 1974.
4. Clauser, F. H., "Turbulent Boundary Layers in Adverse Pressure Gradients," Journal of the Aeronautical Sciences, Vol. 21, pp. 91-108, February 1954.
5. Clauser, F. H., "The Turbulent Boundary Layer," Advances in Applied Mechanics, Vol. 4, pp. 1-51, 1956.
6. Coles, D. E., "The Law of the Wake in the Turbulent Boundary Layer," Journal of Fluid Mechanics, Vol. 1, pp. 191-226, 1956.
7. Coles, D. E. and Hirst, E. A., "Computation of Turbulent Boundary Layers," in Proceedings of the AFSOR-IFP-Standford Conference, Vol. II, August 1968.

8. Deutsch, S. and Zierke, W. C., "Some Measurements of Boundary Layers on the Suction Surface of Double Circular Arc Blades in Cascade," ARL/PSU TM 84-77, The Applied Research Laboratory, The Pennsylvania State University, April 3, 1984.
9. Falkner, V. M. and Skan, S. W., "Some Approximate Solutions of the Boundary Layer Equations," Phil. Mag., Vol. 12, No. 7, pp. 865-896, 193.
10. Hoffman, G. H., "A Rapid Method for Predicting Suction Distributions to Maintain Attached, Laminar Boundary Layers on Bodies of Revolution," ARL/PSU TM 83-201, Applied Research Laboratory, The Pennsylvania University, December 1983.
11. Klock, R., "Evaluation of Boundary Layer Measurements in Two-Dimensional Compressible Subsonic Flow with a Pressure Gradient across the Boundary Layer," ESA-TT-810, European Space Agency, July 1983.
12. Lakshminarayana, B. and Davino, R., "Mean Velocity and Decay Characteristics of the Guide Vane and Stator Blade Wake of an Axial Flow Compressor," Transactions of the ASME, Journal of Engineering for Power, Vol. 102, pp. 50-60, January 1980.
13. Ludweig, H. and Tillman, W., "Untersuchungen über die Wandschubspannung in Turbulenten Reibungsschenkten,: Ing. -Arch. , Vol. 17, pp. 288-299, 1949. (English Transaction, NACA TM 1285.)

14. Mellor, G. L. and Wood, G. M., "An Axial Compressor End-Wall Boundary Layer Theory," Transactions of the ASME, Journal of Basic Engineering, Vol. 93, Series D, No. 1, pp. 300-316, June 1971.
15. Murlis, J., Tsai, H. M., and Bradshaw, P., "The Structure of Turbulent Boundary Layers at Low Reynolds Numbers," Journal of Fluid Mechanics, Vol. 122, pp. 13-56, 1982.
16. Perry, A. E. and Schofield, W. H., "Mean Velocity and Shear Stress Distributions in Turbulent Boundary Layers," Physics of Fluids, Vol. 16, No. 12, pp. 2068-2074, December 1973.
17. Purcell, L. R., Klebanoff, P. S., and Buckley, F. T., "Turbulent Boundary Layers at Low Reynolds Numbers," Physics of Fluids, Vol. 24, pp. 802-811, 1981.
18. Sun, C. C. and Childs, M. E., "Wall-Wake Velocity Profile for Compressible Nonadiabatic Flows," AIAA Journal, Vol. 14, No. 6, pp. 820-822, June 1976.
19. Van Driest, E. R., "Turbulent Boundary Layer in Compressible Fluids," Journal of the Aeronautical Sciences, Vol. 18, pp. 145-160 and 216, 1951.
20. White, F. M., Viscous Fluid Flow, McGraw-Hill, Inc., 1974.

BLADE GEOMETRY

$$C = 228.6 \text{ mm} \quad \sigma = 2.14 \quad \kappa_1 = 53^0$$

$$S = 106.8 \text{ mm} \quad AR = 1.61 \quad \kappa_2 = -12^0$$

$$r_{LE} = r_{TE} = 9.14 \mu\text{m} \quad \gamma = 20.5^0 \quad \phi = 65^0$$

MEASURED FLOW CONDITIONS

$$Re_C \approx 500,000 \quad V_X = 17.55 \text{ m/sec} \quad \bar{\beta}_m = 39.9^0$$

$$i = -5^0 \quad \bar{\beta}_2 = 4^0 \quad \bar{\theta} = 54^0$$

$$\beta_1 = 58^0 \quad \bar{V}_2 = 17.59 \text{ m/sec} \quad \bar{\delta}_D = 16^0$$

$$V_1 = 33.11 \text{ m/sec} \quad \bar{V}_m = 22.88 \text{ m/sec} \quad \bar{\omega} = 0.151$$

$$(\bar{c}_P)_2 = 0.463$$

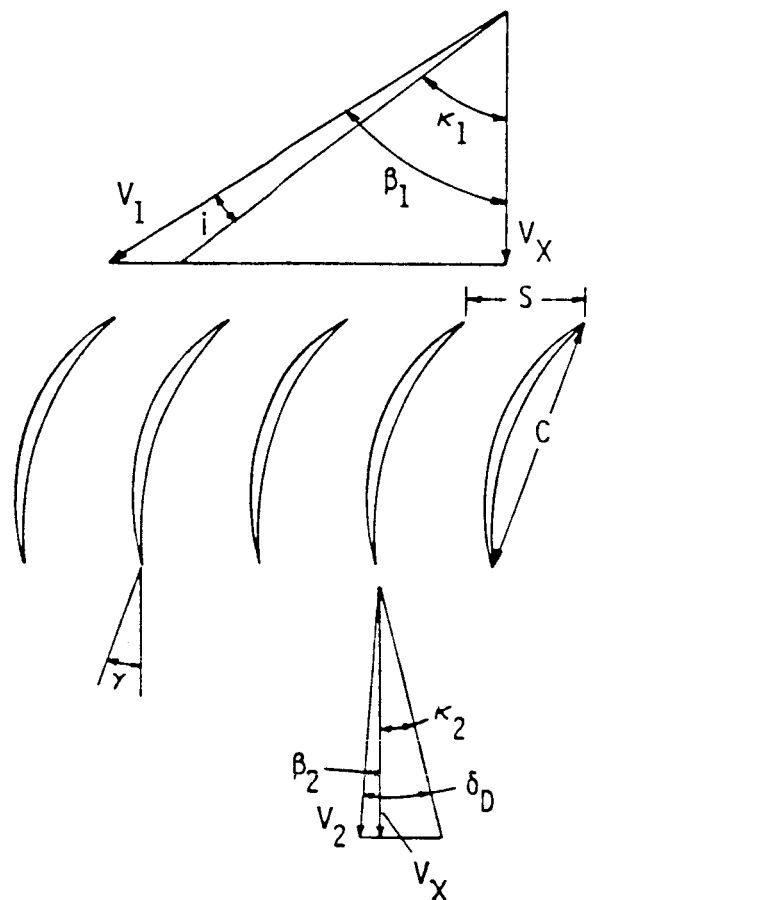


Figure 1. Blade Geometry and Flow Conditions

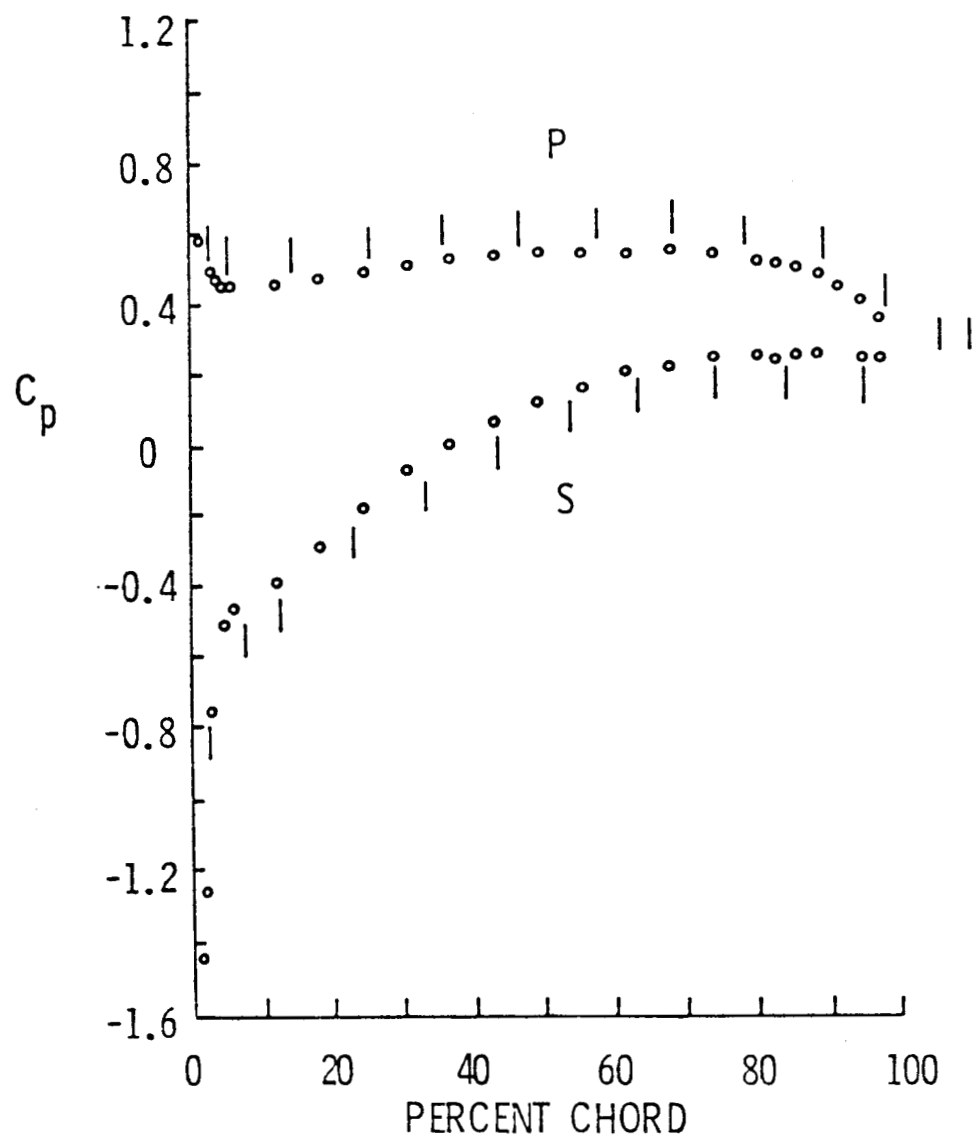


Figure 2. Blade Static-Pressure Distribution (The Vertical Line Segments Represent the Locations of LDV Measurements)
(P - Pressure Surface; S - Suction Surface)

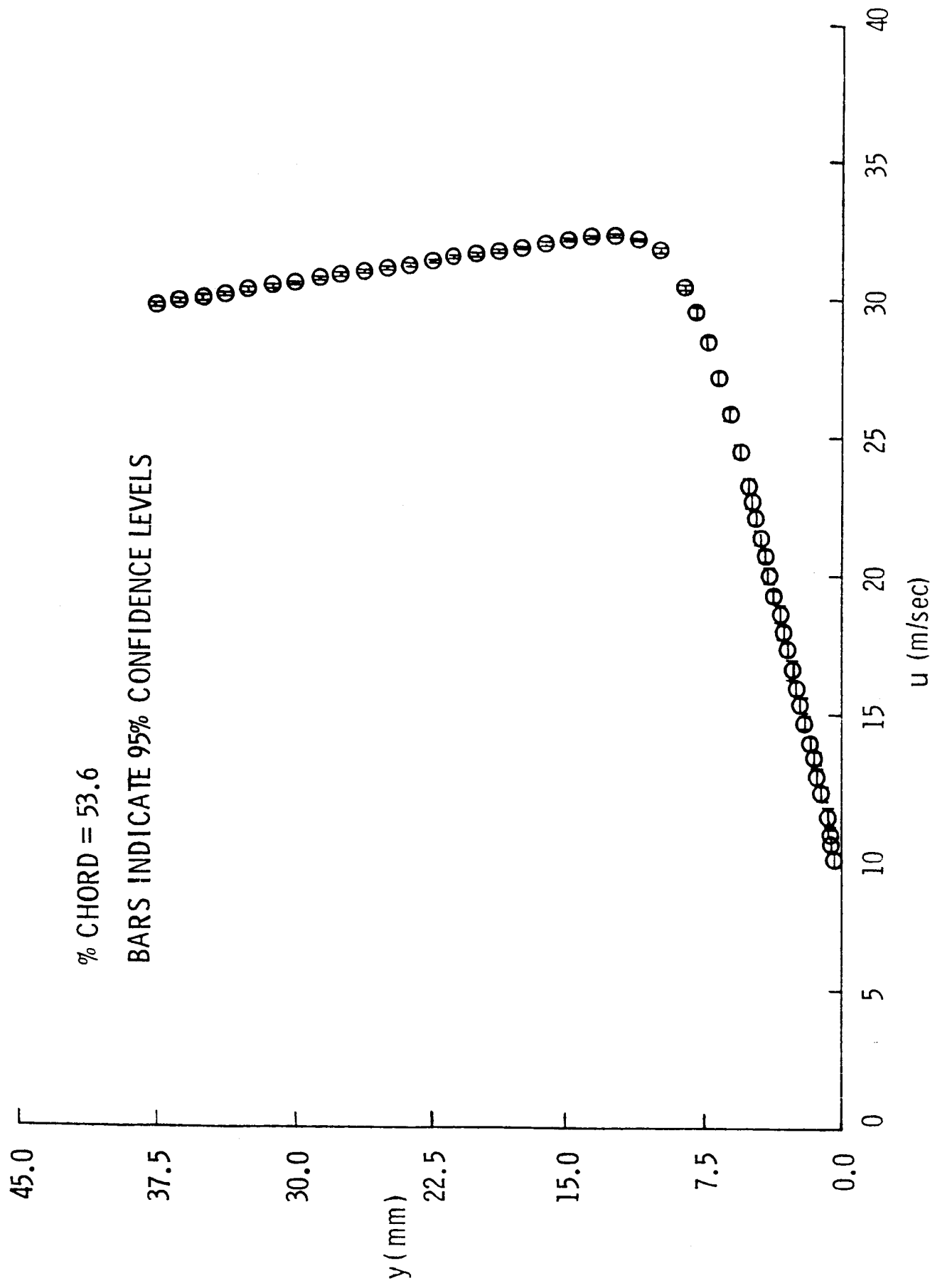


Figure 3. Typical Measured Velocity Profile with $\partial p / \partial y > 0$

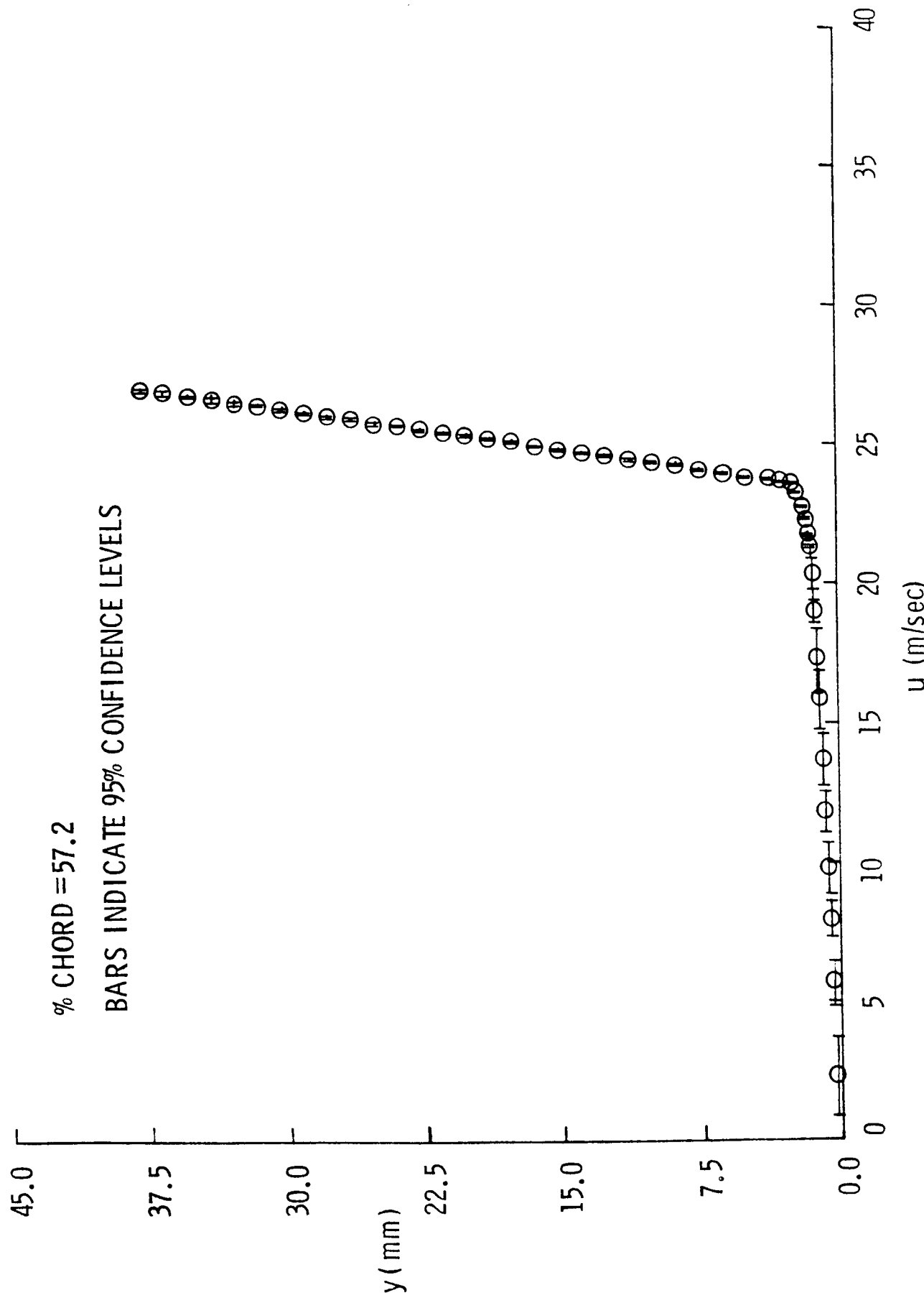


Figure 4. Typical Measured Velocity Profile with $\partial p/\partial y < 0$

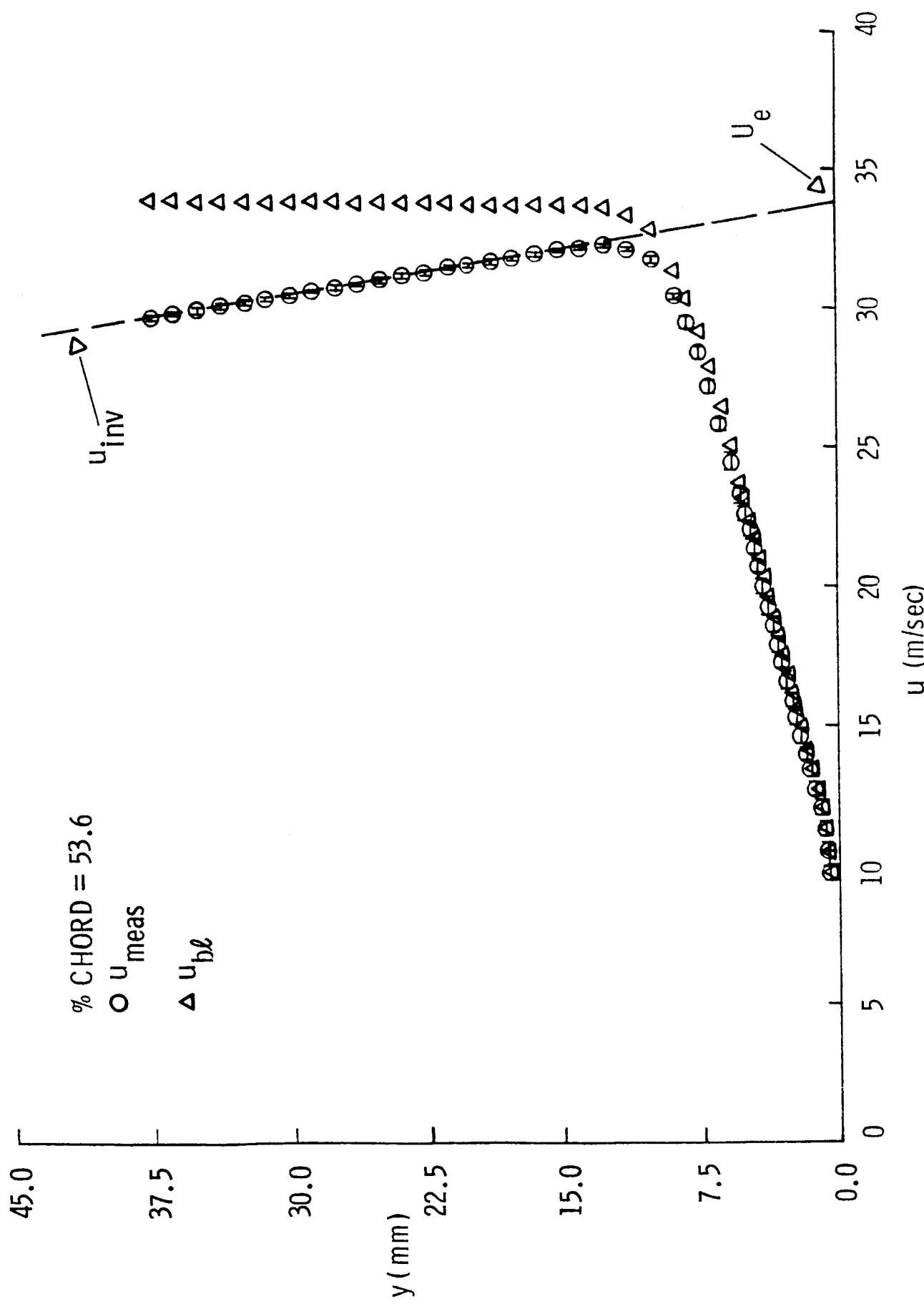


Figure 5. Reconstructed Boundary Layer Velocity Profile with $\partial p / \partial y > 0$

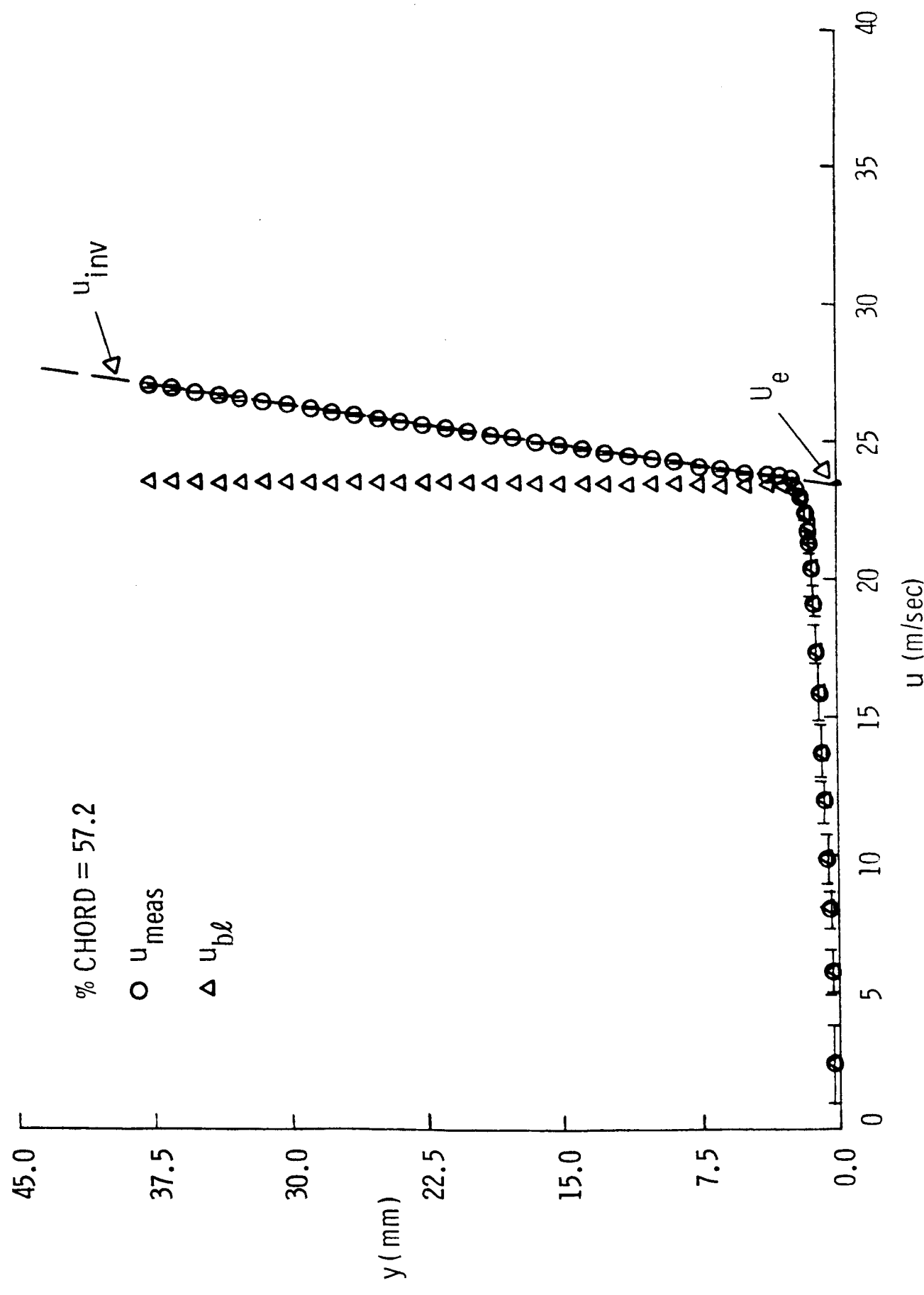


Figure 6. Reconstructed Boundary Layer Velocity Profile with $\frac{\partial p}{\partial y} < 0$

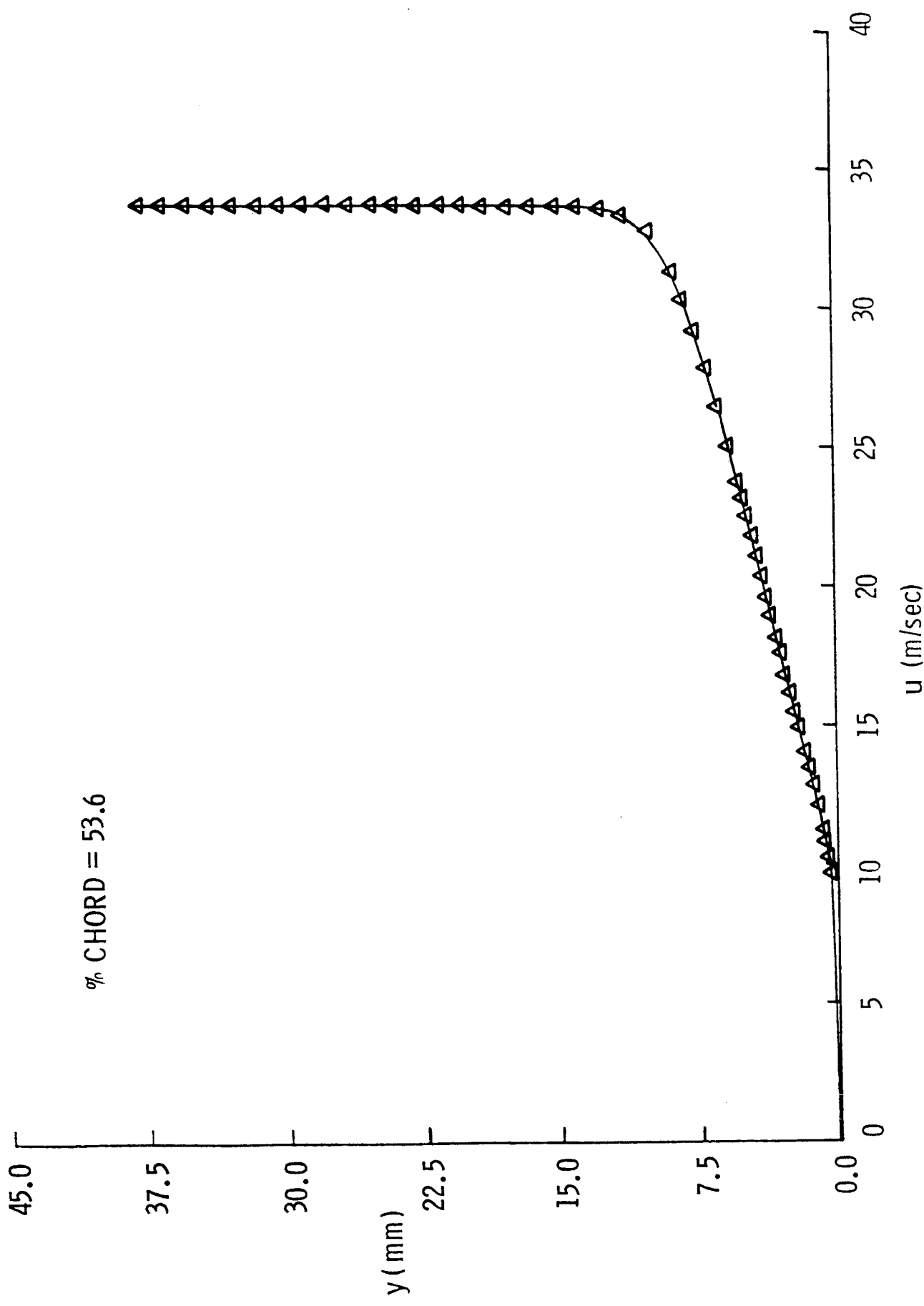


Figure 7. Spline Fit of the Boundary Layer Velocity Profile with $\frac{\partial p}{\partial y} > 0$

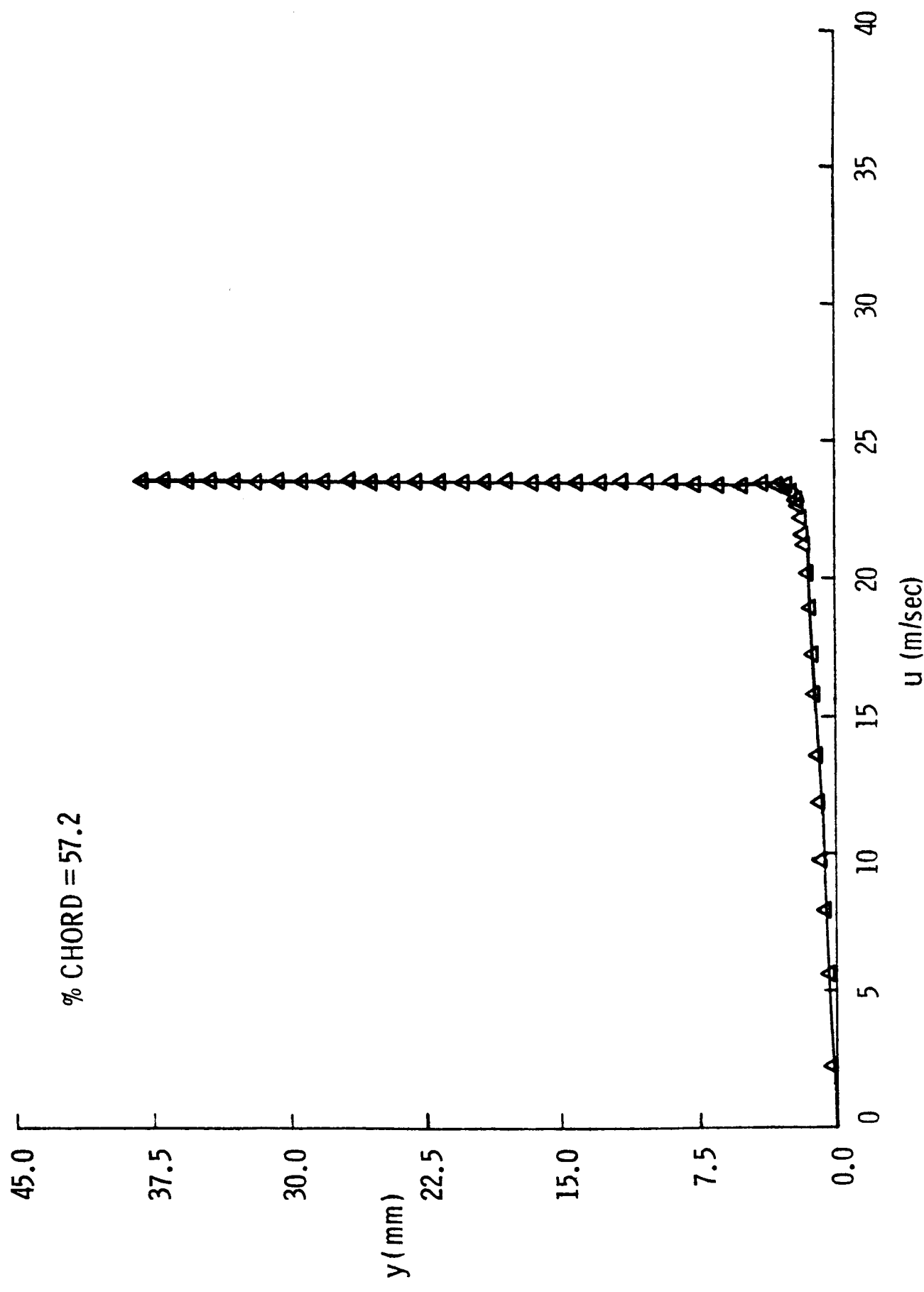


Figure 8. Spline Fit of the Boundary Layer Velocity Profile with $\partial p / \partial y < 0$

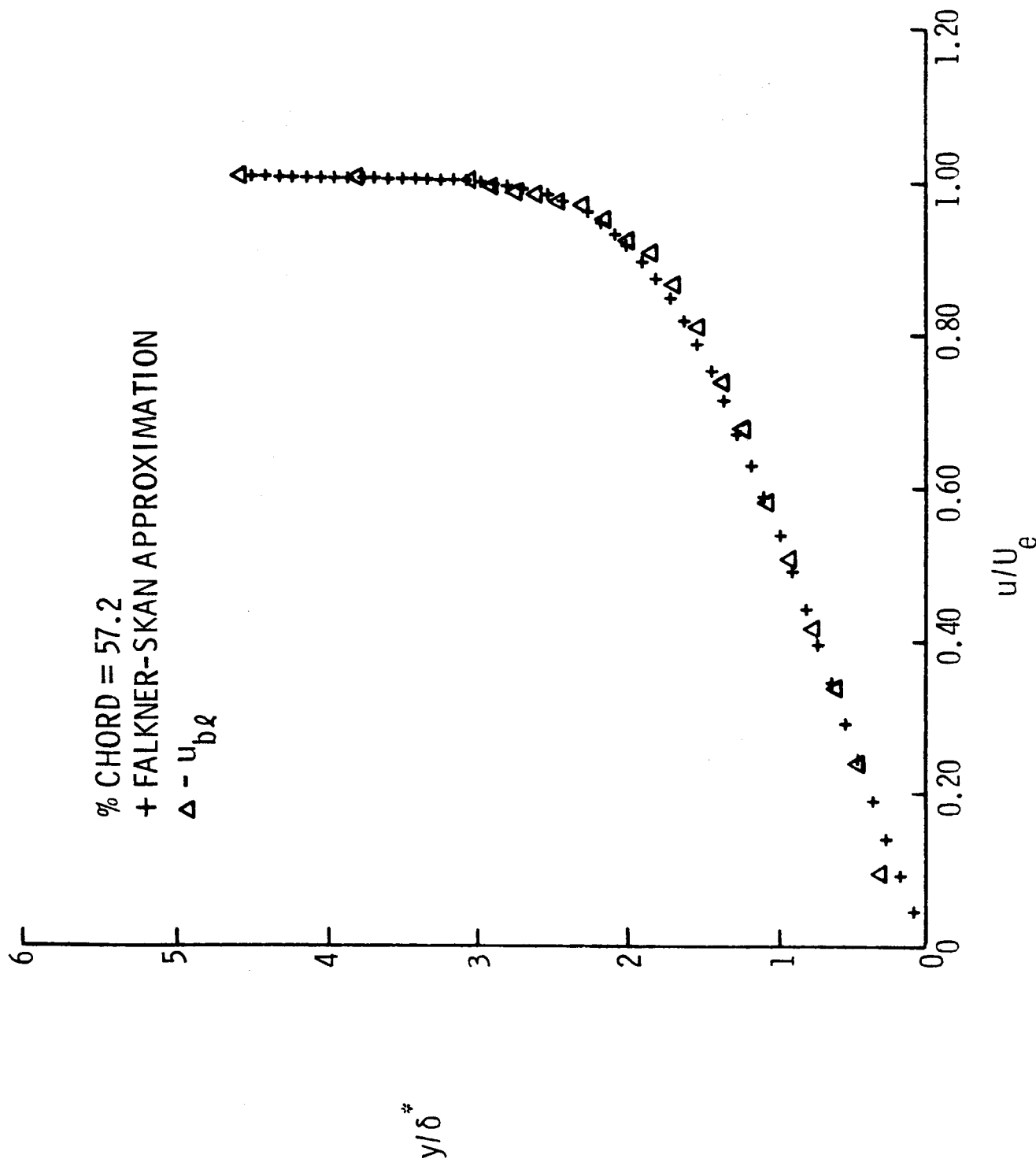


Figure 9. Falkner-Skan Approximation to the Boundary Layer Velocity Profile with $\partial p / \partial y < 0$

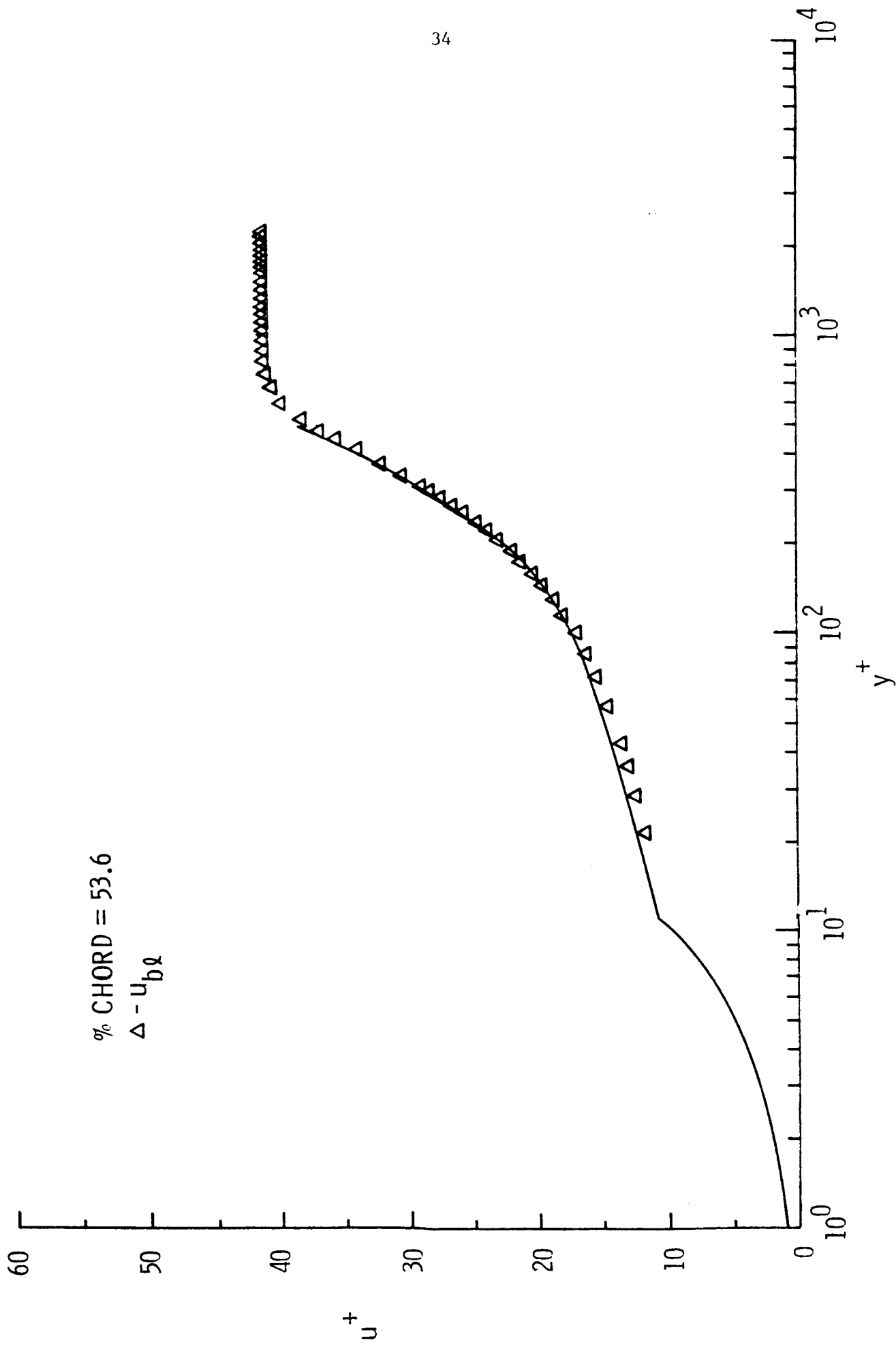


Figure 10. Kállay Wake Approximation to the Boundary Layer Velocity Profile with $\partial p / \partial y > 0$

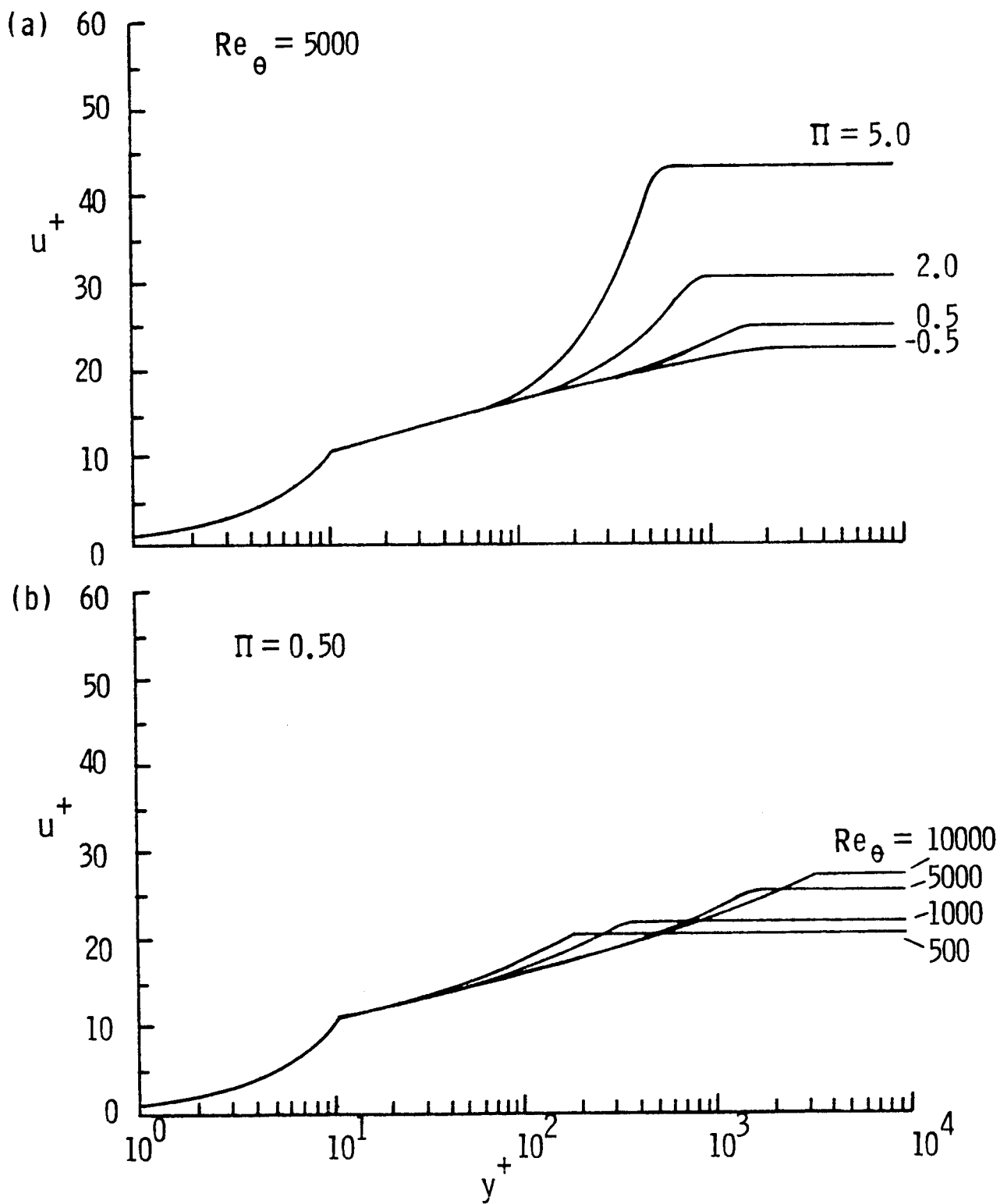


Figure 11. (a) Wall/Wake Composite Profile: Π Varies
 (b) Wall/Wake Composite Profile: Re_{θ} Varies

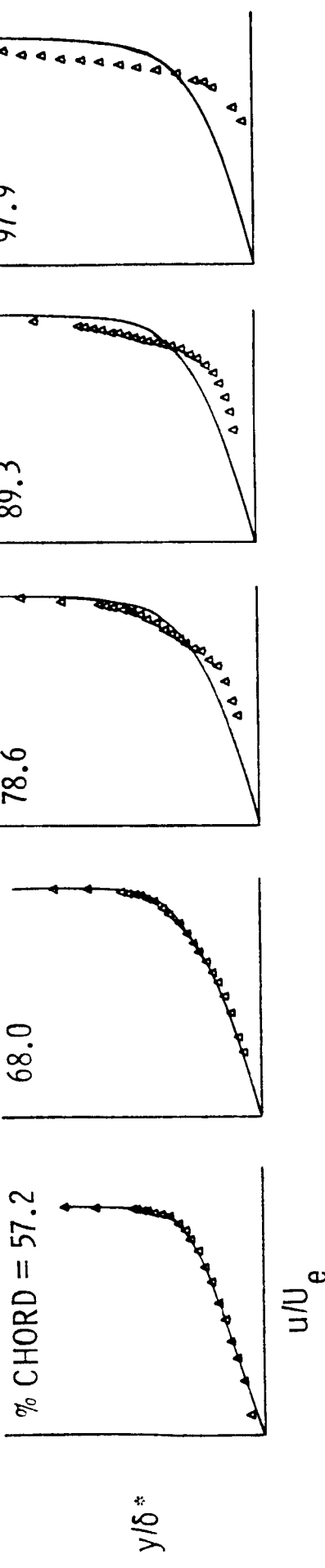


Figure 12. Incomplete Transition of the Pressure Surface Data (Solid Line is the Falkner-Skan Approximation and the Triangles Represent the Reconstructed Boundary Layer Velocity Profiles)

Pressure Surface					
% Chord	C_p	U_e (m/sec)	% Chord	C_p	U_e (m/sec)
1.0	0.685	18.58	49.2	0.588	21.25
3.0	0.547	22.28	55.3	0.588	21.25
4.0	0.523	22.87	61.5	0.590	21.20
5.0	0.508	23.22	67.7	0.597	21.02
6.0	0.508	23.22	73.8	0.584	21.36
12.2	0.509	23.20	80.0	0.565	21.84
18.3	0.526	22.80	82.5	0.551	21.19
24.5	0.545	22.33	85.4	0.543	22.38
30.7	0.553	22.14	88.3	0.523	22.87
36.8	0.574	21.61	91.3	0.494	23.55
43.0	0.583	21.38	94.5	0.456	24.42
			97.3	0.400	25.65

Table 1. Static Pressure Measurements on the Pressure Surface

Suction Surface					
% Chord	C_p	U_e (m/sec)	% Chord	C_p	U_e (m/sec)
1.0	-1.346	50.72	49.2	0.153	30.48
2.0	-1.302	50.24	55.3	0.196	29.69
3.0	-0.936	46.08	61.5	0.243	28.84
5.0	-0.481	40.30	67.7	0.260	28.51
6.0	-0.453	39.92	73.8	0.292	27.89
12.2	-0.349	38.46	80.0	0.301	27.71
18.3	-0.270	37.32	82.5	0.309	27.55
24.5	-0.167	35.77	88.3	0.297	27.79
30.7	-0.067	34.20	94.5	0.307	27.59
36.8	0.038	32.48	97.3	0.308	27.57
43.0	0.097	31.47			

Table 2. Static Pressure Measurements on the Suction Surface

**ORIGINAL
OF POOR QUALITY**

Y (mm)	$\frac{u}{U}$ (m/s)	Local Turbulence Intensity		Skewness		Kurtosis		% Backflow	
		value	deviation	value	deviation	value	deviation	value	deviation
0.127	16.31	4.97	0.225	0.159	-0.782	0.763	4.098	2.185	0.00
0.191	20.00	1.69	0.103	0.047	-1.168	0.641	6.867	3.891	0.00
0.254	21.04	0.31	0.081	0.011	-1.775	0.758	8.380	3.798	0.00
0.318	21.32	0.54	0.073	0.017	-1.764	0.800	8.758	4.301	0.00
0.381	21.28	0.35	0.074	0.014	-1.606	0.569	8.786	3.823	0.00
0.508	21.53	0.26	0.067	0.009	-1.543	0.550	9.060	3.199	0.00
0.762	21.86	0.14	0.060	0.007	-1.918	0.694	12.763	5.664	0.00
1.016	22.14	0.12	0.053	0.010	-1.844	0.989	13.541	8.636	0.00
1.574	22.52	0.02	0.049	0.012	-1.292	2.444	22.163	14.712	0.00
2.032	22.82	0.12	0.046	0.013	-1.168	1.620	12.927	7.082	0.00
2.540	23.22	0.15	0.035	0.007	0.756	0.508	0.756	0.00	0.00
3.810	23.96	0.17	0.034	0.006	0.988	0.730	8.169	2.794	0.00
5.080	24.76	0.29	0.033	0.007	0.833	0.403	5.163	6.204	0.00
6.350	25.36	0.19	0.031	0.005	1.331	1.153	1.381	0.00	0.00
7.620	25.98	0.27	0.031	0.007	0.554	0.886	10.087	11.516	0.00
8.890	26.38	0.23	0.028	0.006	0.743	0.930	5.915	2.566	0.00
10.160	26.77	0.24	0.025	0.005	0.569	0.590	5.893	4.682	0.00
11.430	27.24	0.19	0.023	0.007	-0.002	0.302	4.372	1.873	0.00
12.700	27.60	0.21	0.023	0.004	0.230	0.285	4.365	2.344	0.00
13.970	27.93	0.13	0.023	0.002	0.442	0.401	3.348	0.699	0.00
15.240	28.27	0.09	0.022	0.001	0.077	0.851	4.133	0.960	0.00
16.510	28.54	0.12	0.022	0.002	0.148	0.837	5.362	4.003	0.00
17.780	28.79	0.14	0.021	0.003	0.427	0.356	5.731	3.069	0.00
19.050	29.11	0.14	0.021	0.001	0.378	0.241	3.868	1.477	0.00
20.320	29.33	0.14	0.021	0.003	0.487	0.910	3.580	0.544	0.00
21.590	29.50	0.13	0.020	0.002	-0.209	1.503	5.591	5.863	0.00
22.860	29.72	0.13	0.020	0.002	0.410	0.444	8.036	10.410	0.00
24.130	29.98	0.10	0.020	0.003	-0.207	0.947	3.942	1.768	0.00
25.400	30.17	0.11	0.019	0.001	0.305	0.360	5.671	5.200	0.00
26.670	30.36	0.11	0.019	0.002	0.346	0.197	3.624	0.958	0.00
27.940	30.54	0.11	0.020	0.002	0.409	0.346	3.575	0.631	0.00
29.210	30.77	0.11	0.018	0.001	0.354	0.272	4.652	1.591	0.00
30.480	30.88	0.12	0.020	0.002	0.097	0.164	0.564	0.00	0.00
31.750	31.11	0.11	0.020	0.001	0.254	0.255	3.200	0.367	0.00
33.020	31.28	0.09	0.019	0.002	0.297	0.580	3.384	0.496	0.00
34.290	31.47	0.14	0.020	0.001	0.217	0.275	3.361	2.218	0.00
35.560	31.61	0.17	0.020	0.002	0.146	0.211	3.365	0.761	0.00
36.830	31.81	0.12	0.020	0.001	0.276	0.276	3.272	0.404	0.00
38.100	31.90	0.17	0.021	0.003	-0.493	1.064	5.985	6.849	0.00

Table 3. Boundary Layer Measurements at 2.7% Chord on the Pressure Surface

Y (mm)	u (m/s)	Local Turbulence Intensity	Skewness	Kurtosis	% Backflow
0.318	19.76	1.25	0.105	0.018	-1.263
0.381	22.35	0.70	0.075	0.009	-3.247
0.508	23.76	0.17	0.047	0.005	-3.906
0.762	23.94	0.08	0.042	0.007	-4.236
1.016	24.10	0.10	0.033	0.009	-1.751
1.524	24.28	0.08	0.025	0.002	-0.194
2.032	24.34	0.06	0.023	0.001	-0.245
2.540	24.45	0.03	0.024	0.001	-0.077
3.810	24.69	0.05	0.022	0.001	0.101
5.080	24.92	0.08	0.023	0.002	0.048
6.350	25.18	0.05	0.024	0.004	0.008
7.620	25.52	0.08	0.024	0.001	0.375
8.890	25.80	0.04	0.022	0.002	0.095
10.160	26.05	0.10	0.021	0.001	0.052
11.430	26.37	0.04	0.021	0.002	0.281
12.700	26.66	0.09	0.021	0.002	0.179
13.970	26.92	0.06	0.021	0.001	0.326
15.240	27.20	0.08	0.022	0.001	0.361
16.510	27.46	0.07	0.021	0.001	0.244
17.780	27.71	0.08	0.020	0.001	0.458
19.050	27.99	0.07	0.020	0.001	0.094
20.320	28.19	0.07	0.020	0.001	0.325
21.590	28.41	0.08	0.020	0.001	0.033
22.860	28.63	0.08	0.020	0.001	0.224
24.130	28.86	0.10	0.019	0.002	0.389
25.400	29.06	0.10	0.019	0.001	0.254
26.670	29.30	0.09	0.020	0.001	0.159
27.940	29.47	0.08	0.019	0.001	0.126
29.210	29.68	0.04	0.018	0.001	0.081
30.480	29.83	0.09	0.018	0.001	0.165
31.750	29.98	0.09	0.019	0.002	0.186
33.020	30.21	0.04	0.019	0.001	0.072
34.290	30.45	0.07	0.019	0.001	0.309
35.560	30.60	0.09	0.019	0.001	0.141
36.830	30.77	0.08	0.018	0.001	0.296
38.100	30.91	0.06	0.019	0.002	0.203

Table 4. Boundary Layer Measurements at 5.9% on the Pressure Surface

ORIGINAL PAGE IS
OF POOR QUALITY

y (mm)	u (m/s)	Local Turbulence Intensity	Skewness	Kurtosis	% Backflow
		value deviation	value deviation	value deviation	value deviation
0.254	9.79	0.80	0.187	0.023	0.343
0.318	13.69	0.96	0.133	0.017	0.394
0.381	17.35	1.22	0.112	0.014	-0.010
0.444	20.38	0.90	0.083	0.017	-1.278
0.508	22.29	0.53	0.061	0.011	-2.148
0.762	24.67	0.02	0.020	0.002	-0.152
1.016	24.83	0.07	0.019	0.002	-0.270
1.524	24.95	0.04	0.019	0.002	0.051
2.032	25.00	0.04	0.018	0.001	-0.087
2.540	25.06	0.05	0.019	0.001	-0.030
3.810	25.16	0.03	0.018	0.001	0.183
5.080	25.30	0.06	0.019	0.001	-0.030
6.350	25.44	0.04	0.018	0.002	-0.270
7.620	25.59	0.05	0.019	0.001	-0.063
8.890	25.76	0.07	0.019	0.003	0.034
10.160	25.88	0.03	0.019	0.001	0.063
11.430	26.04	0.04	0.019	0.001	0.357
12.700	26.22	0.04	0.019	0.001	-0.035
13.970	26.35	0.04	0.019	0.001	0.117
15.240	26.51	0.05	0.019	0.002	0.124
16.510	26.65	0.05	0.019	0.002	0.242
17.780	26.85	0.07	0.019	0.002	-0.026
19.050	27.00	0.03	0.019	0.001	0.075
20.320	27.15	0.06	0.019	0.001	0.121
21.590	27.38	0.05	0.018	0.002	0.113
22.860	27.48	0.04	0.019	0.001	0.136
24.130	27.65	0.03	0.019	0.002	0.040
25.400	27.86	0.03	0.019	0.001	0.096
26.670	28.01	0.05	0.020	0.001	-0.005
27.940	28.19	0.06	0.019	0.001	0.281
29.210	28.33	0.03	0.020	0.001	0.258
30.480	28.56	0.04	0.020	0.002	0.157
31.750	28.68	0.05	0.020	0.002	0.265
33.020	28.83	0.05	0.019	0.002	0.280
34.290	29.04	c. c4	c. 019	c. 001	c. 209
35.560	29.22	0.04	0.020	0.001	0.183
36.830	29.36	0.05	0.019	0.001	0.052

Table 5. Boundary Layer Measurements at 19.4% Chord on the Pressure Surface

y (mm)	u (m/s)	Local Turbulence Intensity	Skewness	Kurtosis	% Backflow
0.254	5.60	0.48	0.218	0.036	0.790
0.318	8.23	0.59	0.156	0.017	0.368
0.381	10.54	0.87	0.148	0.019	0.693
0.444	13.60	0.63	0.148	0.017	0.662
0.508	16.06	0.85	0.137	0.029	0.327
0.572	18.52	0.44	0.098	0.012	0.637
0.635	20.14	0.53	0.073	0.011	0.635
0.762	22.35	0.29	0.057	0.009	0.305
0.889	23.57	0.20	0.030	0.008	0.139
1.016	24.11	0.06	0.022	0.002	0.112
1.270	24.36	0.05	0.021	0.002	0.013
1.524	24.41	0.05	0.021	0.002	0.167
2.032	24.46	0.05	0.020	0.004	0.032
2.540	24.57	0.04	0.019	0.001	0.098
3.810	24.65	0.03	0.019	0.001	0.007
5.080	24.75	0.05	0.020	0.002	-0.025
6.350	24.92	0.05	0.020	0.001	0.081
7.620	25.03	0.06	0.020	0.001	0.192
8.890	25.19	0.05	0.019	0.001	0.123
10.160	25.32	0.08	0.020	0.002	0.351
11.430	25.47	0.04	0.019	0.001	-0.050
12.700	25.58	0.07	0.020	0.001	0.082
13.970	25.68	0.06	0.019	0.001	0.010
15.240	25.85	0.04	0.020	0.002	0.226
16.510	25.95	0.02	0.019	0.001	0.113
17.780	26.11	0.04	0.019	0.002	0.013
19.050	26.25	0.07	0.019	0.001	0.117
20.320	26.39	0.05	0.019	0.002	0.170
21.590	26.53	0.03	0.019	0.002	0.220
22.860	26.67	0.04	0.019	0.001	-0.014
24.130	26.73	0.05	0.019	0.001	0.127
25.400	26.92	0.10	0.019	0.002	0.029
26.670	27.06	0.07	0.020	0.002	0.036
27.940	27.22	0.06	0.020	0.001	0.163
29.210	27.32	0.07	0.020	0.001	0.232
30.480	27.51	0.07	0.020	0.001	0.210
31.750	27.65	0.12	0.020	0.001	0.112
33.020	27.80	0.07	0.019	0.001	0.163
34.290	27.94	0.06	0.020	0.000	0.164
35.560	28.05	0.05	0.019	0.001	0.265
36.830	28.22	0.08	0.020	0.001	0.09
38.100	28.36	0.11	0.020	0.002	0.128

Table 6. Boundary Layer Measurements at 25.1% on the Pressure Surface

Y (mm)	u (m/s)	Local Turbulence Intensity			Skewness			% Backflow		
		value	deviation	value	deviation	value	deviation	value	deviation	value
0.381	5.06	0.90	0.260	0.057	0.857	0.969	6.307	6.745	0.00	0.00
0.598	8.43	0.77	0.205	0.018	0.569	0.559	3.888	3.426	0.00	0.00
0.635	12.27	1.01	0.199	0.027	0.067	0.299	3.062	1.659	0.00	0.00
0.762	16.72	0.95	0.158	0.023	-0.806	0.617	4.217	2.580	0.00	0.00
0.889	19.34	0.96	0.110	0.016	-1.384	0.864	7.017	4.403	0.00	0.00
1.016	21.48	0.55	0.081	0.021	-2.326	1.308	15.199	9.532	0.00	0.00
1.143	22.73	0.26	0.058	0.014	-3.323	2.110	25.064	18.008	0.00	0.00
1.270	23.45	0.16	0.040	0.007	-4.125	3.455	42.383	43.486	0.00	0.00
1.524	24.03	0.10	0.020	0.002	0.040	0.199	2.526	1.316	0.00	0.00
2.032	24.14	0.06	0.022	0.002	-0.107	0.546	3.663	2.868	0.00	0.00
2.540	24.19	0.05	0.021	0.002	0.253	0.565	3.362	2.491	0.00	0.00
3.810	24.26	0.05	0.019	0.001	0.136	0.223	2.492	1.332	0.00	0.00
5.080	24.37	0.04	0.020	0.002	0.034	0.240	1.547	1.324	0.00	0.00
6.350	24.48	0.04	0.020	0.001	0.140	0.198	3.135	1.640	0.00	0.00
7.620	24.68	0.07	0.020	0.002	-0.069	0.490	4.287	2.632	0.00	0.00
8.890	24.73	0.05	0.020	0.001	-0.083	0.188	3.315	0.689	0.00	0.00
10.160	24.86	0.10	0.019	0.001	0.042	0.250	3.164	0.566	0.00	0.00
11.430	24.98	0.09	0.019	0.002	0.090	0.197	3.010	0.176	0.00	0.00
12.700	25.15	0.06	0.019	0.002	0.158	0.52	3.262	0.647	0.00	0.00
13.970	25.24	0.09	0.019	0.002	0.2176	0.080	3.182	0.246	0.00	0.00
15.240	25.40	0.09	0.020	0.001	0.176	0.097	3.134	0.712	0.00	0.00
16.510	25.52	0.04	0.019	0.001	0.070	0.141	2.908	0.387	0.00	0.00
17.780	25.65	0.07	0.019	0.001	0.052	0.145	2.859	0.260	0.00	0.00
19.050	25.80	0.02	0.019	0.001	0.040	0.276	2.958	0.359	0.00	0.00
20.320	25.88	0.09	0.020	0.002	0.084	0.52	3.276	0.561	0.00	0.00
21.590	26.05	0.09	0.020	0.002	0.143	0.517	4.049	2.302	0.00	0.00
22.860	26.14	0.09	0.019	0.001	0.009	0.178	2.987	0.380	0.00	0.00
24.130	26.29	0.12	0.019	0.002	0.120	0.195	2.933	0.357	0.00	0.00
25.400	26.39	0.07	0.019	0.001	0.317	0.396	3.667	2.111	0.00	0.00
26.670	26.50	0.07	0.019	0.002	0.124	0.94	2.900	0.488	0.00	0.00
27.940	26.65	0.16	0.019	0.001	0.027	0.134	3.481	0.575	0.00	0.00
29.210	26.80	0.13	0.020	0.002	0.115	0.122	2.805	0.357	0.00	0.00
30.480	26.89	0.06	0.019	0.001	0.058	0.214	3.209	0.390	0.00	0.00
31.750	26.99	0.07	0.019	0.002	0.150	0.109	3.165	0.507	0.00	0.00
33.020	27.16	0.07	0.018	0.001	-0.027	0.088	2.841	0.333	0.00	0.00
34.290	27.32	0.09	0.020	0.004	0.023	0.255	3.305	0.861	0.00	0.00
35.560	27.44	0.09	0.020	0.004	0.164	0.259	3.340	0.542	0.00	0.00
36.830	27.57	0.07	0.020	0.001	0.042	0.107	3.047	0.474	0.00	0.00
38.100	27.74	0.07	0.020	0.002	0.102	0.205	2.930	0.331	0.00	0.00

Table 7. Boundary Layer Measurements at 35.8% Chord on the Pressure Surface

**ORIGINAL PAGE IS
OF POOR QUALITY**

Y_m (mm)	u (m/s)	Local Turbulence Intensity	Skewness	Kurtosis	% Backflow
0.254	2.28	1.43	0.683	0.159	2.557
0.381	5.65	0.82	0.462	0.071	1.664
0.508	7.92	0.67	0.441	0.040	1.227
0.635	9.77	0.91	0.431	0.043	0.657
0.762	11.91	0.85	0.405	0.029	0.233
0.889	13.65	1.05	0.381	0.027	0.011
1.016	15.88	1.07	0.342	0.031	-0.414
1.143	17.35	1.30	0.319	0.041	-0.730
1.270	19.04	0.72	0.270	0.026	-1.145
1.397	20.33	0.97	0.234	0.039	-1.662
1.524	21.32	0.41	0.195	0.019	-2.125
1.651	21.71	0.38	0.183	0.020	-2.345
1.778	22.34	0.19	0.148	0.013	-2.954
1.905	22.77	0.23	0.118	0.019	-3.761
2.032	22.93	0.22	0.107	0.020	-4.057
2.159	23.15	0.11	0.090	0.011	-4.668
2.286	23.25	0.20	0.081	0.026	-4.707
2.413	23.41	0.18	0.057	0.026	-5.202
2.540	23.61	0.06	0.026	0.003	-0.271
3.175	23.68	0.04	0.026	0.005	-0.058
3.810	23.77	0.05	0.024	0.002	0.006
5.080	23.82	0.06	0.025	0.002	0.116
6.350	23.96	0.07	0.024	0.001	0.182
7.620	24.10	0.05	0.023	0.002	0.056
8.890	24.27	0.07	0.024	0.002	0.144
10.160	24.37	0.04	0.024	0.001	0.097
11.430	24.45	0.04	0.024	0.003	-0.038
12.700	24.59	0.09	0.024	0.002	0.126
13.970	24.72	0.07	0.023	0.002	0.199
15.240	24.82	0.06	0.024	0.002	0.040
16.510	24.92	0.07	0.023	0.002	0.057
17.780	25.10	0.06	0.024	0.002	0.097
19.050	25.19	0.06	0.023	0.002	0.109
20.320	25.31	0.07	0.024	0.002	0.105
21.590	25.42	0.07	0.024	0.003	-0.114
22.860	25.51	0.08	0.024	0.001	0.137
24.130	25.66	0.03	0.023	0.002	-0.003
25.400	25.75	0.10	0.024	0.001	0.162
26.670	25.91	0.06	0.023	0.002	-0.034
27.940	26.00	0.07	0.024	0.002	0.211
29.210	26.13	0.06	0.024	0.002	0.018
30.480	26.26	0.03	0.023	0.002	0.064
31.750	26.38	0.04	0.024	0.002	0.141
33.020	26.49	0.11	0.023	0.001	-0.040
34.290	26.59	0.11	0.023	0.002	0.101
35.560	26.73	0.05	0.023	0.001	0.195
36.830	26.86	0.11	0.023	0.001	0.170
38.100	26.96	0.09	0.024	0.001	0.118

PRECEDING PAGE BLANK NOT FILMED

Table 9. Boundary Layer Measurements at 57.2% Chord on the Pressure Surface

y (mm)	u (m/s)	Local Turbulence Intensity	Skewness	Kurtosis	% Backflow
0.318	6.86	1.03	0.474	0.035	1.193
0.381	8.30	1.02	0.449	0.017	0.997
0.508	10.86	0.65	0.411	0.013	0.523
0.635	12.60	0.29	0.376	0.012	0.244
0.762	14.12	0.26	0.338	0.018	0.033
0.889	15.02	0.21	0.314	0.019	0.067
1.016	16.23	0.21	0.300	0.025	-0.021
1.143	17.30	0.34	0.282	0.026	-0.222
1.270	18.36	0.38	0.264	0.024	-0.591
1.397	19.34	0.42	0.241	0.022	-0.621
1.524	20.36	0.67	0.216	0.013	-1.214
1.651	20.98	0.58	0.196	0.017	-1.426
1.778	21.64	0.50	0.174	0.017	-1.825
1.905	22.24	0.40	0.149	0.011	-2.291
2.032	22.53	0.37	0.135	0.015	-2.591
2.159	22.97	0.34	0.109	0.018	-3.207
2.286	23.12	0.19	0.095	0.011	-3.546
2.413	23.28	0.08	0.085	0.004	-3.845
2.540	23.45	0.11	0.072	0.011	-4.146
3.175	23.81	0.07	0.032	0.009	-0.814
3.810	23.90	0.07	0.027	0.001	-0.088
5.080	24.02	0.09	0.025	0.002	0.073
6.350	24.10	0.10	0.026	0.002	0.043
7.620	24.23	0.10	0.026	0.001	0.035
8.890	24.36	0.11	0.027	0.002	-0.163
10.160	24.44	0.05	0.028	0.002	0.054
11.430	24.57	0.07	0.027	0.002	-0.049
12.700	24.68	0.04	0.025	0.002	0.046
13.970	24.79	0.04	0.025	0.002	0.049
15.240	24.91	0.05	0.026	0.001	-0.103
16.510	25.05	0.14	0.026	0.002	0.126
17.780	25.18	0.11	0.027	0.003	-0.020
19.050	25.28	0.10	0.025	0.002	0.159
20.320	25.38	0.10	0.025	0.002	-0.071
21.590	25.48	0.12	0.025	0.002	-0.089
22.860	25.60	0.13	0.026	0.002	-0.039
24.130	25.70	0.14	0.027	0.003	-0.026
25.400	25.81	0.09	0.026	0.002	-0.121
26.670	25.93	0.07	0.025	0.001	0.076
27.940	26.00	0.10	0.026	0.002	-0.097
28.210	26.15	0.13	0.026	0.002	-0.057
29.480	26.28	0.16	0.026	0.002	0.140
30.750	26.37	0.09	0.026	0.001	0.237
33.020	26.51	0.13	0.024	0.001	0.194
34.290	26.64	0.26	0.026	0.003	0.152
35.560	26.72	0.14	0.027	0.002	0.012
36.830	26.83	0.39	0.026	0.001	0.257
38.100	26.97	0.11	0.027	0.001	0.131

Table 10. Boundary Layer Measurements at 68.0% Chord on the Pressure Surface

Y (mm)	u (m/s)	Local Turbulence Intensity				Kurtosis				% Backflow			
		value	deviation	value	deviation	value	deviation	value	deviation	value	deviation	value	deviation
0.318	11.72	1.23	0.367	0.041	0.393	0.244	2.417	0.239	0.00	0.00	0.00	0.00	0.00
0.381	13.10	0.06	0.337	0.040	0.217	0.238	2.222	0.107	0.00	0.00	0.00	0.00	0.00
0.508	15.34	0.56	0.284	0.035	-0.155	0.143	2.200	0.219	0.00	0.00	0.00	0.00	0.00
0.635	16.74	0.58	0.237	0.036	-0.336	0.077	2.474	0.295	0.00	0.00	0.00	0.00	0.00
0.762	17.45	0.59	0.219	0.031	-0.433	0.116	2.729	0.502	0.00	0.00	0.00	0.00	0.00
0.889	18.32	0.56	0.197	0.032	-0.582	0.147	2.970	0.628	0.00	0.00	0.00	0.00	0.00
1.016	18.77	0.46	0.197	0.029	-0.534	0.082	2.676	0.335	0.00	0.00	0.00	0.00	0.00
1.143	19.33	0.33	0.183	0.021	-0.634	0.119	2.946	0.513	0.00	0.00	0.00	0.00	0.00
1.270	19.63	0.26	0.182	0.020	-0.701	0.101	3.171	0.817	0.00	0.00	0.00	0.00	0.00
1.397	20.24	0.47	0.173	0.022	-0.832	0.235	3.214	0.810	0.00	0.00	0.00	0.00	0.00
1.524	20.82	0.33	0.160	0.023	-0.978	0.163	3.492	0.643	0.00	0.00	0.00	0.00	0.00
1.651	21.45	0.24	0.140	0.019	-1.266	0.138	4.515	0.952	0.00	0.00	0.00	0.00	0.00
1.778	21.80	0.48	0.132	0.031	-1.362	0.312	5.140	2.167	0.00	0.00	0.00	0.00	0.00
1.905	22.33	0.41	0.116	0.028	-1.587	0.238	5.635	1.250	0.00	0.00	0.00	0.00	0.00
2.032	22.67	0.20	0.103	0.017	-1.804	0.339	6.709	1.543	0.00	0.00	0.00	0.00	0.00
2.159	22.85	0.21	0.100	0.015	-2.009	0.397	7.706	2.222	0.00	0.00	0.00	0.00	0.00
2.286	23.16	0.09	0.083	0.008	-2.147	0.318	9.004	1.865	0.00	0.00	0.00	0.00	0.00
2.413	23.34	0.15	0.077	0.005	-2.552	0.558	12.431	4.464	0.00	0.00	0.00	0.00	0.00
2.540	23.54	0.09	0.069	0.006	-2.734	0.538	13.506	3.713	0.00	0.00	0.00	0.00	0.00
3.175	23.36	0.09	0.046	0.006	-3.858	0.683	30.580	11.665	0.00	0.00	0.00	0.00	0.00
3.810	24.18	0.07	0.031	0.005	-3.319	1.586	22.588	15.089	0.00	0.00	0.00	0.00	0.00
4.445	24.29	0.07	0.027	0.004	-1.850	2.050	23.292	22.228	0.00	0.00	0.00	0.00	0.00
5.080	24.33	0.05	0.023	0.002	-1.021	0.237	3.039	0.375	0.00	0.00	0.00	0.00	0.00
6.350	24.48	0.10	0.023	0.001	-0.015	0.261	3.408	4.464	0.00	0.00	0.00	0.00	0.00
7.620	24.62	0.09	0.024	0.001	0.117	0.122	2.900	0.552	0.00	0.00	0.00	0.00	0.00
8.890	24.73	0.11	0.023	0.001	0.138	0.192	2.979	0.342	0.00	0.00	0.00	0.00	0.00
10.160	24.87	0.07	0.023	0.002	0.020	0.208	3.102	0.362	0.00	0.00	0.00	0.00	0.00
11.430	24.96	0.06	0.023	0.001	-0.35	0.211	2.947	0.325	0.00	0.00	0.00	0.00	0.00
12.700	25.08	0.13	0.023	0.001	0.095	0.176	2.903	0.229	0.00	0.00	0.00	0.00	0.00
13.970	25.19	0.10	0.023	0.002	-0.075	0.215	2.807	0.278	0.00	0.00	0.00	0.00	0.00
15.240	25.32	0.10	0.023	0.001	-0.127	0.194	3.094	0.458	0.00	0.00	0.00	0.00	0.00
16.510	25.44	0.10	0.023	0.002	0.040	0.128	3.102	0.366	0.00	0.00	0.00	0.00	0.00
17.780	25.52	0.08	0.023	0.002	0.135	0.158	3.060	0.444	0.00	0.00	0.00	0.00	0.00
19.050	25.64	0.08	0.024	0.001	-0.211	0.254	3.052	0.629	0.00	0.00	0.00	0.00	0.00
20.320	25.77	0.07	0.024	0.002	0.089	0.202	3.052	0.335	0.00	0.00	0.00	0.00	0.00
21.590	25.87	0.09	0.024	0.001	-0.037	0.245	3.211	0.805	0.00	0.00	0.00	0.00	0.00
22.860	25.98	0.08	0.024	0.001	-0.005	0.200	3.097	0.506	0.00	0.00	0.00	0.00	0.00
24.130	26.04	0.07	0.024	0.001	0.08	0.164	2.910	0.308	0.00	0.00	0.00	0.00	0.00
25.400	26.15	0.03	0.024	0.002	-0.102	0.156	3.060	0.444	0.00	0.00	0.00	0.00	0.00
26.670	26.23	0.08	0.023	0.001	0.071	0.153	2.937	0.373	0.00	0.00	0.00	0.00	0.00
27.940	26.39	0.09	0.023	0.001	0.138	0.097	2.875	0.244	0.00	0.00	0.00	0.00	0.00
29.210	26.49	0.06	0.024	0.001	0.276	0.199	2.992	0.439	0.00	0.00	0.00	0.00	0.00
30.480	26.61	0.03	0.024	0.002	-0.064	0.119	3.288	0.499	0.00	0.00	0.00	0.00	0.00
31.750	26.68	0.07	0.024	0.001	-0.042	0.211	3.305	0.497	0.00	0.00	0.00	0.00	0.00
33.020	26.78	0.05	0.024	0.002	0.029	0.183	3.301	0.474	0.00	0.00	0.00	0.00	0.00
34.290	26.92	0.03	0.024	0.002	0.046	0.261	3.138	0.351	0.00	0.00	0.00	0.00	0.00
35.560	26.98	0.04	0.025	0.002	0.014	0.217	3.029	0.324	0.00	0.00	0.00	0.00	0.00
36.830	27.07	0.06	0.024	0.001	0.048	0.190	2.813	0.362	0.00	0.00	0.00	0.00	0.00
38.100	27.20	0.07	0.024	0.001	0.050	0.312	2.938	0.244	0.00	0.00	0.00	0.00	0.00

Table 11. Boundary Layer Measurements at 78.6% Chord on the Pressure Surface

ORIGINAL PAGE IS
OF POOR QUALITY

Y (mm)	u (m/s)	Local Turbulence Intensity			Skewness			Kurtosis			% Backflow		
		value	deviation	value	value	deviation	value	value	deviation	value	value	deviation	value
0.254	12.52	1.30	0.329	0.018	0.466	0.267	2.573	0.529	0.00	0.00	0.00	0.00	0.00
0.318	14.57	1.11	0.291	0.026	0.487	0.165	2.097	0.079	0.00	0.00	0.00	0.00	0.00
0.381	16.08	0.75	0.258	0.018	-0.055	0.099	2.100	0.100	0.00	0.00	0.00	0.00	0.00
0.508	17.98	0.59	0.205	0.011	-0.274	0.112	2.309	0.066	0.00	0.00	0.00	0.00	0.00
0.635	19.29	0.40	0.175	0.011	-0.464	0.108	2.651	0.153	0.00	0.00	0.00	0.00	0.00
0.762	20.18	0.35	0.153	0.013	-0.563	0.094	2.937	0.293	0.00	0.00	0.00	0.00	0.00
0.889	20.86	0.18	0.138	0.009	-0.660	0.112	3.250	0.417	0.00	0.00	0.00	0.00	0.00
1.016	21.36	0.26	0.124	0.010	-0.708	0.210	3.526	0.997	0.00	0.00	0.00	0.00	0.00
1.143	21.85	0.21	0.114	0.009	-0.612	0.125	3.037	0.266	0.00	0.00	0.00	0.00	0.00
1.270	22.15	0.26	0.110	0.008	-0.729	0.216	3.386	0.605	0.00	0.00	0.00	0.00	0.00
1.397	22.45	0.30	0.103	0.006	-0.748	0.208	3.577	0.461	0.00	0.00	0.00	0.00	0.00
1.524	22.61	0.27	0.103	0.011	-0.909	0.141	4.106	0.625	0.00	0.00	0.00	0.00	0.00
1.651	23.00	0.30	0.093	0.007	-1.052	0.301	4.789	1.397	0.00	0.00	0.00	0.00	0.00
1.778	23.26	0.30	0.087	0.010	-0.868	0.158	3.580	0.948	0.00	0.00	0.00	0.00	0.00
1.905	23.55	0.22	0.085	0.008	-1.172	0.263	4.779	0.948	0.00	0.00	0.00	0.00	0.00
2.032	23.72	0.18	0.069	0.006	-1.095	0.105	4.292	0.363	0.00	0.00	0.00	0.00	0.00
2.159	23.93	0.22	0.076	0.006	-1.371	0.160	5.767	0.995	0.00	0.00	0.00	0.00	0.00
2.286	24.13	0.24	0.071	0.008	-1.396	0.323	5.802	1.924	0.00	0.00	0.00	0.00	0.00
2.413	24.32	0.17	0.066	0.006	-1.612	0.376	7.187	1.597	0.00	0.00	0.00	0.00	0.00
2.540	24.49	0.18	0.064	0.006	-1.726	0.300	8.069	2.606	0.00	0.00	0.00	0.00	0.00
3.175	25.04	0.67	0.044	0.004	-2.130	0.463	12.512	4.591	0.00	0.00	0.00	0.00	0.00
3.810	25.37	0.37	0.031	0.002	-1.493	0.887	12.936	9.413	0.00	0.00	0.00	0.00	0.00
4.445	25.45	0.45	0.032	0.001	-0.337	0.318	3.881	3.935	0.00	0.00	0.00	0.00	0.00
5.080	25.58	0.58	0.025	0.002	-0.673	0.350	3.051	3.198	0.00	0.00	0.00	0.00	0.00
6.350	25.65	0.65	0.024	0.002	-0.108	0.092	2.835	3.368	0.00	0.00	0.00	0.00	0.00
7.620	25.81	0.51	0.025	0.002	-0.089	0.307	3.350	3.472	0.00	0.00	0.00	0.00	0.00
8.890	25.94	0.47	0.023	0.001	0.104	0.230	3.376	3.378	0.00	0.00	0.00	0.00	0.00
10.160	26.00	0.36	0.025	0.001	-0.078	0.287	3.055	6.620	0.00	0.00	0.00	0.00	0.00
11.430	26.12	0.42	0.024	0.002	0.110	0.273	3.223	3.223	0.00	0.00	0.00	0.00	0.00
12.700	26.24	0.33	0.022	0.001	-0.011	0.146	2.988	2.39	0.00	0.00	0.00	0.00	0.00
13.970	26.32	0.32	0.023	0.003	-0.097	0.248	3.170	1.001	0.00	0.00	0.00	0.00	0.00
15.240	26.42	0.21	0.024	0.002	-0.008	0.121	2.865	1.96	0.00	0.00	0.00	0.00	0.00
16.510	26.47	0.23	0.023	0.002	0.025	0.164	2.987	2.987	0.00	0.00	0.00	0.00	0.00
17.780	26.54	0.22	0.020	0.001	-0.005	0.299	3.227	3.227	0.00	0.00	0.00	0.00	0.00
19.050	26.63	0.21	0.022	0.001	-0.158	0.253	3.297	5.521	0.00	0.00	0.00	0.00	0.00
20.320	26.65	0.19	0.020	0.002	-0.089	0.101	3.237	3.459	0.00	0.00	0.00	0.00	0.00
21.590	26.72	0.19	0.020	0.002	-0.039	0.158	3.178	3.178	0.00	0.00	0.00	0.00	0.00
22.860	26.77	0.14	0.024	0.002	0.008	0.327	3.284	3.284	0.00	0.00	0.00	0.00	0.00
24.130	26.91	0.12	0.020	0.003	-0.024	0.248	3.056	6.263	0.00	0.00	0.00	0.00	0.00
25.400	26.96	0.12	0.020	0.004	-0.095	0.187	3.106	3.106	0.00	0.00	0.00	0.00	0.00
26.670	27.05	0.05	0.020	0.002	-0.167	0.237	3.153	3.153	0.00	0.00	0.00	0.00	0.00
27.940	27.12	0.12	0.020	0.003	-0.248	0.171	3.441	3.441	0.00	0.00	0.00	0.00	0.00
29.210	27.20	0.12	0.020	0.002	-0.002	0.124	2.848	2.848	0.00	0.00	0.00	0.00	0.00
30.480	27.25	0.12	0.020	0.002	-0.028	0.302	3.252	3.252	0.00	0.00	0.00	0.00	0.00
31.750	27.29	0.12	0.020	0.001	-0.013	0.143	3.291	3.291	0.00	0.00	0.00	0.00	0.00
33.020	27.45	0.12	0.020	0.002	-0.191	0.253	3.451	3.451	0.00	0.00	0.00	0.00	0.00
34.290	27.48	0.12	0.020	0.002	-0.286	0.267	3.235	3.235	0.00	0.00	0.00	0.00	0.00
35.560	27.56	0.12	0.020	0.002	-0.123	0.216	3.291	3.291	0.00	0.00	0.00	0.00	0.00
36.830	27.58	0.12	0.020	0.002	-0.078	0.187	3.173	3.173	0.00	0.00	0.00	0.00	0.00
38.100	27.60	0.12	0.020	0.002	-0.032	0.282	3.295	3.295	0.00	0.00	0.00	0.00	0.00

Table 12. Boundary Layer Measurements at 89.3% Chord on the Pressure Surface

**ORIGINAL PAGE IS
OF POOR QUALITY**

Y (mm)	U (m/s)	Local Turbulence Intensity	Skewness	Kurtosis	% Backflow
0.064	17.76	2.00	0.234	0.036	0.110
0.127	19.57	1.10	0.201	0.025	-0.144
0.254	21.75	0.64	0.155	0.013	-0.488
0.318	22.38	0.66	0.141	0.014	-0.603
0.381	22.73	0.65	0.132	0.016	-0.621
0.508	23.47	0.67	0.118	0.016	-0.815
0.635	23.96	0.44	0.108	0.013	-0.828
0.762	24.42	0.53	0.103	0.014	-0.986
0.889	24.91	0.35	0.093	0.010	-0.952
1.016	25.22	0.38	0.087	0.008	-0.961
1.143	25.45	0.25	0.084	0.008	-1.022
1.270	25.57	0.39	0.086	0.012	-1.382
1.397	26.04	0.23	0.076	0.011	-1.264
1.524	26.30	0.33	0.072	0.012	-1.275
1.651	26.45	0.23	0.072	0.011	-1.533
1.778	26.70	0.28	0.067	0.014	-1.456
1.905	26.79	0.24	0.067	0.014	-1.602
2.032	26.96	0.19	0.063	0.008	-1.676
2.159	27.15	0.22	0.059	0.007	-1.834
2.286	27.30	0.22	0.055	0.010	-1.704
2.413	27.46	0.18	0.054	0.010	-2.023
2.540	27.58	0.15	0.050	0.008	-1.935
3.175	27.99	0.15	0.038	0.007	-2.076
3.810	28.25	0.15	0.027	0.001	-0.244
5.080	28.27	0.18	0.022	0.002	-0.116
6.350	28.24	0.15	0.023	0.002	-0.008
7.620	28.18	0.10	0.023	0.001	-0.093
8.890	28.18	0.16	0.024	0.001	-0.119
10.160	28.15	0.14	0.024	0.001	0.217
11.430	28.14	0.14	0.023	0.002	0.028
12.700	28.16	0.15	0.023	0.001	0.095
13.970	28.15	0.14	0.023	0.001	0.004
15.240	28.13	0.13	0.023	0.001	0.021
16.510	28.08	0.17	0.023	0.002	0.086
17.780	28.10	0.19	0.023	0.001	-0.007
19.050	28.10	0.16	0.024	0.002	-0.104
20.320	28.08	0.16	0.024	0.002	-0.008
22.590	28.07	0.13	0.023	0.002	-0.160
22.860	28.03	0.12	0.024	0.003	0.138
24.130	28.07	0.15	0.024	0.001	-0.009
25.400	28.05	0.17	0.024	0.001	-0.122
26.670	28.04	0.12	0.025	0.002	0.075
27.940	28.06	0.13	0.024	0.002	-0.111
29.210	28.06	0.14	0.026	0.003	-0.005
30.480	28.05	0.14	0.025	0.002	0.050
31.750	28.15	0.19	0.024	0.001	0.062
33.020	28.15	0.20	0.025	0.000	-0.025
34.290	28.14	0.21	0.025	0.002	0.046
35.560	28.17	0.19	0.024	0.002	0.012
36.830	28.22	0.24	0.025	0.002	0.074
38.100	28.21	0.26	0.027	0.002	-0.028

Table 13. Boundary Layer Measurements at 97.9% Chord on the Pressure Surface

ORIGINAL PAGE IS
OF POOR QUALITY

Y (mm)	u (m/s)	Local Turbulence Intensity		Skewness		Kurtosis		% Backflow	
		value	deviation	value	deviation	value	deviation	value	deviation
0.254	20.46	0.54	0.240	0.012	---	---	---	---	---
0.391	21.60	0.75	0.259	0.016	---	---	---	---	---
0.508	23.53	1.26	0.276	0.015	---	---	---	---	---
0.635	26.05	0.89	0.278	0.017	---	---	---	---	---
0.762	27.96	1.10	0.271	0.016	---	---	---	---	---
0.889	30.35	1.41	0.269	0.014	---	---	---	---	---
1.016	33.88	1.36	0.248	0.008	---	---	---	---	---
1.143	36.63	1.47	0.239	0.013	---	---	---	---	---
1.270	39.21	0.91	0.223	0.011	---	---	---	---	---
1.397	41.61	1.08	0.202	0.013	---	---	---	---	---
1.524	44.68	1.03	0.173	0.013	---	---	---	---	---
1.651	46.94	1.11	0.141	0.019	---	---	---	---	---
1.778	48.77	1.01	0.113	0.022	---	---	---	---	---
2.032	50.83	0.54	0.079	0.020	---	---	---	---	---
2.286	51.84	0.24	0.059	0.008	---	---	---	---	---
2.540	52.01	0.14	0.052	0.006	---	---	---	---	---
3.175	51.35	0.22	0.046	0.009	---	---	---	---	---
3.810	50.65	0.22	0.034	0.002	---	---	---	---	---
4.445	49.78	0.19	0.031	0.002	---	---	---	---	---
5.080	48.96	0.17	0.032	0.005	---	---	---	---	---
5.715	48.49	0.21	0.029	0.003	---	---	---	---	---
6.350	47.95	0.19	0.027	0.002	---	---	---	---	---
7.620	46.86	0.14	0.026	0.003	---	---	---	---	---
8.890	46.11	0.19	0.025	0.003	---	---	---	---	---
10.160	45.37	0.19	0.025	0.004	---	---	---	---	---
11.430	44.76	0.19	0.025	0.002	---	---	---	---	---
12.700	44.25	0.15	0.024	0.001	---	---	---	---	---
13.970	43.78	0.12	0.023	0.002	---	---	---	---	---
15.240	43.33	0.17	0.023	0.002	---	---	---	---	---

Table 14. Boundary Layer Measurements at 2.6% on the Suction Surface

**ORIGINAL PAGE IS
OF POOR QUALITY**

y (mm)	u (m/s)	Local Turbulence Intensity		Skewness		Kurtosis		% Backflow	
		value	deviation	value	deviation	value	deviation	value	deviation
0.127	24.48	1.20	0.238	0.020	---	---	---	---	---
0.191	25.67	0.57	0.230	0.011	---	---	---	---	---
0.254	26.33	0.43	0.228	0.007	---	---	---	---	---
0.381	27.43	0.22	0.224	0.012	---	---	---	---	---
0.508	28.19	0.38	0.225	0.012	---	---	---	---	---
0.635	29.52	0.33	0.221	0.007	---	---	---	---	---
0.762	30.59	0.30	0.215	0.008	---	---	---	---	---
0.889	31.81	0.52	0.211	0.005	---	---	---	---	---
1.016	32.87	0.45	0.208	0.005	---	---	---	---	---
1.143	34.25	0.39	0.201	0.004	---	---	---	---	---
1.270	35.27	0.46	0.197	0.006	---	---	---	---	---
1.397	36.61	0.56	0.185	0.004	---	---	---	---	---
1.524	37.81	0.31	0.172	0.005	---	---	---	---	---
1.651	38.81	0.48	0.161	0.007	---	---	---	---	---
1.778	40.09	0.45	0.143	0.011	---	---	---	---	---
1.905	40.87	0.40	0.135	0.008	---	---	---	---	---
2.032	41.54	0.32	0.125	0.007	---	---	---	---	---
2.159	42.45	0.17	0.106	0.009	---	---	---	---	---
2.286	42.94	0.19	0.093	0.011	---	---	---	---	---
2.413	43.47	0.37	0.083	0.013	---	---	---	---	---
2.540	43.87	0.28	0.075	0.018	---	---	---	---	---
3.175	44.81	0.29	0.046	0.006	---	---	---	---	---
3.810	45.03	0.30	0.033	0.006	---	---	---	---	---
4.445	44.92	0.17	0.031	0.005	---	---	---	---	---
5.080	44.86	0.26	0.029	0.009	---	---	---	---	---
5.715	44.76	0.25	0.030	0.012	---	---	---	---	---
6.350	44.72	0.18	0.026	0.003	---	---	---	---	---
7.620	44.46	0.24	0.025	0.004	---	---	---	---	---
8.890	44.28	0.30	0.024	0.003	---	---	---	---	---
10.160	44.02	0.25	0.023	0.002	---	---	---	---	---
11.430	43.81	0.24	0.024	0.002	---	---	---	---	---
12.700	43.58	0.30	0.024	0.004	---	---	---	---	---
13.970	43.25	0.27	0.023	0.002	---	---	---	---	---
15.240	43.00	0.31	0.024	0.002	---	---	---	---	---
16.510	42.78	0.27	0.023	0.001	---	---	---	---	---
17.780	42.57	0.30	0.023	0.003	---	---	---	---	---
19.050	42.31	0.26	0.022	0.002	---	---	---	---	---
20.320	42.12	0.20	0.024	0.003	---	---	---	---	---
21.590	41.87	0.23	0.024	0.003	---	---	---	---	---
22.860	41.63	0.24	0.024	0.003	---	---	---	---	---

Table 15. Boundary Layer Measurements at 7.6% Chord on the Suction Surface

Y (mm)	u (m/s)	Local Turbulence Intensity	Skewness	Kurtosis	% Backflow
0.102	21.67	1.69	0.261	0.023	---
0.152	24.43	0.99	0.225	0.016	---
0.203	25.78	0.70	0.209	0.006	---
0.254	27.02	0.40	0.191	0.007	---
0.318	27.87	0.35	0.184	0.005	---
0.381	28.63	0.42	0.176	0.004	---
0.508	29.79	0.20	0.171	0.006	---
0.635	30.67	0.37	0.168	0.005	---
0.762	31.34	0.33	0.165	0.003	---
0.889	32.00	0.39	0.165	0.003	---
1.016	32.56	0.37	0.161	0.005	---
1.143	33.42	0.37	0.159	0.006	---
1.270	34.07	0.32	0.156	0.003	---
1.397	34.62	0.13	0.156	0.004	---
1.524	35.14	0.28	0.155	0.004	---
1.651	35.83	0.41	0.150	0.003	---
1.778	36.30	0.26	0.150	0.002	---
1.905	37.26	0.35	0.141	0.004	---
2.032	37.70	0.41	0.138	0.006	---
2.286	39.06	0.19	0.125	0.004	---
2.540	40.10	0.33	0.113	0.006	---
2.794	41.29	0.28	0.092	0.009	---
3.048	41.87	0.21	0.087	0.005	---
3.302	42.69	0.13	0.064	0.010	---
3.556	43.02	0.22	0.053	0.011	---
3.810	43.25	0.14	0.045	0.010	---
4.445	43.62	0.11	0.030	0.005	---
5.080	43.55	0.13	0.024	0.002	---
5.715	43.52	0.08	0.022	0.003	---
6.350	43.39	0.07	0.021	0.001	---
7.620	43.14	0.07	0.020	0.002	---
8.890	42.95	0.07	0.020	0.001	---
10.160	42.70	0.10	0.019	0.001	---
11.430	42.50	0.06	0.019	0.001	---
12.700	42.34	0.07	0.019	0.002	---
13.970	42.10	0.14	0.019	0.002	---
15.240	41.87	0.05	0.021	0.002	---
16.510	41.67	0.14	0.019	0.002	---
17.780	41.55	0.08	0.021	0.001	---
19.050	41.30	0.08	0.019	0.002	---
20.320	41.11	0.09	0.019	0.002	---
21.590	40.93	0.12	0.019	0.002	---
22.860	40.79	0.13	0.018	0.003	---
24.130	40.64	0.09	0.019	0.001	---
25.400	40.48	0.12	0.020	0.002	---
26.670	40.28	0.07	0.019	0.002	---
27.940	40.15	0.10	0.019	0.001	---
29.210	40.01	0.10	0.019	0.002	---
30.480	39.88	0.09	0.019	0.002	---
31.750	39.76	0.06	0.019	0.002	---
33.020	39.63	0.12	0.019	0.002	---
34.290	39.50	0.05	0.020	0.001	---

Table 16. Boundary Layer Measurements at 12.7% Chord on the Suction Surface

ORIGINAL PAGE IS
OF POOR QUALITY

Y (mm)	u (m/s)	Local Turbulence Intensity	Skewness	Kurtosis	% Backflow
0.127	20.00	0.59	0.271	0.013	
0.191	21.76	0.39	0.239	0.006	
0.254	23.59	0.23	0.195	0.005	
0.318	24.46	0.19	0.179	0.007	
0.381	25.41	0.10	0.169	0.003	
0.508	26.47	0.31	0.155	0.005	
0.635	27.25	0.22	0.150	0.003	
0.762	27.92	0.10	0.145	0.004	
0.889	28.62	0.27	0.143	0.004	
1.016	29.24	0.16	0.139	0.006	
1.143	29.68	0.26	0.139	0.004	
1.270	30.30	0.30	0.134	0.003	
1.524	31.28	0.27	0.130	0.004	
1.778	32.28	0.32	0.128	0.003	
2.032	33.00	0.21	0.124	0.003	
2.286	33.92	0.10	0.120	0.004	
2.540	34.97	0.30	0.113	0.004	
2.794	35.75	0.16	0.109	0.002	
3.048	36.40	0.23	0.105	0.004	
3.302	37.21	0.23	0.098	0.005	
3.556	37.92	0.16	0.090	0.005	
3.810	38.59	0.32	0.080	0.008	
4.445	39.83	0.10	0.054	0.005	
5.080	40.25	0.13	0.043	0.011	
5.715	40.52	0.14	0.031	0.006	
6.350	40.55	0.18	0.026	0.002	
7.620	40.40	0.13	0.023	0.002	
8.890	40.14	0.06	0.022	0.002	
10.160	39.97	0.17	0.022	0.001	
11.430	39.80	0.20	0.023	0.003	
12.700	39.51	0.11	0.022	0.001	
13.970	39.20	0.12	0.021	0.002	
15.240	39.01	0.09	0.021	0.002	
16.510	38.84	0.13	0.021	0.002	
17.780	38.63	0.13	0.021	0.003	
19.050	38.40	0.12	0.021	0.003	
20.320	38.20	0.08	0.020	0.001	
21.590	38.04	0.11	0.021	0.001	
22.860	37.83	0.06	0.020	0.002	
24.130	37.60	0.35	0.020	0.001	
25.400	37.43	0.12	0.020	0.001	
26.670	37.27	0.03	0.021	0.003	
27.940	37.03	0.07	0.020	0.002	
29.210	36.88	0.07	0.021	0.002	
30.480	36.66	0.08	0.020	0.002	
31.750	36.50	0.06	0.020	0.002	
33.020	36.33	0.11	0.020	0.001	
34.290	36.12	0.11	0.020	0.002	
35.560	35.95	0.07	0.020	0.002	
36.830	35.79	0.08	0.020	0.001	
38.100	35.64	0.07	0.019	0.001	

Table 17. Boundary Layer Measurements at 23.0% Chord on the Suction Surface

y (mm)	u (m/s)	Local Turbulence Intensity	Skewness	Kurtosis	% Backflow
0.127	14.58	0.33	0.281	0.009	---
0.254	17.07	0.38	0.233	0.010	---
0.381	18.48	0.33	0.211	0.004	---
0.508	19.48	0.20	0.197	0.005	---
0.635	20.28	0.20	0.187	0.006	---
0.762	21.06	0.22	0.183	0.005	---
1.016	22.23	0.37	0.176	0.004	---
1.270	23.32	0.31	0.170	0.004	---
1.524	24.35	0.28	0.158	0.004	---
1.778	25.35	0.37	0.152	0.004	---
2.032	26.25	0.28	0.143	0.003	---
2.286	27.01	0.36	0.136	0.004	---
2.540	27.75	0.30	0.128	0.004	---
2.794	28.47	0.23	0.123	0.004	---
3.048	28.94	0.21	0.116	0.003	---
3.302	29.57	0.16	0.109	0.003	---
3.556	30.17	0.24	0.103	0.002	---
3.810	30.45	0.21	0.101	0.002	---
4.064	31.01	0.20	0.098	0.003	---
4.318	31.40	0.20	0.095	0.003	---
4.572	31.76	0.31	0.095	0.003	---
4.826	32.21	0.34	0.093	0.003	---
5.080	32.56	0.29	0.091	0.004	---
5.334	32.85	0.41	0.090	0.003	---
5.842	33.74	0.39	0.086	0.003	---
6.350	34.61	0.36	0.078	0.004	---
7.620	36.01	0.13	0.048	0.004	---
8.890	36.41	0.15	0.024	0.005	---
10.160	36.33	0.19	0.020	0.003	---
11.430	36.14	0.11	0.018	0.002	---
12.700	35.93	0.08	0.018	0.001	---
13.970	35.72	0.12	0.017	0.001	---
15.240	35.52	0.10	0.017	0.001	---
16.510	35.31	0.15	0.017	0.001	---
17.780	35.13	0.14	0.017	0.001	---
19.050	34.96	0.12	0.016	0.001	---
20.320	34.77	0.12	0.017	0.001	---
21.590	34.55	0.10	0.017	0.002	---
22.860	34.41	0.06	0.017	0.002	---
24.130	34.19	0.07	0.017	0.002	---
25.400	33.99	0.08	0.016	0.001	---
26.670	33.76	0.06	0.017	0.001	---
27.940	33.60	0.06	0.018	0.001	---
29.210	33.42	0.08	0.017	0.001	---
30.480	33.20	0.08	0.017	0.001	---
31.750	33.03	0.06	0.018	0.002	---
33.020	32.84	0.07	0.017	0.002	---
34.290	32.63	0.06	0.018	0.001	---
35.560	32.43	0.07	0.017	0.002	---
36.830	32.24	0.06	0.017	0.001	---
38.100	32.03	0.09	0.018	0.001	---

Table 18. Boundary Layer Measurements at 33.2% Chord on the Suction Surface

ORIGINAL PAGE IS
OF POOR QUALITY

Y (m)	u (m/s)	Local Turbulence Intensity		Skewness		Kurtosis		% Backflow	
		value	deviation	value	deviation	value	deviation	value	deviation
0.127	10.63	0.61	0.346	0.020	0.015	0.006	0.002	0.004	0.004
0.254	12.87	0.31	0.277	0.015	0.011	0.005	0.002	0.003	0.003
0.381	14.23	0.35	0.241	0.011	0.005	0.003	0.002	0.002	0.002
0.508	14.95	0.22	0.225	0.011	0.005	0.003	0.002	0.002	0.002
0.635	15.60	0.21	0.213	0.005	0.005	0.003	0.002	0.002	0.002
0.762	16.15	0.23	0.203	0.006	0.006	0.003	0.002	0.002	0.002
1.016	17.12	0.20	0.193	0.008	0.008	0.004	0.003	0.003	0.003
1.270	18.07	0.24	0.191	0.008	0.008	0.004	0.003	0.003	0.003
1.524	18.80	0.32	0.186	0.003	0.003	0.002	0.001	0.001	0.001
1.778	19.65	0.32	0.180	0.005	0.005	0.003	0.002	0.002	0.002
2.032	20.39	0.32	0.173	0.004	0.004	0.002	0.001	0.001	0.001
2.286	21.30	0.28	0.170	0.004	0.004	0.002	0.001	0.001	0.001
2.540	22.04	0.33	0.166	0.005	0.005	0.003	0.002	0.002	0.002
2.794	22.86	0.42	0.157	0.003	0.003	0.002	0.001	0.001	0.001
3.048	23.60	0.32	0.158	0.005	0.005	0.003	0.002	0.002	0.002
3.302	24.50	0.35	0.148	0.005	0.005	0.003	0.002	0.002	0.002
3.556	25.23	0.60	0.141	0.008	0.008	0.005	0.003	0.003	0.003
3.810	26.05	0.36	0.135	0.003	0.003	0.002	0.001	0.001	0.001
4.064	26.75	0.27	0.129	0.003	0.003	0.002	0.001	0.001	0.001
4.318	27.35	0.30	0.125	0.005	0.005	0.003	0.002	0.002	0.002
4.572	28.02	0.32	0.118	0.006	0.006	0.004	0.002	0.002	0.002
4.826	28.57	0.27	0.114	0.002	0.002	0.001	0.001	0.001	0.001
5.080	29.16	0.26	0.107	0.005	0.005	0.003	0.002	0.002	0.002
5.334	29.65	0.28	0.102	0.006	0.006	0.004	0.003	0.003	0.003
5.842	30.46	0.28	0.093	0.004	0.004	0.003	0.002	0.002	0.002
6.350	31.25	0.24	0.084	0.004	0.004	0.003	0.002	0.002	0.002
6.985	32.05	0.32	0.075	0.005	0.005	0.003	0.002	0.002	0.002
7.620	32.70	0.14	0.065	0.003	0.003	0.002	0.001	0.001	0.001
8.255	33.27	0.12	0.052	0.005	0.005	0.003	0.002	0.002	0.002
8.890	33.76	0.19	0.039	0.004	0.004	0.003	0.002	0.002	0.002
9.525	33.97	0.08	0.031	0.003	0.003	0.002	0.001	0.001	0.001
10.160	34.04	0.13	0.024	0.003	0.003	0.002	0.001	0.001	0.001
11.430	34.01	0.17	0.075	0.005	0.005	0.003	0.002	0.002	0.002
12.700	33.85	0.12	0.065	0.003	0.003	0.002	0.001	0.001	0.001
13.970	33.67	0.15	0.018	0.001	0.001	0.001	0.000	0.000	0.000
15.240	33.50	0.20	0.019	0.002	0.002	0.001	0.001	0.001	0.001
16.510	33.34	0.21	0.019	0.003	0.003	0.002	0.001	0.001	0.001
17.780	33.23	0.24	0.018	0.003	0.003	0.002	0.001	0.001	0.001
19.050	33.02	0.20	0.018	0.002	0.002	0.001	0.001	0.001	0.001
20.320	32.82	0.26	0.018	0.002	0.002	0.001	0.001	0.001	0.001
21.590	32.69	0.22	0.019	0.003	0.003	0.002	0.002	0.002	0.002
22.860	32.54	0.17	0.019	0.002	0.002	0.001	0.001	0.001	0.001
24.130	32.36	0.17	0.019	0.002	0.002	0.001	0.001	0.001	0.001
25.400	32.17	0.16	0.019	0.002	0.002	0.001	0.001	0.001	0.001
26.670	32.08	0.23	0.019	0.001	0.001	0.001	0.001	0.001	0.001
27.940	31.88	0.26	0.019	0.003	0.003	0.002	0.002	0.002	0.002
29.210	31.68	0.20	0.018	0.002	0.002	0.001	0.001	0.001	0.001
30.480	31.55	0.21	0.019	0.003	0.003	0.002	0.002	0.002	0.002
31.750	31.38	0.27	0.019	0.004	0.004	0.003	0.002	0.002	0.002
33.020	31.21	0.20	0.019	0.002	0.002	0.001	0.001	0.001	0.001
34.290	31.04	0.23	0.019	0.002	0.002	0.001	0.001	0.001	0.001
35.560	30.88	0.21	0.020	0.002	0.002	0.001	0.001	0.001	0.001

Table 19. Boundary Layer Measurements at 43.3% Chord on the Suction Surface

Table 19. (Continued)

36.830	30.71	0.21	0.019	0.003	---	---	---
38.100	30.52	0.21	0.019	0.003	---	---	---

**ORIGINAL PAGE IS
OF POOR QUALITY**

y (mm)	u (m/s)	Local Turbulence Intensity		Skewness		Kurtosis		% Backflow	
		value	deviation	value	deviation	value	deviation	value	deviation
0.381	9.68	0.24	0.308	0.020	-----	-----	-----	-----	-----
0.508	10.24	0.29	0.295	0.010	-----	-----	-----	-----	-----
0.635	10.75	0.25	0.280	0.014	-----	-----	-----	-----	-----
0.762	11.17	0.40	0.277	0.009	-----	-----	-----	-----	-----
1.016	12.06	0.31	0.256	0.010	-----	-----	-----	-----	-----
1.270	12.75	0.40	0.250	0.008	-----	-----	-----	-----	-----
1.524	13.39	0.40	0.241	0.008	-----	-----	-----	-----	-----
1.778	13.91	0.28	0.233	0.012	-----	-----	-----	-----	-----
2.032	14.72	0.37	0.225	0.010	-----	-----	-----	-----	-----
2.286	15.26	0.37	0.213	0.006	-----	-----	-----	-----	-----
2.540	15.94	0.31	0.208	0.006	-----	-----	-----	-----	-----
2.794	16.57	0.40	0.207	0.010	-----	-----	-----	-----	-----
3.048	17.33	0.32	0.198	0.008	-----	-----	-----	-----	-----
3.302	17.88	0.39	0.188	0.007	-----	-----	-----	-----	-----
3.556	18.64	0.38	0.188	0.008	-----	-----	-----	-----	-----
3.810	19.23	0.27	0.183	0.009	-----	-----	-----	-----	-----
4.064	19.97	0.32	0.181	0.007	-----	-----	-----	-----	-----
4.318	20.70	0.22	0.169	0.010	-----	-----	-----	-----	-----
4.572	21.36	0.26	0.166	0.006	-----	-----	-----	-----	-----
4.826	22.04	0.27	0.164	0.008	-----	-----	-----	-----	-----
5.080	22.65	0.31	0.160	0.008	-----	-----	-----	-----	-----
5.334	23.22	0.34	0.155	0.005	-----	-----	-----	-----	-----
5.842	24.50	0.29	0.145	0.004	-----	-----	-----	-----	-----
6.350	25.83	0.22	0.134	0.003	-----	-----	-----	-----	-----
6.985	27.18	0.23	0.121	0.005	-----	-----	-----	-----	-----
7.620	28.44	0.24	0.107	0.004	-----	-----	-----	-----	-----
8.255	29.52	0.29	0.094	0.003	-----	-----	-----	-----	-----
8.890	30.44	0.11	0.079	0.003	-----	-----	-----	-----	-----
10.160	31.78	0.13	0.048	0.008	-----	-----	-----	-----	-----
11.430	32.18	0.18	0.032	0.002	-----	-----	-----	-----	-----
12.700	32.29	0.97	0.026	0.004	-----	-----	-----	-----	-----
13.970	32.21	0.67	0.022	0.003	-----	-----	-----	-----	-----
15.240	32.09	0.97	0.019	0.001	-----	-----	-----	-----	-----
16.510	31.95	0.22	0.018	0.001	-----	-----	-----	-----	-----
17.780	31.79	0.35	0.018	0.001	-----	-----	-----	-----	-----
19.050	31.68	0.33	0.019	0.002	-----	-----	-----	-----	-----
20.320	31.54	0.19	0.019	0.002	-----	-----	-----	-----	-----
21.590	31.44	0.33	0.013	0.002	-----	-----	-----	-----	-----
22.860	31.28	0.42	0.018	0.002	-----	-----	-----	-----	-----
24.130	31.13	0.41	0.018	0.001	-----	-----	-----	-----	-----
25.400	30.98	0.13	0.016	0.001	-----	-----	-----	-----	-----
26.670	30.83	0.18	0.017	0.001	-----	-----	-----	-----	-----
27.940	30.72	0.11	0.017	0.001	-----	-----	-----	-----	-----
29.210	30.58	0.16	0.018	0.001	-----	-----	-----	-----	-----
30.480	30.41	0.13	0.013	0.001	-----	-----	-----	-----	-----
31.750	30.27	0.13	0.017	0.002	-----	-----	-----	-----	-----
33.020	30.15	0.13	0.017	0.001	-----	-----	-----	-----	-----
34.290	29.98	0.19	0.018	0.002	-----	-----	-----	-----	-----
35.560	29.84	0.12	0.017	0.001	-----	-----	-----	-----	-----
36.830	29.73	0.11	0.017	0.001	-----	-----	-----	-----	-----
38.100	29.56	0.11	0.017	0.001	-----	-----	-----	-----	-----

Table 20. Boundary Layer Measurements at 53.6% Chord on the Suction Surface

**ORIGINAL PAGE IS
OF POOR QUALITY**

Y (mm)	u (m/s)	Local Turbulence Intensity	Kurtosis	% Backflow
0.254	3.38	0.23	0.704	0.030
0.508	4.53	0.24	0.579	0.024
0.762	5.13	0.24	0.548	0.035
1.016	5.75	0.31	0.495	0.037
1.270	6.29	0.32	0.466	0.031
1.524	6.71	0.27	0.453	0.024
1.778	7.29	0.36	0.417	0.017
2.032	7.70	0.35	0.406	0.011
2.286	8.35	0.35	0.395	0.022
2.540	8.91	0.26	0.378	0.017
2.794	9.11	0.48	0.377	0.018
3.048	9.88	0.35	0.353	0.018
3.302	10.50	0.41	0.345	0.021
3.556	10.93	0.60	0.335	0.027
3.810	11.55	0.51	0.322	0.023
4.064	12.12	0.41	0.312	0.011
4.318	12.78	0.45	0.298	0.016
4.572	13.11	0.41	0.297	0.019
4.826	13.89	0.40	0.286	0.015
5.080	14.42	0.40	0.278	0.012
5.334	14.95	0.44	0.273	0.015
5.842	16.21	0.47	0.254	0.012
6.350	17.30	0.57	0.247	0.020
6.985	19.16	0.51	0.219	0.026
7.620	20.89	0.30	0.191	0.012
8.255	22.34	0.44	0.178	0.020
8.890	23.70	0.34	0.156	0.008
9.525	24.94	0.38	0.146	0.008
10.160	26.25	0.24	0.122	0.006
10.795	27.12	0.33	0.117	0.009
11.430	28.05	0.06	0.101	0.004
12.065	28.77	0.18	0.085	0.005
12.700	29.31	0.13	0.073	0.004
13.335	29.68	0.13	0.057	0.005
13.970	29.87	0.16	0.046	0.006
15.240	30.06	0.05	0.030	0.007
16.510	30.07	0.09	0.023	0.005
17.780	29.91	0.03	0.013	0.003
19.050	29.32	0.04	0.018	0.001
20.320	29.74	0.12	0.018	0.001
21.590	29.58	0.05	0.018	0.001
22.860	29.41	0.11	0.018	0.001
24.130	29.33	0.33	0.013	0.001
25.400	29.18	0.11	0.018	0.002
26.670	29.08	0.04	0.017	0.001
27.940	28.99	0.33	0.017	0.001
29.210	28.83	0.08	0.017	0.001
30.480	28.73	0.24	0.017	0.002
31.750	28.59	0.27	0.017	0.002
33.020	28.45	0.39	0.017	0.002
34.290	28.35	0.04	0.018	0.002
35.560	28.21	0.39	0.017	0.002

Table 21. Boundary Layer Measurements at 63.2% Chord on the Suction Surface

Table 21. (Continued)

36.830	28.07	0.07	0.018	0.003	0.015	0.267	3.409	0.382	0.00
38.100	27.90	0.11	0.018	0.001	0.143	0.223	3.315	0.485	0.00

y (mm)	u (m/s)	Local Turbulence Intensity	Kurtosis	% Backflow
0.254	0.77	0.11	2.271	0.474
0.508	1.44	0.12	1.579	0.139
0.762	1.76	0.08	1.378	0.088
1.016	1.84	0.18	1.351	0.158
1.270	2.18	0.21	1.241	0.228
1.524	2.53	0.32	1.129	0.052
1.778	2.76	0.16	0.983	0.193
2.032	3.01	0.13	0.950	0.092
2.286	3.27	0.14	0.876	0.052
2.540	3.49	0.31	0.842	0.118
2.794	3.94	0.17	0.751	0.044
3.048	4.30	0.26	0.679	0.062
3.302	4.46	0.12	0.680	0.045
3.556	4.79	0.31	0.653	0.083
3.810	5.18	0.19	0.600	0.026
4.064	5.29	0.36	0.599	0.054
4.318	5.81	0.34	0.557	0.048
4.572	5.97	0.27	0.558	0.038
4.826	6.39	0.37	0.514	0.048
5.080	6.65	0.44	0.518	0.084
5.334	7.02	0.44	0.487	0.045
5.842	7.99	0.39	0.432	0.033
6.350	8.51	0.23	0.408	0.011
6.985	9.73	0.49	0.573	0.044
7.620	10.73	0.39	0.359	0.022
8.255	12.10	0.20	0.374	0.019
8.890	12.95	0.47	0.309	0.026
9.525	14.22	0.36	0.298	0.032
10.160	15.89	0.39	0.256	0.018
10.795	17.15	0.76	0.240	0.025
11.430	18.39	0.56	0.222	0.020
12.065	19.55	0.65	0.211	0.015
12.700	20.83	0.40	0.198	0.011
13.335	22.10	0.49	0.178	0.010
13.970	23.32	0.59	0.169	0.016
14.605	24.53	0.33	0.145	0.014
15.240	25.36	0.54	0.135	0.011
15.875	26.36	0.50	0.121	0.012
16.510	26.98	0.28	0.112	0.015
17.145	27.80	0.30	0.088	0.008
17.780	28.36	0.26	0.069	0.011
19.050	29.15	0.30	0.044	0.016
20.320	29.31	0.05	0.017	0.002
21.590	29.26	0.07	0.017	0.001
22.860	29.21	0.07	0.020	0.002
24.130	29.14	0.03	0.020	0.001
25.400	29.09	0.05	0.016	0.003
26.670	29.00	0.07	0.017	0.002
27.940	28.91	0.08	0.017	0.001
29.210	28.83	0.07	0.017	0.003
30.480	28.73	0.07	0.017	0.041
31.750	28.59	0.37	0.016	0.002

Table 22. Boundary Layer Measurements at 74.0% Chord on the Suction Surface

33.020	28.49	0.06	0.017	0.001	0.033	0.323	3.160	0.537	0.00
34.290	28.38	0.03	0.017	0.001	0.188	0.303	3.866	0.913	0.00
35.560	28.26	0.06	0.017	0.001	0.091	0.325	3.303	0.605	0.00
36.830	28.20	0.05	0.018	0.001	0.205	0.189	3.773	1.140	0.00
38.100	28.07	0.04	0.018	0.002	0.335	0.353	3.710	1.540	0.00

Table 22. (Continued)

**ORIGINAL PAGE IS
OF POOR QUALITY**

y (mm)	u (m/s)	Local Turbulence Intensity		Skewness		Kurtosis		% Backflow		
		value	deviation	value	deviation	value	deviation	value	deviation	
0.254	0.07	0.16	2.950	14.003	0.075	0.086	4.045	0.780	47.70	
0.508	0.10	0.29	-13.032	28.063	0.135	0.065	3.283	0.271	48.55	
0.762	0.06	0.26	47.825	94.944	0.080	2.050	50.13	0.298	5.92	
1.016	0.07	0.23	43.326	71.541	0.125	0.130	2.819	0.263	50.54	
1.270	0.07	0.39	44.847	126.134	0.172	0.168	2.728	0.176	50.78	
1.524	0.25	0.17	-8.016	43.288	0.166	0.124	2.780	0.228	48.03	
1.778	0.34	-7.968	62.888	0.083	0.080	2.568	0.101	46.53	4.53	
2.032	0.26	0.33	5.179	7.535	0.226	0.180	2.638	0.234	48.65	
2.286	0.41	0.23	10.223	9.121	0.129	0.078	2.566	0.173	45.38	
2.540	0.52	6.120	2.346	0.157	0.150	2.685	0.315	44.68	4.98	
2.794	0.83	0.10	3.453	0.443	0.026	0.063	2.483	0.186	39.78	1.57
3.048	1.00	0.41	3.227	1.180	0.016	0.100	2.511	0.134	37.63	5.38
3.302	1.32	0.41	2.268	0.720	-0.048	0.084	2.672	0.207	33.05	6.37
3.556	1.36	0.30	2.264	0.534	-0.022	0.082	2.506	0.130	33.42	3.26
3.810	1.41	0.33	2.249	0.641	-0.028	0.039	2.485	0.118	32.82	4.60
4.064	1.64	0.21	1.819	0.231	-0.047	0.195	2.760	0.347	30.15	2.75
4.318	1.82	0.20	1.676	0.213	-0.061	0.104	2.718	0.149	27.83	3.19
4.572	1.93	0.38	1.650	0.352	-0.106	0.077	2.742	0.258	27.55	5.23
4.826	2.21	0.31	1.417	0.296	-0.137	0.124	2.690	0.197	24.47	4.79
5.080	2.38	0.20	1.357	0.133	-0.105	0.064	2.634	0.146	24.20	2.62
5.715	2.91	0.40	1.131	0.207	-0.253	0.097	2.790	0.109	19.23	3.82
6.350	3.70	0.53	0.900	0.211	-0.201	0.107	3.035	0.371	13.45	5.36
6.985	4.21	0.35	0.785	0.111	-0.248	0.091	3.010	0.189	10.70	3.43
7.620	4.72	0.31	0.712	0.098	-0.266	0.106	3.119	0.169	9.03	3.47
8.255	5.40	0.37	0.630	0.073	-0.287	0.090	3.078	0.232	6.77	2.21
8.890	6.09	0.30	0.587	0.044	-0.283	0.172	3.338	0.397	5.25	1.15
9.525	6.76	0.34	0.531	0.031	-0.259	0.067	3.369	0.162	3.95	0.66
10.160	7.49	0.29	0.481	0.026	-0.268	0.098	3.321	0.100	2.98	0.77
10.795	8.36	0.41	0.454	0.053	-0.191	0.184	3.314	0.180	1.46	2.17
11.430	8.71	0.71	0.441	0.043	-0.277	0.060	3.287	0.162	2.23	1.28
12.065	9.64	0.25	0.410	0.028	-0.223	0.142	3.158	0.318	1.28	0.75
12.700	10.43	0.31	0.391	0.026	-0.282	0.126	3.286	0.160	1.10	0.46
13.335	11.49	0.52	0.358	0.033	-0.283	0.075	3.275	0.145	0.85	0.52
13.970	12.32	0.25	0.345	0.024	-0.282	0.117	3.261	0.287	0.70	0.39
14.605	13.10	0.40	0.330	0.027	-0.280	0.146	3.246	0.333	0.55	0.35
15.240	14.25	0.46	0.302	0.022	-0.345	0.099	3.253	0.171	0.32	0.37
15.875	15.44	0.51	0.284	0.023	-0.370	0.193	3.266	0.371	2.20	0.24
16.510	16.36	0.47	0.272	0.020	-0.381	0.032	3.253	0.133	0.13	0.13
17.145	17.42	0.47	0.257	0.023	-0.516	0.146	4.404	0.466	0.17	0.13
17.780	18.39	0.36	0.241	0.017	-0.588	0.139	3.415	0.460	0.10	0.13
18.415	19.58	0.47	0.222	0.017	-0.578	0.072	3.423	0.213	0.00	0.00
19.050	20.60	0.61	0.207	0.021	-0.599	0.081	3.265	0.175	0.00	0.00
19.685	21.52	0.52	0.198	0.021	-0.813	0.133	3.563	0.592	0.00	0.00
20.320	22.42	0.86	0.191	0.029	-0.896	0.133	3.952	0.647	0.00	0.00
20.955	23.34	0.64	0.172	0.020	-0.950	0.160	4.071	0.607	0.00	0.00
21.590	24.33	0.72	0.163	0.034	-1.238	0.203	4.389	0.787	0.00	0.00
22.225	25.47	0.53	0.153	0.024	-1.277	0.190	4.572	0.766	0.00	0.00
22.860	26.26	0.59	0.116	0.018	-1.421	0.251	5.478	1.073	0.03	0.00
24.130	27.23	0.27	0.092	0.007	-1.842	0.254	7.312	1.528	0.09	0.00
25.400	28.05	0.16	0.067	0.006	-2.515	0.418	12.216	3.795	0.01	0.00
26.670	28.44	0.20	0.048	0.009	-2.923	0.969	18.306	13.731	0.00	0.00
27.940	28.65	0.05	0.036	0.008	-3.018	1.911	25.014	19.497	0.00	0.00

Table 23. Boundary Layer Measurements at 84.2% Chord on the Suction Surface

29.210	28.68	0.08	0.030	0.009	2.920	39.089	0.00
30.480	28.68	0.04	0.023	0.005	-3.345	2.920	0.00
31.750	28.61	0.06	0.022	0.006	-1.171	14.473	25.276
33.020	28.59	0.05	0.021	0.006	-0.501	2.481	0.00
34.290	28.49	0.05	0.019	0.001	-1.114	1.648	8.335
35.560	28.42	0.10	0.021	0.010	0.286	3.016	10.331
36.830	28.37	0.05	0.023	0.017	-0.715	16.814	32.413
38.100	28.30	0.04	0.017	0.002	-0.982	2.764	1.845
39.370	28.24	0.07	0.017	0.001	0.212	2.224	4.418
40.640	28.15	0.07	0.018	0.005	0.041	0.377	21.068
41.910	28.06	0.09	0.024	0.015	-0.874	0.252	9.708
					-1.975	3.459	11.987
						21.302	0.801
						26.337	0.754
						13.282	26.337
						21.302	0.00
						32.120	0.00
							0.00

Table 23. (Continued)

Y (m)	u_y (m/s)	Local Turbulence Intensity			Skewness			Kurtosis			% Backflow		
		value	deviation	value	value	deviation	value	value	deviation	value	value	deviation	
0.254	-0.19	0.53	-6.251	8.006	-0.052	0.196	3.407	0.445	52.57	9.61	5.56	6.32	
0.508	-0.33	0.41	-5.906	1.185	0.055	0.094	2.467	0.188	54.45	6.32	3.64	3.64	
0.762	-0.76	0.24	-4.112	2.021	0.248	0.109	2.367	0.279	61.32	7.43	6.52	7.43	
1.016	-0.94	0.50	-4.016	2.707	0.290	0.127	2.550	0.402	64.57	6.52	6.52	6.52	
1.270	-0.86	0.43	-4.317	2.749	0.130	0.225	2.522	0.225	62.73	6.54	6.54	6.54	
1.524	-0.80	0.49	-31.485	72.719	0.305	0.134	2.485	0.211	62.95	7.84	7.84	7.84	
1.778	-0.82	0.49	-9.630	16.156	0.339	0.195	2.655	0.351	62.95	5.56	5.56	5.56	
2.032	-0.43	0.41	5.144	5.144	0.304	0.137	2.651	0.341	57.83	6.08	6.08	6.08	
2.286	-0.53	0.40	-1.130	8.828	0.306	0.135	2.580	0.268	58.70	3.31	3.31	3.31	
2.540	-0.53	0.22	-6.537	4.104	0.328	0.107	2.592	0.214	59.43	7.29	7.29	7.29	
2.794	-0.61	0.49	-3.453	9.676	0.360	0.156	2.719	0.199	60.43	8.11	8.11	8.11	
3.048	-0.53	0.49	-3.933	6.047	0.409	0.173	2.809	0.312	58.63	5.94	5.94	5.94	
3.302	-0.47	0.40	-2.121	7.001	0.362	0.118	2.655	0.121	59.52	4.53	4.53	4.53	
3.556	-0.27	0.30	10.290	29.646	0.298	0.080	2.645	0.124	56.63	7.23	7.23	7.23	
3.810	-0.23	0.47	-7.149	8.792	0.313	0.125	2.653	0.108	56.57	8.56	8.56	8.56	
4.064	-0.08	0.55	7.149	20.580	0.338	0.179	2.786	0.300	54.03	11.05	11.05	11.05	
4.318	0.06	0.49	-23.302	49.905	0.306	0.119	2.860	0.229	52.63	7.19	7.19	7.19	
4.572	0.02	0.62	-5.260	8.816	0.286	0.119	2.576	0.138	53.32	7.82	7.82	7.82	
4.826	0.01	0.50	-8.087	15.067	0.310	0.105	2.742	0.186	53.85	7.27	7.27	7.27	
5.080	0.23	0.67	-36.749	68.697	0.250	0.230	2.766	0.192	49.68	9.83	9.83	9.83	
5.715	0.38	0.61	13.332	21.366	0.196	0.186	2.765	0.284	46.97	8.69	8.69	8.69	
6.350	0.70	0.80	2.977	5.996	0.168	0.192	2.792	0.355	43.68	6.95	6.95	6.95	
6.985	1.03	0.79	-3.987	17.794	0.161	0.139	2.636	0.179	39.75	9.61	9.61	9.61	
7.620	1.26	0.83	4.231	4.484	0.204	0.292	2.981	0.468	36.52	8.88	8.88	8.88	
8.255	1.57	0.83	3.276	2.932	0.232	0.266	3.114	0.806	32.66	8.88	8.88	8.88	
8.890	1.76	0.76	2.320	1.527	0.108	0.175	2.866	0.261	31.05	9.06	9.06	9.06	
9.525	2.06	0.71	1.809	0.819	0.051	0.106	2.802	0.123	27.60	7.92	7.92	7.92	
10.160	2.37	0.60	1.484	0.528	-0.015	0.159	2.783	0.098	24.40	6.95	6.95	6.95	
10.795	2.60	0.86	1.468	0.753	-0.010	0.138	2.853	0.186	22.80	8.51	8.51	8.51	
11.430	3.07	1.00	1.212	0.428	-0.020	0.153	2.914	0.278	19.87	7.79	7.79	7.79	
12.065	3.30	0.81	0.294	0.294	-0.023	0.123	2.888	0.240	18.33	6.16	6.16	6.16	
12.700	3.76	0.78	0.939	0.209	-0.082	0.155	3.074	0.401	14.18	5.99	5.99	5.99	
13.335	4.51	0.75	0.807	0.140	-0.182	0.131	3.043	0.130	10.87	4.21	4.21	4.21	
13.970	4.77	0.75	0.761	0.128	-0.187	0.070	3.122	0.138	9.62	3.16	3.16	3.16	
14.605	5.49	0.93	0.675	0.118	-0.105	0.087	3.015	0.119	7.63	3.09	3.09	3.09	
15.240	5.79	0.89	0.636	0.090	-0.149	0.138	3.052	0.222	5.90	2.35	2.35	2.35	
15.875	6.20	0.84	0.599	0.088	-0.124	0.069	3.131	0.262	5.37	2.45	2.45	2.45	
16.510	6.56	0.94	0.589	0.083	-0.150	0.086	3.043	0.214	5.33	2.23	2.23	2.23	
17.145	7.20	0.97	0.530	0.081	-0.153	0.064	3.022	0.201	3.72	1.99	1.99	1.99	
17.780	7.61	0.93	0.507	0.072	-0.073	0.064	2.916	0.151	2.83	0.75	0.75	0.75	
18.415	8.17	1.12	0.492	0.074	-0.149	0.106	3.163	0.197	2.67	1.76	1.76	1.76	
19.050	8.39	0.75	0.477	0.073	-0.092	0.070	2.974	0.174	2.13	1.29	1.29	1.29	
19.685	9.33	1.29	0.449	0.074	-0.118	0.099	2.966	0.241	1.75	1.19	1.19	1.19	
20.320	9.85	1.33	0.428	0.067	-0.120	0.096	2.955	0.201	1.37	1.02	1.02	1.02	
20.955	10.88	0.97	0.383	0.081	-0.170	0.087	2.984	0.062	0.88	0.75	0.75	0.75	
21.590	11.69	0.95	0.373	0.041	-0.138	0.106	2.226	0.087	0.45	0.55	0.55	0.55	
22.225	12.36	0.98	0.364	0.041	-0.146	0.064	2.900	0.096	0.47	0.53	0.53	0.53	
22.860	13.29	0.84	0.329	0.033	-0.239	0.080	2.975	0.140	0.35	0.25	0.25	0.25	
23.495	13.95	1.08	0.323	0.047	-0.206	0.126	2.938	0.165	0.20	0.33	0.33	0.33	
24.130	14.97	0.90	0.302	0.043	-0.308	0.068	3.021	0.221	0.18	0.23	0.23	0.23	
24.765	15.86	0.88	0.286	0.042	-0.340	0.075	2.947	0.138	0.05	0.13	0.13	0.13	
25.400	16.65	1.06	0.279	0.041	-0.340	0.065	3.045	0.205	0.07	0.09	0.09	0.09	

Table 24. Boundary Layer Measurements 94.9% on the Suction Surface

17.46	0.86	0.265	0.024	-0.487	0.091	0.05	0.09
26.035	0.72	0.247	0.035	-0.426	0.051	2.988	0.04
26.670	0.77	0.232	0.044	-0.513	0.069	0.175	0.02
27.305	20.31	0.92	0.224	0.038	-0.613	0.162	0.250
27.940	21.34	1.00	0.207	0.035	-0.708	0.053	0.07
28.575	22.52	0.68	0.186	0.022	-0.783	0.143	0.360
29.210	23.49	0.73	0.172	0.032	-0.946	0.199	0.388
29.845	24.12	0.81	0.157	0.026	-1.058	0.265	0.435
30.480	25.03	0.80	0.148	0.020	-1.375	0.424	0.502
31.115	25.98	0.76	0.121	0.014	-1.671	0.602	0.502
31.750	26.47	0.69	0.113	0.023	-1.946	0.514	0.00
32.385	26.86	0.56	0.100	0.021	-2.084	0.533	0.00
33.020	27.53	0.47	0.077	0.028	-2.287	0.414	0.00
34.290	28.05	0.27	0.052	0.011	-2.925	0.795	0.00
35.560	28.28	0.15	0.040	0.011	-3.083	1.764	15.960
36.830	28.28	0.12	0.031	0.005	-1.794	1.133	6.984
38.100	28.28	0.10	0.025	0.002	-0.212	0.726	2.891
39.370	28.38	0.13	0.023	0.004	0.075	0.330	7.865
40.640	28.36	0.11	0.021	0.001	-0.122	0.280	8.938
41.910	28.26	0.14	0.020	0.002	0.010	0.002	2.709
43.180							3.462

Table 24. (Continued)

Y (mm)	u (m/s)	Local Turbulence Intensity	Kurtosis	% Backflow
-63, 500	28, 98	0.14	0.019	0.001
-62, 230	29, 00	0.09	0.019	0.056
-60, 960	29, 02	0.14	0.021	0.082
-59, 690	29, 11	0.18	0.020	0.034
-58, 420	29, 07	0.13	0.021	0.003
-57, 150	29, 01	0.12	0.020	0.163
-55, 880	29, 08	0.08	0.020	0.002
-54, 610	29, 11	0.09	0.021	0.001
-53, 340	29, 13	0.17	0.020	0.002
-52, 070	29, 16	0.14	0.022	0.003
-50, 800	29, 13	0.15	0.022	0.001
-49, 530	29, 27	0.11	0.023	0.001
-48, 260	29, 19	0.06	0.027	0.011
-46, 990	29, 26	0.16	0.026	0.009
-45, 720	29, 22	0.06	0.033	0.016
-44, 450	29, 28	0.14	0.022	0.002
-43, 180	29, 21	0.09	0.038	0.009
-41, 910	29, 05	0.08	0.052	0.011
-40, 640	28, 66	0.13	0.069	0.012
-39, 370	28, 05	0.18	0.085	0.007
-38, 100	26, 84	0.24	0.114	0.009
-37, 465	26, 16	0.17	0.131	0.017
-36, 830	25, 24	0.30	0.151	0.017
-36, 195	24, 32	0.43	0.168	0.010
-35, 560	23, 19	0.36	0.183	0.012
-34, 925	22, 06	0.48	0.199	0.007
-34, 290	21, 09	0.43	0.223	0.017
-33, 655	20, 05	0.21	0.242	0.009
-33, 020	18, 87	0.62	0.266	0.026
-32, 385	17, 84	0.47	0.275	0.012
-31, 750	17, 15	0.51	0.278	0.021
-31, 115	16, 07	0.80	0.304	0.026
-30, 480	15, 07	0.36	0.327	0.013
-29, 845	13, 97	0.44	0.348	0.013
-29, 210	13, 30	0.15	0.360	0.016
-28, 575	12, 37	0.52	0.382	0.020
-27, 940	11, 51	0.49	0.419	0.026
-27, 305	10, 56	0.26	0.458	0.018
-26, 670	9, 53	0.63	0.514	0.057
-26, 035	8, 92	0.59	0.541	0.046
-25, 400	8, 32	0.44	0.577	0.047
-24, 765	7, 57	0.61	0.635	0.088
-24, 130	6, 87	0.41	0.708	0.077
-23, 495	6, 35	0.22	0.751	0.050
-22, 860	5, 54	0.41	0.865	0.082
-22, 225	4, 99	0.53	0.979	0.157
-21, 590	4, 33	0.51	1.121	0.159
-20, 955	3, 96	0.62	1.228	0.200
-20, 320	3, 37	0.73	1.450	0.363
-19, 685	2, 83	0.52	1.700	0.349
-19, 050	2, 22	0.33	2.109	0.297
-18, 415	1, 90	0.32	2.486	0.434

Table 25. Wake Measurements at 105.4% Chord

ORIGINAL PAGE IS
OF POOR QUALITY

4.47	4.99	4.19	4.22	37.78
4.65	4.50	4.20	2.45	0.154
0.65	0.37	0.146	2.299	42.32
0.65	0.37	0.146	2.299	46.50
0.40	0.40	0.216	0.051	49.36
-15.875	-15.875	0.194	2.281	4.20
-15.240	-0.11	0.216	0.145	3.39
-14.605	-0.14	0.09	2.391	51.42
-10.795	-1.15	0.31	0.133	0.47
-10.160	-1.71	0.19	0.100	53.70
-11.335	-0.63	0.45	2.435	0.311
-12.700	-0.94	0.29	0.265	2.578
-12.065	-1.29	0.57	0.125	0.244
-11.430	-1.26	0.32	0.118	0.149
-10.795	-1.15	0.31	0.118	58.44
-10.160	-1.71	0.19	0.118	4.88
-11.335	-1.93	0.14	2.416	4.31
-8.890	-2.02	0.29	0.136	6.18
-8.255	-2.08	0.29	0.136	6.38
-7.620	-2.21	0.21	0.136	6.96
-6.985	-2.19	0.21	0.138	6.46
-6.350	-2.24	0.22	0.138	3.42
-5.715	-1.88	0.16	0.138	3.42
-5.080	-0.98	0.32	0.138	3.42
-4.445	-1.17	0.73	0.138	3.42
-3.810	4.50	0.95	0.138	3.42
-3.175	8.65	0.87	0.138	3.42
-2.540	14.29	0.99	0.138	3.42
-1.105	20.46	0.75	0.138	3.42
-1.270	25.01	0.18	0.138	3.42
-0.635	27.55	0.23	0.138	3.42
0.000	28.63	0.19	0.063	0.000
1.270	29.53	0.15	0.038	0.000
2.540	29.62	0.22	0.031	0.000
3.810	29.48	0.21	0.030	0.000
5.080	29.44	0.27	0.025	0.000
6.350	29.25	0.19	0.021	0.000
7.620	29.19	0.16	0.020	0.000
8.890	29.11	0.23	0.021	0.000
10.160	29.05	0.19	0.021	0.000
11.430	28.93	0.17	0.022	0.000
12.700	28.93	0.26	0.022	0.000
13.970	28.80	0.22	0.022	0.000
15.240	28.75	0.27	0.021	0.000
16.510	28.64	0.16	0.022	0.000
17.780	28.56	0.25	0.022	0.000
25.400	28.37	0.29	0.021	0.000
26.670	28.33	0.20	0.022	0.000
27.940	28.28	0.21	0.022	0.000
29.210	28.36	0.29	0.023	0.000
30.480	28.22	0.22	0.022	0.000
31.750	28.26	0.23	0.023	0.000
33.020	28.24	0.25	0.022	0.000
34.290	28.24	0.27	0.022	0.000

Table 25. (Continued)

y (mm)	u (m/s)	Local Turbulence Intensity		Skewness		Kurtosis		% Backflow	
		value	deviation	value	deviation	value	deviation	value	deviation
-66.040	28.78	0.05	0.023	0.001	-0.121	0.205	3.284	0.562	0.00
-64.770	28.82	0.13	0.023	0.003	-0.010	0.250	3.585	0.826	0.00
-63.500	28.90	0.20	0.023	0.004	-0.081	0.596	4.305	2.665	0.00
-62.230	28.88	0.17	0.024	0.002	-0.285	0.515	4.521	1.627	0.00
-60.960	28.90	0.22	0.024	0.002	0.022	0.297	3.599	0.684	0.00
-59.690	28.90	0.09	0.023	0.002	-0.038	0.297	3.125	0.470	0.00
-58.420	28.87	0.24	0.025	0.004	-0.225	0.542	3.921	1.833	0.00
-57.150	28.91	0.12	0.026	0.005	-0.783	2.063	9.722	17.049	0.00
-55.880	28.98	0.09	0.026	0.003	-0.122	0.428	3.480	1.123	0.00
-54.610	29.01	0.18	0.026	0.005	-0.095	0.243	3.681	0.606	0.00
-53.340	29.08	0.15	0.028	0.003	-0.282	0.936	4.773	4.025	0.00
-52.070	28.95	0.09	0.028	0.005	-0.182	0.273	4.428	1.448	0.00
-50.800	28.95	0.17	0.039	0.024	-0.982	2.197	8.591	9.754	0.00
-49.530	28.94	0.12	0.043	0.009	-2.576	1.804	12.500	0.00	0.00
-48.260	28.91	0.13	0.045	0.009	-2.360	1.402	15.603	10.570	0.00
-46.990	28.79	0.16	0.054	0.015	-2.838	1.561	19.676	14.531	0.00
-45.720	28.79	0.10	0.053	0.007	-2.750	0.783	15.900	8.641	0.00
-44.450	27.43	0.38	0.104	0.016	-2.146	0.524	10.051	3.976	0.00
-43.815	27.39	0.51	0.104	0.023	-2.213	0.386	10.821	3.542	0.00
-43.180	26.65	0.31	0.121	0.015	-1.719	0.269	7.478	2.267	0.00
-42.545	25.87	0.60	0.143	0.016	-1.608	0.407	6.630	2.517	0.00
-41.910	25.42	0.66	0.148	0.018	-1.501	0.088	6.250	0.611	0.00
-41.275	24.41	0.70	0.171	0.021	-1.196	0.261	4.985	1.304	0.00
-40.640	23.87	0.73	0.186	0.020	-1.203	0.193	0.501	0.00	0.00
-40.005	22.62	0.55	0.205	0.016	-1.012	0.179	4.964	0.564	0.00
-39.370	21.47	0.63	0.230	0.018	-0.903	0.142	4.344	0.800	0.04
-38.735	20.80	0.94	0.246	0.020	-0.837	0.175	3.776	0.522	0.10
-38.100	19.53	1.03	0.263	0.027	-0.762	0.122	3.712	0.562	0.12
-37.465	18.90	0.84	0.271	0.030	-0.638	0.090	3.443	0.476	0.20
-36.830	17.85	0.41	0.299	0.014	-0.648	0.193	3.557	0.712	0.38
-36.195	16.84	0.39	0.318	0.014	-1.012	0.179	4.344	0.217	0.15
-35.560	16.11	0.61	0.338	0.022	-0.537	0.074	3.361	0.522	0.20
-34.925	14.90	0.72	0.374	0.020	-0.590	0.220	3.448	0.627	0.32
-34.290	13.85	0.73	0.410	0.029	-0.524	0.159	3.393	0.264	0.84
-33.655	13.39	0.85	0.466	0.032	-0.464	0.121	3.300	0.217	0.18
-33.020	12.33	0.47	0.469	0.008	-0.453	0.181	3.74	0.643	0.22
-32.385	11.51	0.52	0.482	0.021	-0.443	0.103	3.209	0.172	0.19
-31.750	10.57	0.53	0.542	0.028	-0.475	0.079	3.361	0.207	0.07
-31.115	9.94	0.66	0.552	0.046	-0.379	0.106	3.170	0.255	0.82
-30.480	8.91	0.65	0.625	0.059	-0.443	0.107	3.111	0.157	0.94
-29.845	7.98	0.46	0.583	0.072	-0.381	0.116	3.238	0.253	1.86
-29.210	7.52	0.33	0.726	0.056	-0.397	0.063	3.036	0.173	0.99
-28.575	6.65	0.26	0.838	0.044	-0.311	0.101	2.892	0.214	0.50
-27.940	6.34	0.40	0.873	0.070	-0.344	0.060	2.849	0.201	0.67
-27.305	5.46	0.28	0.911	0.094	-0.263	0.103	2.767	0.169	0.72
-26.670	5.26	0.39	1.232	0.117	-0.274	0.088	2.762	0.199	1.00
-26.035	4.24	0.66	1.307	0.207	-0.205	0.079	2.553	0.189	2.78
-25.400	3.86	0.55	1.416	0.197	-0.111	0.055	2.474	0.180	2.56
-24.765	3.05	0.43	1.772	0.300	-0.042	0.179	2.434	0.979	1.92
-24.130	2.81	0.46	1.946	0.431	-0.079	0.190	2.423	0.117	1.96
-23.495	2.15	0.61	2.546	0.614	-0.015	0.123	2.271	0.140	3.33
-22.860	1.57	0.31	3.308	1.57	0.570	0.083	2.386	0.142	3.48

Table 26. Wake Measurements at 109.6% Chord

ORIGINAL PAGE IS
OF POOR QUALITY

3.67	42.32	0.084	2.280
2.50	-22.225	0.076	1.726
2.50	-21.590	0.189	6.107
2.50	-20.955	0.143	14.843
2.50	-20.320	0.143	47.234
2.50	-19.685	0.156	20.164
2.50	-19.050	0.155	10.418
2.50	-18.415	0.226	3.518
2.50	-17.780	0.675	0.653
2.50	-17.145	0.637	0.584
2.50	-16.510	0.585	0.703
2.50	-15.875	0.491	0.488
2.50	-15.240	0.605	0.200
2.50	-14.605	0.29	0.278
2.50	-14.03	0.27	0.193
2.50	-13.970	0.30	0.329
2.50	-13.335	0.24	0.363
2.50	-12.700	0.43	0.140
2.50	-12.065	0.43	0.140
2.50	-11.430	0.11	0.123
2.50	-10.795	0.29	0.074
2.50	-10.160	0.07	0.054
2.50	-9.525	0.23	0.397
2.50	-8.890	0.31	0.186
2.50	-8.255	0.56	0.286
2.50	-7.620	0.14	0.187
2.50	-7.000	0.54	0.969
2.50	-6.350	0.82	0.664
2.50	-5.715	0.14	0.517
2.50	-5.080	1.13	0.403
2.50	-4.445	1.15	0.318
2.50	-3.810	1.19	0.239
2.50	-3.175	0.54	0.113
2.50	-2.540	0.34	0.119
2.50	-1.270	0.23	0.085
2.50	0.000	0.11	0.047
2.50	2.14	0.16	0.043
2.50	2.54	0.15	0.027
2.50	2.91	0.19	0.025
2.50	3.29	0.16	0.020
2.50	3.67	0.17	0.024
2.50	4.05	0.14	0.022
2.50	4.42	0.19	0.024
2.50	4.79	0.16	0.023
2.50	5.17	0.12	0.023
2.50	5.54	0.09	0.023
2.50	5.91	0.14	0.024
2.50	6.28	0.16	0.024
2.50	6.55	0.11	0.023
2.50	6.82	0.16	0.023
2.50	7.19	0.12	0.023
2.50	7.56	0.09	0.023
2.50	7.93	0.14	0.024
2.50	8.30	0.16	0.024
2.50	8.67	0.12	0.023
2.50	9.04	0.13	0.023
2.50	9.41	0.17	0.023
2.50	9.78	0.16	0.023
2.50	10.15	0.12	0.023
2.50	10.52	0.13	0.023
2.50	10.89	0.11	0.023
2.50	11.26	0.17	0.023
2.50	11.63	0.16	0.023
2.50	12.00	0.12	0.023
2.50	12.37	0.19	0.023
2.50	12.74	0.14	0.024
2.50	13.11	0.16	0.024
2.50	13.48	0.12	0.023
2.50	13.85	0.17	0.023
2.50	14.22	0.14	0.024
2.50	14.59	0.11	0.023
2.50	14.96	0.16	0.024
2.50	15.33	0.12	0.023
2.50	15.70	0.17	0.023
2.50	16.07	0.14	0.024
2.50	16.44	0.11	0.023
2.50	16.81	0.16	0.024
2.50	17.18	0.12	0.023
2.50	17.55	0.19	0.024
2.50	17.92	0.14	0.023
2.50	18.29	0.11	0.023
2.50	18.66	0.16	0.024
2.50	19.03	0.12	0.023
2.50	19.40	0.17	0.023
2.50	19.77	0.14	0.024
2.50	20.14	0.11	0.023
2.50	20.51	0.16	0.024
2.50	20.88	0.12	0.023
2.50	21.25	0.17	0.023
2.50	21.62	0.14	0.024
2.50	22.00	0.11	0.023
2.50	22.37	0.16	0.024
2.50	22.74	0.12	0.023
2.50	23.11	0.17	0.023
2.50	23.48	0.14	0.024
2.50	23.85	0.11	0.023
2.50	24.22	0.16	0.024
2.50	24.59	0.12	0.023
2.50	24.96	0.17	0.023
2.50	25.33	0.14	0.024
2.50	25.70	0.11	0.023
2.50	26.07	0.16	0.024
2.50	26.44	0.12	0.023
2.50	26.81	0.17	0.023
2.50	27.18	0.14	0.024
2.50	27.55	0.11	0.023
2.50	27.92	0.16	0.024
2.50	28.29	0.12	0.023
2.50	28.66	0.17	0.023
2.50	29.03	0.14	0.024
2.50	29.40	0.11	0.023
2.50	29.77	0.16	0.024
2.50	30.14	0.12	0.023
2.50	30.51	0.17	0.023
2.50	30.88	0.14	0.024
2.50	31.25	0.11	0.023
2.50	31.62	0.16	0.024
2.50	32.00	0.12	0.023
2.50	32.37	0.17	0.023
2.50	32.74	0.14	0.024
2.50	33.11	0.11	0.023
2.50	33.48	0.16	0.024
2.50	33.85	0.12	0.023
2.50	34.22	0.17	0.023
2.50	34.59	0.14	0.024
2.50	34.96	0.11	0.023
2.50	35.33	0.16	0.024
2.50	35.70	0.12	0.023
2.50	36.07	0.17	0.023
2.50	36.44	0.14	0.024
2.50	36.81	0.11	0.023
2.50	37.18	0.16	0.024
2.50	37.55	0.12	0.023
2.50	37.92	0.17	0.023
2.50	38.29	0.14	0.024
2.50	38.66	0.11	0.023
2.50	39.03	0.16	0.024
2.50	39.40	0.12	0.023
2.50	39.77	0.17	0.023
2.50	40.14	0.14	0.024
2.50	40.51	0.11	0.023
2.50	40.88	0.16	0.024
2.50	41.25	0.12	0.023
2.50	41.62	0.17	0.023
2.50	42.00	0.14	0.024
2.50	42.37	0.11	0.023
2.50	42.74	0.16	0.024
2.50	43.11	0.12	0.023
2.50	43.48	0.17	0.023
2.50	43.85	0.14	0.024
2.50	44.22	0.11	0.023
2.50	44.59	0.16	0.024
2.50	44.96	0.12	0.023
2.50	45.33	0.17	0.023
2.50	45.70	0.14	0.024
2.50	46.07	0.11	0.023
2.50	46.44	0.16	0.024
2.50	46.81	0.12	0.023
2.50	47.18	0.17	0.023
2.50	47.55	0.14	0.024
2.50	47.92	0.11	0.023
2.50	48.29	0.16	0.024
2.50	48.66	0.12	0.023
2.50	49.03	0.17	0.023
2.50	49.40	0.14	0.024
2.50	49.77	0.11	0.023
2.50	50.14	0.16	0.024
2.50	50.51	0.12	0.023
2.50	50.88	0.17	0.023
2.50	51.25	0.14	0.024
2.50	51.62	0.11	0.023
2.50	52.00	0.16	0.024
2.50	52.37	0.12	0.023
2.50	52.74	0.17	0.023
2.50	53.11	0.14	0.024
2.50	53.48	0.11	0.023
2.50	53.85	0.16	0.024
2.50	54.22	0.12	0.023
2.50	54.59	0.17	0.023
2.50	54.96	0.14	0.024
2.50	55.33	0.11	0.023
2.50	55.70	0.16	0.024
2.50	56.07	0.12	0.023
2.50	56.44	0.17	0.023
2.50	56.81	0.14	0.024
2.50	57.18	0.11	0.023
2.50	57.55	0.16	0.024
2.50	57.92	0.12	0.023
2.50	58.29	0.17	0.023
2.50	58.66	0.14	0.024
2.50	59.03	0.11	0.023
2.50	59.40	0.16	0.024
2.50	59.77	0.12	0.023
2.50	60.14	0.17	0.023
2.50	60.51	0.14	0.024
2.50	60.88	0.11	0.023
2.50	61.25	0.16	0.024
2.50	61.62	0.12	0.023
2.50	62.00	0.17	0.023
2.50	62.37	0.14	0.024
2.50	62.74	0.11	0.023
2.50	63.11	0.16	0.024
2.50	63.48	0.12	0.023
2.50	63.85	0.17	0.023
2.50	64.22	0.14	0.024
2.50	64.59	0.11	0.023
2.50	64.96	0.16	0.024
2.50	65.33	0.12	0.023
2.50	65.70	0.17	0.023
2.50	66.07	0.14	0.024
2.50	66.44	0.11	0.023
2.50	66.81	0.16	0.024
2.50	67.18	0.12	0.023
2.50	67.55	0.17	0.023
2.50	67.92	0.14	0.024
2.50	68.29	0.11	0.023
2.50	68.66	0.16	0.024
2.50	69.03	0.12	0.023
2.50	69.40	0.17	0.023
2.50	69.77	0.14	0.024
2.50	70.14	0.11	0.023
2.50	70.51	0.16	0.024
2.50	70.88	0.12	0.023
2.50	71.25	0.17	0.023
2.50	71.62	0.14	0.024
2.50	72.00	0.11	0.023
2.50	72.37	0.16	0.024
2.50	72.74	0.12	0.023
2.50	73.11	0.17	0.023
2.50	73.48	0.14	0.024
2.50	73.85	0.11	0.023
2.50	74.22	0.16	0.024
2.50	74.59	0.12	0.023
2.50	74.96	0.17	0.023
2.50	75.33	0.14	0.024
2.50	75.70	0.11	0.023
2.50	76.07	0.16	0.024
2.50	76.44	0.12	0.023
2.50	76.81	0.17	0.023
2.50	77.18	0.14	0.024
2.50	77.55	0.11	0.023
2.50	77.92	0.16	0.024
2.50	78.29	0.12	0.023
2.50	78.66	0.17	0.023
2.50	79.03	0.14	0.024
2.50	79.40	0.11	0.023
2.50	79.77	0.16	0.024
2.50	80.14	0.12	0.023
2.50	80.51	0.17	0.023
2.50	80.88	0.14	0.024
2.50	81.25	0.11	0.023
2.50	81.62	0.16	0.024
2.50	82.00	0.12	0.023
2.50	82.37	0.17	0.023
2.50	82.74	0.14	0.024
2.50	83.11	0.11	0.023
2.50	83.48	0.16	0.024
2.50	83.85	0.12	0.023
2.50	84.22	0.17	0.023
2.50	84.59	0.14	0.024
2.50	84.96	0.11	0.023
2.50	85.33	0.16	0.024
2.50	85.70	0.12	0.023
2.50	86.07	0.17	0.023
2.50	86.44	0.14	0.024
2.50	86.81	0.11	0.023
2.50	87.18	0.16	0.024
2.50	87.55	0.12	0.023
2.50	87.92	0.17	0.023
2.50	88.29	0.14	0.024
2.50	88.66	0.11	0.023
2.50	89.03	0.16	0.024
2.50	89.40	0.12	0.023
2.50	89.77	0.17	0.023
2.50	90.14	0.14	0.024
2.50	90.51	0.11	0.023
2.50	90.88	0.16	0.024
2.50	91.25	0.12	0.023
2.50	91.62	0.17	0.023
2.50	92.00	0.14	0.024
2.50	92.37	0.11	0.023
2.50	92.74	0.16	0.024
2.50	93.11	0.12	0.023
2.50	93.48	0.17	0.023
2.50	93.85	0.14	0.024
2.50	94.22	0.11	0.023
2.50	94.59	0.16	0.024
2.50	94.96	0.12	0.023
2.50	95.		

Table 26. (Continued)

**ORIGINAL PAGE IS
OF POOR QUALITY**

Y (mm)	u (m/s)	Local Turbulence Intensity		Skewness		Kurtosis		% Backflow	
		value	deviation	value	deviation	value	deviation	value	deviation
-134.137	26.26	0.07	---	---	---	---	---	---	---
-130.962	26.25	0.14	---	---	---	---	---	---	---
-127.787	26.15	0.19	---	---	---	---	---	---	---
-124.612	26.04	0.23	---	---	---	---	---	---	---
-121.437	25.79	0.25	---	---	---	---	---	---	---
-118.262	25.38	0.20	---	---	---	---	---	---	---
-115.087	25.02	0.20	---	---	---	---	---	---	---
-111.912	24.60	0.28	---	---	---	---	---	---	---
-108.737	23.77	0.27	---	---	---	---	---	---	---
-105.562	22.64	0.52	---	---	---	---	---	---	---
-102.387	22.12	0.91	---	---	---	---	---	---	---
-99.212	20.81	0.77	---	---	---	---	---	---	---
-96.037	19.32	0.61	---	---	---	---	---	---	---
-92.862	18.04	1.07	---	---	---	---	---	---	---
-89.687	16.33	0.62	---	---	---	---	---	---	---
-86.512	14.69	0.84	---	---	---	---	---	---	---
-83.337	13.17	0.82	---	---	---	---	---	---	---
-80.162	11.84	0.40	---	---	---	---	---	---	---
-76.987	10.74	0.76	---	---	---	---	---	---	---
-73.812	9.69	0.49	---	---	---	---	---	---	---
-70.637	9.32	0.59	---	---	---	---	---	---	---
-67.462	9.16	0.39	---	---	---	---	---	---	---
-64.287	9.58	0.57	---	---	---	---	---	---	---
-61.112	10.60	0.74	---	---	---	---	---	---	---
-57.937	12.26	0.51	---	---	---	---	---	---	---
-54.762	14.20	0.88	---	---	---	---	---	---	---
-51.587	16.11	0.95	---	---	---	---	---	---	---
-48.412	18.33	0.96	---	---	---	---	---	---	---
-45.237	20.22	0.99	---	---	---	---	---	---	---
-42.062	22.08	0.68	---	---	---	---	---	---	---
-38.887	23.55	0.55	---	---	---	---	---	---	---
-35.712	24.78	0.48	---	---	---	---	---	---	---
-32.537	25.43	0.29	---	---	---	---	---	---	---
-29.362	25.90	0.17	---	---	---	---	---	---	---
-26.187	26.05	0.19	---	---	---	---	---	---	---
-23.012	26.16	0.18	---	---	---	---	---	---	---
-19.837	26.15	0.25	---	---	---	---	---	---	---
-16.662	26.17	0.07	---	---	---	---	---	---	---
-13.487	26.14	0.36	---	---	---	---	---	---	---

Table 27. Wake Measurements at 152.6% Chord

Suction Surface Boundary Layer at 53.6% Chord ($\partial p/\partial y > 0$)

<u>N_{inv}</u>	<u>U_e, m/sec</u>	<u>δ, mm</u>
11	33.64	11.30
12	33.74	11.42
13	33.83	11.54
14	34.00	11.77
15	33.84	11.55
16	33.76	11.46
17	<u>33.64</u>	<u>11.32</u>
	33.78 ± 0.13	11.48 ± 0.16

Pressure Surface Boundary Layer at 57.2% Chord ($\partial p/\partial y < 0$)

<u>N_{inv}</u>	<u>U_e, m/sec</u>	<u>δ, mm</u>
14	23.37	2.31
15	23.38	2.33
16	23.39	2.34
17	23.41	2.37
18	23.40	2.35
19	23.40	2.35
20	23.40	2.35
21	23.40	2.35
22	<u>23.40</u>	<u>2.35</u>
	23.39 ± 0.02	2.34 ± 0.02

Table 28. Variation of U_e and δ with the Number of Parts used in the Polynomial Fit of the Inviscid Region

Parameters	Suction Surface Boundary Layer at 53.6% Chord $(\partial p/\partial y > 0)$		Pressure Surface Boundary Layer at 57.2% Chord $(\partial p/\partial y < 0)$	
	Spline Fit	Fit of Wall-Wake Eq.	Spline Fit	Falkner-Skan Solution
δ^* , (mm)	3.50	3.46	0.83	0.59
θ , (mm)	1.80	1.82	0.29	0.22
δ_3 , (mm)	2.88	2.91	0.46	-----
Re_{δ^*}	7881	7795	1295	835
Re_{θ}	4041	4095	451	310
Re_{δ_3}	6489	6557	213	-----
H_{12}	1.95	1.90	2.87	2.70
H_{32}	1.61	1.60	1.58	-----
u_τ , (m/sec)	0.850 ⁽¹⁾	0.823	0.385 ⁽¹⁾	0.337
Π	-----	4.496	-----	-----
β_c	-----	7.362	-----	-----
β	-----	-----	-----	- 0.0588

(1) Calculated from the Ludweig-Tillman Equation.

Table 29. Boundary Layer Parameters

% Chord	Pressure Tap Measurements			LDV Measurements	
	C _p	U _e (m/s)	U _e (m/s)	δ (mm)	δ (mm)
2.7	0.555	21.95	21.45	0.68 (?)	
5.9	0.509	23.22	23.70 ± 0.07	0.50 ± 0.01	
14.4	0.512	23.10	24.50 ± 0.13	0.66 ± 0.01	
25.1	0.546	22.31	24.34 ± 0.04	1.16 ± 0.03	
35.8	0.570	21.70	23.83 ± 0.03	1.36 ± 0.01	
46.5	0.584	21.34	23.63 ± 0.01	1.68 ± 0.02	
57.2	0.591	21.17	23.39 ± 0.02	2.34 ± 0.02	
68.0	0.591	21.19	23.56 ± 0.02	2.77 ± 0.03	
78.6	0.571	21.70	24.08 ± 0.03	3.47 ± 0.09	
89.3	0.512	23.13	25.52 ± 0.01	4.65 ± 0.11	
97.9	0.393	25.99	28.11 ± 0.05	2.68	

Table 30. Boundary Layer Edge Velocities and Boundary Layer Thicknesses on the Pressure Surface

<i>y</i> (mm)	<i>u</i> (m/s)	Turbulence Intensity
0.127	16.22	0.171
0.190	19.87	0.096
0.254	20.85	0.080
0.317	21.09	0.072
0.381	21.01	0.074
0.508	21.18	0.067
0.762	21.33	0.061
1.016	21.43	0.055
1.524	21.47	0.052
2.032	21.45	0.048
2.540	21.54	0.038
3.810	21.53	0.038
5.080	21.63	0.038
6.350	21.60	0.036
7.620	21.64	0.038
8.890	21.51	0.034
10.160	21.42	0.031
11.430	21.45	0.030
12.700	21.40	0.030
13.970	21.37	0.031
15.240	21.37	0.030
16.510	21.34	0.030
17.780	21.32	0.028
19.050	21.39	0.029
20.320	21.38	0.029
21.590	21.34	0.028
22.860	21.37	0.028
24.130	21.45	0.028
25.400	21.46	0.028
26.670	21.49	0.027
27.940	21.50	0.028
29.210	21.56	0.026
30.480	21.51	0.028
31.750	21.55	0.029
33.020	21.54	0.028
34.290	21.53	0.029
35.560	21.45	0.029
36.830	21.41	0.029
38.100	21.24	0.031

Table 31. Reconstructed Boundary Layer at 2.7% on the Pressure Surface

<i>y</i> (mm)	<i>u</i> (m/s)	Turbulence Intensity
0.317	19.76	0.088
0.381	22.33	0.071
0.508	23.70	0.047
0.762	23.82	0.042
1.016	23.92	0.034
1.524	23.96	0.026
2.032	23.89	0.024
2.540	23.88	0.025
3.810	23.79	0.023
5.080	23.72	0.025
6.350	23.67	0.025
7.620	23.71	0.024
8.890	23.69	0.024
10.160	23.65	0.023
11.430	23.70	0.024
12.700	23.71	0.023
13.970	23.70	0.024
15.240	23.71	0.025
16.510	23.72	0.025
17.780	23.72	0.024
19.050	23.76	0.024
20.320	23.72	0.023
21.590	23.70	0.024
22.860	23.70	0.024
24.130	23.70	0.023
25.400	23.68	0.023
26.670	23.71	0.024
27.940	23.69	0.023
29.210	23.70	0.023
30.480	23.66	0.022
31.750	23.62	0.023
33.020	23.67	0.024
34.290	23.74	0.024
35.560	23.72	0.025
36.830	23.73	0.024
38.100	23.71	0.025

Table 32. Reconstructed Boundary Layer at 5.9% Chord on the Pressure Surface

<i>y</i> (mm)	<i>u</i> (m/s)	Turbulence Intensity
0.254	9.70	0.075
0.317	13.59	0.074
0.381	17.24	0.080
0.444	20.26	0.069
0.508	22.17	0.056
0.762	24.52	0.020
1.016	24.64	0.020
1.524	24.70	0.019
2.032	24.69	0.019
2.540	24.68	0.019
3.810	24.62	0.019
5.080	24.59	0.019
6.350	24.58	0.019
7.620	24.57	0.020
8.890	24.57	0.020
10.160	24.53	0.020
11.430	24.53	0.021
12.700	24.54	0.020
13.970	24.50	0.021
15.240	24.50	0.021
16.510	24.47	0.020
17.780	24.51	0.021
19.050	24.50	0.021
20.320	24.48	0.021
21.590	24.54	0.021
22.860	24.47	0.022
24.130	24.47	0.021
25.400	24.52	0.022
26.670	24.50	0.023
27.940	24.51	0.022
29.210	24.48	0.023
30.480	24.54	0.023
31.750	24.50	0.023
33.020	24.47	0.023
34.290	24.51	0.023
35.560	24.52	0.024
36.830	24.48	0.023

Table 33. Reconstructed Boundary Layer at 14.4% Chord on the Pressure Surface

<i>y</i> (mm)	<i>u</i> (m/s)	Turbulence Intensity
0.254	5.58	0.050
0.317	8.21	0.053
0.381	10.52	0.064
0.444	13.57	0.083
0.508	16.02	0.090
0.571	18.48	0.074
0.635	20.10	0.060
0.762	22.29	0.052
0.889	23.50	0.029
1.016	24.02	0.022
1.270	24.25	0.021
1.524	24.28	0.021
2.032	24.28	0.020
2.540	24.34	0.020
3.810	24.29	0.019
5.080	24.27	0.020
6.350	24.32	0.020
7.620	24.31	0.020
8.890	24.34	0.020
10.160	24.34	0.020
11.430	24.36	0.020
12.700	24.35	0.021
13.970	24.31	0.020
15.240	24.35	0.021
16.510	24.32	0.020
17.780	24.35	0.020
19.050	24.35	0.020
20.320	24.36	0.021
21.590	24.35	0.021
22.860	24.36	0.021
24.130	24.28	0.021
25.400	24.33	0.021
26.670	24.33	0.022
27.940	24.35	0.022
29.210	24.32	0.022
30.480	24.36	0.023
31.750	24.35	0.022
33.020	24.36	0.022
34.290	24.36	0.022
35.560	24.32	0.023
36.830	24.34	0.024
38.100	24.33	0.023

Table 34. Reconstructed Boundary Layer at 25.1% Chord on the Pressure Surface

y (mm)	u (m/s)	Turbulence Intensity
0.381	5.01	0.055
0.508	8.37	0.072
0.635	12.20	0.103
0.762	16.63	0.111
0.889	19.24	0.090
1.016	21.37	0.073
1.143	22.61	0.055
1.270	23.31	0.039
1.524	23.86	0.020
2.032	23.92	0.022
2.540	23.92	0.021
3.810	23.87	0.020
5.080	23.85	0.020
6.350	23.82	0.021
7.620	23.90	0.021
8.890	23.82	0.021
10.160	23.82	0.019
11.430	23.81	0.020
12.700	23.85	0.020
13.970	23.81	0.021
15.240	23.85	0.021
16.510	23.84	0.021
17.780	23.84	0.021
19.050	23.86	0.021
20.320	23.82	0.021
21.590	23.86	0.022
22.860	23.82	0.021
24.130	23.85	0.021
25.400	23.82	0.021
26.670	23.79	0.021
27.940	23.82	0.022
29.210	23.84	0.022
30.480	23.80	0.021
31.750	23.78	0.021
33.020	23.82	0.020
34.290	23.84	0.023
35.560	23.84	0.023
36.830	23.84	0.023
38.100	23.88	0.023

Table 35. Reconstructed Boundary Layer at 35.8% Chord on the Pressure Surface

<i>Y (mm)</i>	<i>u (m/s)</i>	Turbulence Intensity
0.254	2.23	0.039
0.381	5.20	0.062
0.508	7.69	0.095
0.635	10.60	0.142
0.762	13.53	0.169
0.889	16.23	0.179
1.016	18.88	0.167
1.143	20.78	0.137
1.270	21.99	0.113
1.397	22.78	0.083
1.524	23.02	0.081
1.651	23.37	0.055
1.778	23.50	0.049
1.905	23.55	0.042
2.032	23.61	0.037
2.159	23.58	0.043
2.286	23.61	0.033
2.413	23.62	0.036
2.540	23.65	0.026
3.175	23.62	0.033
3.810	23.67	0.021
5.080	23.64	0.021
6.350	23.66	0.020
7.620	23.64	0.021
8.890	23.59	0.021
10.160	23.62	0.022
11.430	23.67	0.020
12.700	23.62	0.023
13.970	23.62	0.021
15.240	23.64	0.022
16.510	23.63	0.022
17.780	23.62	0.021
19.050	23.64	0.022
20.320	23.62	0.022
21.590	23.62	0.022
22.860	23.63	0.022
24.130	23.65	0.022
25.400	23.67	0.022
26.670	23.63	0.022
27.940	23.60	0.023
29.210	23.63	0.024
30.480	23.62	0.024
31.750	23.58	0.024
33.020	23.65	0.025
34.290	23.63	0.024
35.560	23.64	0.024
36.830	23.62	0.024
38.100	23.65	0.024

Table 36. Reconstructed Boundary Layer at 46.5% Chord on the Pressure Surface

<i>Y (mm)</i>	<i>u (m/s)</i>	Turbulence Intensity
0.254	2.25	0.067
0.381	5.61	0.112
0.508	7.87	0.149
0.635	9.71	0.180
0.762	11.83	0.206
0.889	13.56	0.222
1.016	15.77	0.232
1.143	17.23	0.236
1.270	18.91	0.220
1.397	20.19	0.204
1.524	21.17	0.178
1.651	21.54	0.170
1.778	22.17	0.141
1.905	22.59	0.114
2.032	22.73	0.105
2.159	22.94	0.089
2.286	23.02	0.080
2.413	23.17	0.057
2.540	23.36	0.026
3.175	23.37	0.027
3.810	23.41	0.025
5.080	23.34	0.026
6.350	23.36	0.024
7.620	23.38	0.024
8.890	23.43	0.025
10.160	23.41	0.025
11.430	23.38	0.025
12.700	23.39	0.025
13.970	23.40	0.025
15.240	23.38	0.025
16.510	23.37	0.024
17.780	23.42	0.026
19.050	23.40	0.025
20.320	23.40	0.026
21.590	23.39	0.027
22.860	23.36	0.026
24.130	23.39	0.025
25.400	23.37	0.026
26.670	23.41	0.026
27.940	23.37	0.026
29.210	23.39	0.027
30.480	23.40	0.026
31.750	23.40	0.027
33.020	23.39	0.026
34.290	23.37	0.027
35.560	23.40	0.027
36.830	23.40	0.027
38.100	23.39	0.028

Table 37. Reconstructed Boundary Layer at 57.2% Chord on the Pressure Surface

<i>y</i> (mm)	<i>u</i> (m/s)	Turbulence Intensity
0.317	6.81	0.138
0.381	8.24	0.158
0.508	10.80	0.189
0.635	12.52	0.201
0.762	14.04	0.202
0.889	14.92	0.200
1.016	16.12	0.207
1.143	17.18	0.207
1.270	18.23	0.206
1.397	19.20	0.198
1.524	20.20	0.187
1.651	20.82	0.175
1.778	21.46	0.160
1.905	22.05	0.140
2.032	22.33	0.129
2.159	22.76	0.106
2.286	22.90	0.094
2.413	23.05	0.084
2.540	23.20	0.071
3.175	23.50	0.033
3.810	23.55	0.027
5.080	23.55	0.026
6.350	23.52	0.027
7.620	23.54	0.026
8.890	23.55	0.027
10.160	23.52	0.029
11.430	23.54	0.028
12.700	23.54	0.027
13.970	23.54	0.026
15.240	23.54	0.027
16.510	23.57	0.028
17.780	23.59	0.029
19.050	23.57	0.026
20.320	23.56	0.027
21.590	23.55	0.027
22.860	23.56	0.029
24.130	23.54	0.029
25.400	23.54	0.026
26.670	23.55	0.027
27.940	23.51	0.029
29.210	23.55	0.028
30.480	23.57	0.029
31.750	23.54	0.029
33.020	23.57	0.027
34.290	23.59	0.030
35.560	23.56	0.030
36.830	23.56	0.030
38.100	23.59	0.030

Table 38. Reconstructed Boundary Layer at 68.0% on the Pressure Surface

<i>y</i> (mm)	<i>u</i> (m/s)	Turbulence Intensity
0.317	11.68	0.179
0.381	13.05	0.183
0.508	15.29	0.181
0.635	16.67	0.165
0.762	17.38	0.159
0.889	18.23	0.150
1.016	18.68	0.153
1.143	19.23	0.147
1.270	19.51	0.148
1.397	20.11	0.145
1.524	20.69	0.138
1.651	21.31	0.125
1.778	21.64	0.119
1.905	22.16	0.107
2.032	22.49	0.097
2.159	22.67	0.094
2.286	22.96	0.080
2.413	23.14	0.075
2.540	23.32	0.067
3.175	23.69	0.046
3.810	23.86	0.031
4.445	23.91	0.027
5.080	23.91	0.023
6.350	23.95	0.024
7.620	23.99	0.024
8.890	23.99	0.024
10.160	24.03	0.024
11.430	24.02	0.024
12.700	24.03	0.024
13.970	24.04	0.024
15.240	24.07	0.025
16.510	24.08	0.024
17.780	24.06	0.025
19.050	24.08	0.025
20.320	24.10	0.026
21.590	24.10	0.026
22.860	24.10	0.025
24.130	24.06	0.026
25.400	24.06	0.026
26.670	24.04	0.025
27.940	24.10	0.026
29.210	24.09	0.027
30.480	24.11	0.027
31.750	24.08	0.026
33.020	24.07	0.026
34.290	24.11	0.027
35.560	24.06	0.028
36.830	24.05	0.027
38.100	24.08	0.027

Table 39. Reconstructed Boundary Layer at 78.6% Chord on the Pressure Surface

y (mm)	u (m/s)	Turbulence Intensity
0.254	12.51	0.161
0.317	14.55	0.166
0.381	16.06	0.162
0.508	17.95	0.144
0.635	19.26	0.132
0.762	20.14	0.121
0.889	20.81	0.113
1.016	21.30	0.104
1.143	21.79	0.097
1.270	22.08	0.095
1.397	22.37	0.091
1.524	22.53	0.091
1.651	22.90	0.084
1.778	23.16	0.079
1.905	23.45	0.078
2.032	23.61	0.074
2.159	23.81	0.071
2.286	24.00	0.067
2.413	24.18	0.063
2.540	24.34	0.058
3.175	24.86	0.043
3.810	25.15	0.031
4.445	25.20	0.026
5.080	25.29	0.025
6.350	25.29	0.024
7.620	25.38	0.025
8.890	25.44	0.025
10.160	25.42	0.025
11.430	25.47	0.024
12.700	25.52	0.023
13.970	25.52	0.024
15.240	25.55	0.025
16.510	25.53	0.024
17.780	25.53	0.025
19.050	25.54	0.026
20.320	25.50	0.026
21.590	25.50	0.026
22.860	25.47	0.026
24.130	25.53	0.026
25.400	25.52	0.026
26.670	25.53	0.026
27.940	25.53	0.026
29.210	25.54	0.027
30.480	25.52	0.026
31.750	25.49	0.026
33.020	25.57	0.027
34.290	25.53	0.028
35.560	25.54	0.029
36.830	25.49	0.029
38.100	25.50	0.027

Table 40. Reconstructed Boundary Layer at 89.3% Chord on the Pressure Surface

<i>y</i> (mm)	<i>u</i> (m/s)	Turbulence Intensity
0.063	17.76	0.148
0.127	19.57	0.140
0.254	21.75	0.120
0.317	22.38	0.112
0.381	22.73	0.107
0.508	23.47	0.099
0.635	23.96	0.092
0.762	24.42	0.089
0.889	24.90	0.083
1.016	25.22	0.078
1.143	25.45	0.076
1.270	25.56	0.078
1.397	26.04	0.071
1.524	26.30	0.067
1.651	26.44	0.068
1.778	26.69	0.064
1.905	26.79	0.064
2.032	26.96	0.061
2.159	27.15	0.057
2.286	27.29	0.053
2.413	27.46	0.053
2.540	27.57	0.049
3.175	27.99	0.038
3.810	28.24	0.027
5.080	28.27	0.024
6.350	28.23	0.024
7.620	28.18	0.023
8.890	28.17	0.024
10.160	28.14	0.024
11.430	28.13	0.023
12.700	28.14	0.024
13.970	28.14	0.023
15.240	28.11	0.023
16.510	28.06	0.023
17.780	28.07	0.023
19.050	28.08	0.024
20.320	28.05	0.024
21.590	28.05	0.023
22.860	28.00	0.024
24.130	28.04	0.024
25.400	28.02	0.024
26.670	28.01	0.025
27.940	28.03	0.024
29.210	28.03	0.026
30.480	28.01	0.025
31.750	28.11	0.024
33.020	28.11	0.025
34.290	28.10	0.026
35.560	28.13	0.024
36.830	28.18	0.026
38.100	28.16	0.027

Table 41. Reconstructed Boundary Layer at 97.9% on the Pressure Surface

% Chord	Spline Fit						Ludweig-Tillman Equation		
	δ^* (mm)	θ (mm)	δ_3 (mm)	H_{12}	H_{32}	Re_θ	u_τ (m/s)	τ_w (Pa)	C_f
2.7	0.076	0.006 (?)	-0.001 (?)	12.24 (?)	-0.20 (?)	9 (?)	---	---	---
5.9	0.187	0.027 (?)	0.027 (?)	6.79 (?)	0.97 (?)	4.3 (?)	---	---	---
14.4	0.248	0.036 (?)	0.031 (?)	6.86 (?)	0.86 (?)	59 (?)	---	---	---
25.1	0.448	0.145	0.232	3.09	1.60	235	---	---	---
35.8	0.619	0.160	0.238	3.88	1.49	254	---	---	---
46.5	0.708	0.207	0.317	3.43	1.54	326	---	---	---
57.2	0.830	0.290	0.457	2.87	1.58	451	---	---	---
68.0	0.801	0.356	0.583	2.25	1.64	559	---	---	---
78.6	0.708	0.397	0.693	1.78	1.75	637	---	---	---
89.3	0.640	0.393	0.705	1.63	1.79	669	---	---	---
97.9	0.284	0.207	0.377	1.37	1.82	388	1.521	2.786	0.00585

Table 42. Pressure Surface Boundary Layer Parameters Determined From a Parametric Cubic Spline Fit of the Data

Falkner-Skan Solution									
% Chord	ξ	β	δ^* (mm)	θ (mm)	H_{12}	$Re\theta$	u_T (m/s)	τ_w (Pa)	C_f
2.7	0.0102	0.1811	0.071	0.029	2.43	43	1.171	1.653	0.00569
5.9	0.0323	0.0267	0.140	0.055	2.56	84	0.852	0.874	0.00269
14.4	0.0921	-0.0775	0.278	0.101	2.74	156	0.547	0.361	0.00112
25.1	0.1654	-0.1487	0.459	0.152	3.01	227	0.346	0.144	0.00048
35.8	0.2365	-0.1506	0.568	0.188	3.03	272	0.296	0.106	0.00037
46.5	0.3060	-0.1042	0.580	0.206	2.82	293	0.323	0.126	0.00046
57.2	0.3744	-0.0588	0.592	0.219	2.70	310	0.337	0.136	0.00051
68.0	0.4433	0.1261	0.508	0.206	2.47	291	0.407	0.200	0.00074
78.6	0.5124	0.5917	0.389	0.170	2.29	246	0.523	0.329	0.00116
89.3	0.5844	1.4414	0.288	0.131	2.20	201	0.696	0.583	0.00181
97.9	0.6472	3.8382	0.179	0.083	2.17	143	1.079	1.403	0.00345

Table 43. Pressure Surface Boundary Layer Parameters Determined from a Falkner-Skan Solution

% Chord	Pressure Tap Measurements			LDV Measurements	
	C_p	U_e (m/s)	U_e (m/s)	U_e (m/s)	δ (mm)
2.6	-1.048	47.63	55.94 ± 0.85	2.28 ± 0.14	
7.6	-0.424	39.42	45.89 ± 0.04	3.25 ± 0.03	
12.7	-0.342	38.34	44.73 ± 0.08	4.02 ± 0.08	
23.0	-0.196	36.22	41.75 ± 0.10	5.24 ± 0.11	
33.2	-0.021	33.41	37.78 ± 0.08	8.26 ± 0.08	
43.3	0.108	31.32	35.31 ± 0.12	9.26 ± 0.11	
53.6	0.185	29.90	33.78 ± 0.13	11.48 ± 0.16	
63.2	0.245	28.74	31.77 ± 0.06	14.44 ± 0.14	
74.0	0.292	27.87	31.26 ± 0.05	20.06 ± 0.09	
84.2	0.301	27.67	30.48 ± 0.12	27.50 ± 0.23	
94.9	0.305	27.61	29.72	36.56	

Table 44. Boundary Layer Edge Velocities and Boundary Layer Thicknesses on the Suction Surface

<i>Y (mm)</i>	<i>u (m/s)</i>	Turbulence Intensity
0.254	20.02	0.088
0.381	21.41	0.100
0.508	23.59	0.116
0.635	26.35	0.129
0.762	28.50	0.135
0.889	31.13	0.146
1.016	34.89	0.150
1.143	37.87	0.157
1.270	40.68	0.156
1.397	43.30	0.150
1.524	46.59	0.138
1.651	49.06	0.118
1.778	51.10	0.099
2.032	53.57	0.072
2.286	54.99	0.055
2.540	55.53	0.049
3.175	55.79	0.042
3.810	55.94	0.031
4.445	55.84	0.028
5.080	55.72	0.028
5.715	55.90	0.026
6.350	55.96	0.023
7.620	55.89	0.022
8.890	55.99	0.021
10.160	55.95	0.020
11.430	55.93	0.020
12.700	55.93	0.019
13.970	55.94	0.018
15.240	55.94	0.017

Table 45. Reconstructed Boundary Layer at 2.6% Chord on the Suction Surface

<i>y</i> (mm)	<i>u</i> (m/s)	Turbulence Intensity
0.127	24.49	0.127
0.190	25.69	0.129
0.254	26.37	0.131
0.381	27.49	0.134
0.508	28.27	0.138
0.635	29.63	0.142
0.762	30.72	0.143
0.889	31.96	0.147
1.016	33.05	0.149
1.143	34.45	0.150
1.270	35.49	0.152
1.397	36.86	0.148
1.524	38.08	0.142
1.651	39.10	0.136
1.778	40.41	0.125
1.905	41.21	0.120
2.032	41.90	0.113
2.159	42.84	0.098
2.286	43.36	0.087
2.413	43.91	0.078
2.540	44.33	0.072
3.175	45.40	0.045
3.810	45.73	0.032
4.445	45.74	0.030
5.080	45.80	0.029
5.715	45.82	0.030
6.350	45.89	0.025
7.620	45.87	0.024
8.890	45.93	0.024
10.160	45.90	0.023
11.430	45.93	0.022
12.700	45.94	0.022
13.970	45.85	0.022
15.240	45.84	0.022
16.510	45.85	0.021
17.780	45.88	0.021
19.050	45.86	0.021
20.320	45.91	0.022
21.590	45.89	0.022
22.860	45.94	0.022

Table 46. Reconstructed Boundary Layer at 7.6% Chord on the Suction Surface

<i>y</i> (mm)	<i>u</i> (m/s)	Turbulence Intensity
0.102	21.72	0.126
0.152	24.49	0.123
0.203	25.85	0.120
0.254	27.10	0.116
0.317	27.96	0.114
0.381	28.74	0.112
0.508	29.92	0.114
0.635	30.83	0.115
0.762	31.53	0.116
0.889	32.21	0.118
1.016	32.80	0.117
1.143	33.69	0.119
1.270	34.36	0.119
1.397	34.94	0.121
1.524	35.49	0.122
1.651	36.20	0.120
1.778	36.70	0.122
1.905	37.68	0.118
2.032	38.15	0.117
2.286	39.56	0.109
2.540	40.65	0.101
2.794	41.89	0.085
3.048	42.52	0.081
3.302	43.40	0.061
3.556	43.77	0.051
3.810	44.06	0.043
4.445	44.55	0.029
5.080	44.60	0.024
5.715	44.70	0.021
6.350	44.69	0.020
7.620	44.67	0.019
8.890	44.72	0.019
10.160	44.69	0.018
11.430	44.72	0.018
12.700	44.77	0.018
13.970	44.74	0.018
15.240	44.71	0.020
16.510	44.72	0.018
17.780	44.79	0.019
19.050	44.72	0.018
20.320	44.71	0.018
21.590	44.71	0.018
22.860	44.74	0.017
24.130	44.75	0.017
25.400	44.75	0.018
26.670	44.70	0.017
27.940	44.72	0.017
29.210	44.73	0.017
30.480	44.73	0.017
31.750	44.74	0.017
33.020	44.74	0.017
34.290	44.72	0.017

Table 47. Reconstructed Boundary Layer at 12.7% Chord on the Suction Surface

<i>y</i> (mm)	<i>u</i> (m/s)	Turbulence Intensity
0.127	20.04	0.130
0.190	21.81	0.125
0.254	23.65	0.110
0.317	24.54	0.105
0.381	25.50	0.103
0.508	26.58	0.098
0.635	27.39	0.098
0.762	28.08	0.097
0.889	28.80	0.098
1.016	29.45	0.097
1.143	29.91	0.099
1.270	30.55	0.097
1.524	31.58	0.098
1.778	32.63	0.099
2.032	33.40	0.098
2.286	34.36	0.098
2.540	35.46	0.095
2.794	36.29	0.094
3.048	36.99	0.091
3.302	37.84	0.087
3.556	38.59	0.082
3.810	39.31	0.074
4.445	40.67	0.051
5.080	41.20	0.041
5.715	41.59	0.030
6.350	41.73	0.025
7.620	41.80	0.022
8.890	41.77	0.021
10.160	41.82	0.021
11.430	41.87	0.022
12.700	41.79	0.021
13.970	41.70	0.019
15.240	41.72	0.020
16.510	41.76	0.020
17.780	41.76	0.020
19.050	41.73	0.019
20.320	41.73	0.018
21.590	41.77	0.019
22.860	41.76	0.019
24.130	41.73	0.018
25.400	41.75	0.018
26.670	41.78	0.019
27.940	41.73	0.018
29.210	41.77	0.018
30.480	41.73	0.017
31.750	41.75	0.018
33.020	41.76	0.017
34.290	41.73	0.017
35.560	41.73	0.017
36.830	41.75	0.017
38.100	41.77	0.016

Table 48. Reconstructed Boundary Layer at 23.0% Chord on the Suction Surface

<i>y</i> (mm)	<i>u</i> (m/s)	Turbulence Intensity
0.127	14.59	0.108
0.254	17.09	0.105
0.381	18.52	0.103
0.508	19.54	0.102
0.635	20.36	0.100
0.762	21.16	0.102
1.016	22.37	0.104
1.270	23.49	0.105
1.524	24.57	0.102
1.778	25.59	0.102
2.032	26.54	0.100
2.286	27.34	0.097
2.540	28.11	0.094
2.794	28.87	0.093
3.048	29.38	0.089
3.302	30.04	0.085
3.556	30.68	0.082
3.810	31.00	0.082
4.064	31.59	0.080
4.318	32.02	0.079
4.572	32.43	0.079
4.826	32.91	0.080
5.080	33.29	0.079
5.334	33.62	0.078
5.842	34.59	0.077
6.350	35.53	0.071
7.620	37.12	0.045
8.890	37.71	0.023
10.160	37.82	0.019
11.430	37.82	0.018
12.700	37.80	0.018
13.970	37.78	0.016
15.240	37.77	0.016
16.510	37.75	0.016
17.780	37.77	0.016
19.050	37.79	0.015
20.320	37.78	0.015
21.590	37.76	0.016
22.860	37.81	0.015
24.130	37.78	0.016
25.400	37.78	0.015
26.670	37.75	0.015
27.940	37.78	0.016
29.210	37.79	0.015
30.480	37.77	0.015
31.750	37.79	0.015
33.020	37.79	0.015
34.290	37.78	0.015
35.560	37.78	0.014
36.830	37.79	0.015
38.100	37.77	0.015

Table 49. Reconstructed Boundary Layer at 33.2% Chord on the Suction Surface

<i>Y</i> (mm)	<i>u</i> (m/s)	Turbulence Intensity
0.127	10.77	0.104
0.254	13.03	0.101
0.381	14.40	0.097
0.508	15.13	0.095
0.635	15.79	0.094
0.762	16.36	0.093
1.016	17.35	0.094
1.270	18.34	0.098
1.524	19.09	0.099
1.778	19.97	0.100
2.032	20.74	0.100
2.286	21.67	0.103
2.540	22.45	0.104
2.794	23.29	0.102
3.048	24.06	0.106
3.302	24.99	0.103
3.556	25.75	0.101
3.810	26.60	0.100
4.064	27.32	0.098
4.318	27.95	0.097
4.572	28.65	0.094
4.826	29.23	0.093
5.080	29.85	0.089
5.334	30.36	0.085
5.842	31.23	0.080
6.350	32.08	0.074
6.985	32.95	0.068
7.620	33.67	0.060
8.255	34.31	0.049
8.890	34.88	0.038
9.525	35.16	0.030
10.160	35.30	0.023
11.430	35.42	0.019
12.700	35.41	0.019
13.970	35.38	0.018
15.240	35.36	0.018
16.510	35.35	0.018
17.780	35.39	0.017
19.050	35.34	0.017
20.320	35.30	0.017
21.590	35.32	0.017
22.860	35.33	0.018
24.130	35.31	0.017
25.400	35.28	0.017
26.670	35.35	0.018
27.940	35.31	0.017
29.210	35.28	0.016
30.480	35.31	0.017
31.750	35.31	0.017
33.020	35.31	0.017
34.290	35.31	0.016
35.560	35.32	0.017
36.830	35.32	0.017
38.100	35.30	0.017

Table 50. Reconstructed Boundary Layer at 43.3% Chord on the Suction Surface

<i>y</i> (mm)	<i>u</i> (m/s)	Turbulence Intensity
0.381	9.67	0.088
0.508	10.24	0.089
0.635	10.77	0.089
0.762	11.20	0.092
1.016	12.12	0.091
1.270	12.84	0.094
1.524	13.50	0.096
1.778	14.06	0.096
2.032	14.89	0.098
2.286	15.46	0.096
2.540	16.17	0.098
2.794	16.83	0.101
3.048	17.61	0.101
3.302	18.20	0.100
3.556	18.99	0.104
3.810	19.60	0.104
4.064	20.37	0.107
4.318	21.13	0.103
4.572	21.82	0.105
4.826	22.53	0.107
5.080	23.17	0.107
5.334	23.77	0.107
5.842	25.10	0.105
6.350	26.49	0.102
6.985	27.91	0.098
7.620	29.24	0.090
8.255	30.39	0.082
8.890	31.39	0.072
10.160	32.86	0.045
11.430	33.41	0.031
12.700	33.66	0.025
13.970	33.73	0.021
15.240	33.74	0.018
16.510	33.75	0.017
17.780	33.73	0.017
19.050	33.76	0.017
20.320	33.76	0.017
21.590	33.81	0.017
22.860	33.79	0.017
24.130	33.78	0.016
25.400	33.77	0.016
26.670	33.76	0.016
27.940	33.80	0.016
29.210	33.80	0.016
30.480	33.77	0.016
31.750	33.77	0.015
33.020	33.80	0.016
34.290	33.77	0.016
35.560	33.77	0.015
36.830	33.80	0.015
38.100	33.77	0.015

Table 51. Reconstructed Boundary Layer at 53.6% Chord on the Suction Surface

<i>Y (mm)</i>	<i>u (m/s)</i>	Turbulence Intensity
0.254	3.43	0.075
0.508	4.61	0.083
0.762	5.23	0.088
1.016	5.88	0.090
1.270	6.45	0.092
1.524	6.89	0.096
1.778	7.49	0.096
2.032	7.93	0.098
2.286	8.61	0.104
2.540	9.19	0.106
2.794	9.52	0.109
3.048	10.22	0.110
3.302	10.86	0.114
3.556	11.31	0.115
3.810	11.96	0.117
4.064	12.56	0.119
4.318	13.24	0.120
4.572	13.59	0.123
4.826	14.40	0.125
5.080	14.95	0.126
5.334	15.51	0.129
5.842	16.82	0.130
6.350	17.96	0.135
6.985	19.88	0.132
7.620	21.68	0.126
8.255	23.19	0.125
8.890	24.61	0.116
9.525	25.92	0.114
10.160	27.29	0.100
10.795	28.22	0.100
11.430	29.22	0.089
12.065	30.01	0.077
12.700	30.60	0.065
13.335	31.03	0.053
13.970	31.29	0.043
15.240	31.60	0.028
16.510	31.74	0.022
17.780	31.71	0.017
19.050	31.75	0.017
20.320	31.79	0.017
21.590	31.76	0.017
22.860	31.74	0.017
24.130	31.76	0.016
25.400	31.73	0.017
26.670	31.76	0.016
27.940	31.80	0.015
29.210	31.77	0.015
30.480	31.79	0.015
31.750	31.78	0.015
33.020	31.77	0.015
34.290	31.79	0.016
35.560	31.78	0.015
36.830	31.77	0.016
38.100	31.73	0.016

Table 52. Reconstructed Boundary Layer at 63.2% Chord on the Suction Surface

<i>y</i> (mm)	<i>u</i> (m/s)	Turbulence Intensity
0.254	0.90	0.056
0.508	1.58	0.073
0.762	1.93	0.078
1.016	2.03	0.080
1.270	2.39	0.087
1.524	2.76	0.091
1.778	3.02	0.087
2.032	3.28	0.092
2.286	3.56	0.092
2.540	3.80	0.094
2.794	4.28	0.095
3.048	4.65	0.093
3.302	4.84	0.097
3.556	5.18	0.100
3.810	5.59	0.099
4.064	5.73	0.101
4.318	6.26	0.103
4.572	6.45	0.107
4.826	6.89	0.105
5.080	7.17	0.110
5.334	7.56	0.109
5.842	8.57	0.110
6.350	9.13	0.111
6.985	10.40	0.116
7.620	11.45	0.123
8.255	12.88	0.126
8.890	13.78	0.128
9.525	15.10	0.135
10.160	16.82	0.130
10.795	18.13	0.132
11.430	19.42	0.131
12.065	20.63	0.132
12.700	21.97	0.132
13.335	23.28	0.126
13.970	24.56	0.126
14.605	25.81	0.114
15.240	26.70	0.110
15.875	27.74	0.102
16.510	28.42	0.097
17.145	29.29	0.078
17.780	29.91	0.063
19.050	30.80	0.041
20.320	31.06	0.029
21.590	31.11	0.024
22.860	31.16	0.019
24.130	31.19	0.019
25.400	31.24	0.017
26.670	31.27	0.016
27.940	31.27	0.016
29.210	31.30	0.016
30.480	31.30	0.016
31.750	31.26	0.015
33.020	31.26	0.016
34.290	31.26	0.016
35.560	31.24	0.015
36.830	31.28	0.016
38.100	31.25	0.016

Table 53. Reconstructed Boundary Layer at 74.0% Chord on the Suction Surface

C-2

y (mm)	u (m/s)	Turbulence Intensity
0.254	-0.05	0.006
0.508	0.00	-0.043
0.762	-0.02	0.101
1.016	0.00	0.103
1.270	0.02	0.108
1.524	0.21	-0.067
1.778	0.31	-0.088
2.032	0.25	0.045
2.286	0.41	0.136
2.540	0.54	0.104
2.794	0.86	0.094
3.048	1.05	0.106
3.302	1.39	0.103
3.556	1.44	0.101
3.810	1.51	0.104
4.064	1.76	0.098
4.318	1.95	0.100
4.572	2.07	0.104
4.826	2.37	0.103
5.080	2.55	0.106
5.715	3.12	0.108
6.350	3.95	0.109
6.985	4.50	0.108
7.620	5.05	0.110
8.255	5.77	0.112
8.890	6.49	0.117
9.525	7.20	0.118
10.160	7.97	0.118
10.795	8.88	0.124
11.430	9.27	0.126
12.065	10.24	0.130
12.700	11.07	0.134
13.335	12.16	0.135
13.970	13.04	0.140
14.605	13.86	0.142
15.240	15.04	0.141
15.875	16.27	0.144
16.510	17.23	0.146
17.145	18.33	0.147
17.780	19.33	0.146
18.415	20.57	0.143
19.050	21.62	0.140
19.685	22.58	0.140
20.320	23.52	0.141
20.955	24.48	0.131
21.590	25.51	0.130
22.225	26.69	0.109
22.860	27.52	0.100
24.130	28.56	0.082
25.400	29.46	0.062
26.670	29.92	0.045
27.940	30.21	0.033
29.210	30.32	0.028
30.480	30.40	0.021
31.750	30.40	0.020
33.020	30.46	0.020
34.290	30.44	0.018
35.560	30.44	0.020
36.830	30.47	0.022
38.100	30.48	0.016

Table 54. Reconstructed Boundary Layer at 84.2% Chord on the Suction Surface



39.370	30.49	0.016
40.640	30.48	0.017
41.910	30.47	0.022

Table 54. (Continued)

<i>y</i> (mm)	<i>u</i> (m/s)	Turbulence Intensity
0.254	-0.18	0.040
0.508	-0.32	0.066
0.762	-0.74	0.106
1.016	-0.90	0.127
1.270	-0.82	0.125
1.524	-0.75	0.848
1.778	-0.76	0.265
2.032	-0.36	-0.075
2.286	-0.46	0.020
2.540	-0.45	0.118
2.794	-0.51	0.009
3.048	-0.30	0.054
3.302	-0.36	0.033
3.556	-0.15	-0.094
3.810	-0.10	0.057
4.064	0.06	-0.019
4.318	0.20	-0.044
4.572	0.17	-0.004
4.826	0.17	-0.002
5.080	0.39	-0.278
5.715	0.57	0.170
6.350	0.91	0.070
6.985	1.26	-0.138
7.620	1.51	0.179
8.255	1.85	0.173
8.890	2.06	0.138
9.525	2.38	0.125
10.160	2.71	0.118
10.795	2.96	0.128
11.430	3.45	0.125
12.065	3.71	0.123
12.700	4.18	0.119
13.335	4.96	0.122
13.970	5.24	0.122
14.605	5.98	0.125
15.240	6.30	0.124
15.875	6.73	0.125
16.510	7.11	0.130
17.145	7.77	0.128
17.780	8.21	0.130
18.415	8.79	0.135
19.050	9.31	0.139
19.685	9.99	0.141
20.320	10.53	0.142
20.955	11.58	0.142
21.590	12.41	0.147
22.225	13.10	0.151
22.860	14.05	0.147
23.495	14.73	0.152
24.130	15.77	0.152
24.765	16.63	0.152
25.400	17.50	0.156
26.035	18.33	0.155
26.670	19.33	0.153
27.305	20.36	0.152
27.940	21.24	0.153
28.575	22.29	0.148
29.210	23.50	0.141
29.845	24.48	0.136
30.480	25.14	0.127

Table 55. Reconstructed Boundary Layer at 94.9% Chord on the Suction Surface

31.115	26.07	0.125
31.750	27.04	0.105
32.385	27.55	0.100
33.020	27.96	0.090
34.290	28.68	0.071
35.560	29.24	0.049
36.830	29.51	0.038
38.100	29.56	0.030
39.370	29.70	0.023
40.640	29.71	0.022
41.910	29.76	0.020
43.180	29.71	0.019

Table 55. (Continued)

% Chord	Spline Fit						Ludweig-Tillman Equation		
	δ^* (mm)	θ (mm)	δ_3 (mm)	H_{12}	H_{32}	$Re \theta$	u_T (m/s)	τ_w (Pa)	c_f
2.6	0.820	0.371	0.590	2.21	1.59	1384	1.328	2.124	0.00113
7.6	0.653	0.415	0.713	1.57	1.72	1270	1.807	3.935	0.00310
12.7	0.725	0.497	0.872	1.46	1.75	1482	1.888	4.294	0.00356
23.0	0.937	0.636	1.110	1.47	1.75	1769	1.702	3.491	0.00332
33.2	1.660	1.096	1.884	1.51	1.72	2760	1.405	2.378	0.00277
43.3	2.189	1.310	2.177	1.67	1.66	3083	1.145	1.579	0.00210
53.6	3.500	1.795	2.882	1.95	1.61	4041	0.850	0.870	0.00127
63.2	5.557	2.262	3.471	2.46	1.53	4790	0.526	0.333	0.00055
74.0	9.438	2.973	4.431	3.17	1.49	6195	0.285	0.098	0.00017
84.2	14.844	3.703	5.481	4.01	1.48	7525	0.141	0.024	0.00004
94.9	22.434	4.406	6.467	5.09	1.45	8731	0.058	0.004	0.0001

Table 56. Suction Surface Boundary Layer Parameters Determined from a Parametric Cubic Spline Fit of the data

Fit of Wall-Wake Equation

Ludweig-Tillman Equation

% Chord	δ^* (mm)	θ (mm)	δ_3 (mm)	H ₁₂	H ₃₂	Reθ	u_τ (m/s)	τ_w (Pa)	C _f
2.6	0.802	0.388	0.616	2.07	1.59	1448	1.475	2.621	0.00139
7.6	0.645	0.420	0.721	1.54	1.72	1285	1.860	4.170	0.00329
12.7	0.717	0.499	0.875	1.44	1.75	1489	1.922	4.450	0.00369
23.0	0.923	0.640	1.118	1.44	1.75	1782	1.743	3.662	0.00349
33.2	1.652	1.108	1.905	1.49	1.72	2791	1.429	2.462	0.00286
43.3	2.178	1.312	2.179	1.66	1.66	3089	1.155	1.607	0.00214
53.6	3.461	1.819	2.912	1.90	1.60	4097	0.880	0.933	0.00136
63.2	5.551	2.279	3.484	2.44	1.53	4827	0.534	0.344	0.00057
74.0	9.422	2.979	4.448	3.16	1.49	6208	0.288	0.100	0.00017
84.2	---	---	---	---	---	---	---	---	---
94.0	---	---	---	---	---	---	---	---	---

Table 57. Suction Surface Boundary Layer Parameters Determined from a Least-Squares Fit of the Data to the Wall-Wake Equation

% Chord	Fit of Wall-Wake Equation						Viscous Sublayer	
	β_c	Δ (mm)	G	H	τ_w (Pa)	c_f	c_f	
2.6	19.675	31.878	20.50	4.284	1.408	2.388	0.00127	---
7.6	0.796	15.846	8.57	1.147	1.868	4.203	0.00331	---
12.7	0.572	16.570	7.01	0.486	1.935	4.514	0.00374	---
23.0	1.130	22.057	7.32	0.617	1.747	3.676	0.00350	---
33.2	3.003	44.431	8.86	1.186	1.405	2.377	0.00276	---
43.3	3.652	68.904	12.57	2.558	1.116	1.502	0.00200	0.00204
53.6	7.362	142.073	19.47	4.496	0.823	0.816	0.00119	---
63.2	32.765	375.548	39.87	10.215	0.470	0.266	0.00044	0.00040
74.0	120.629	1426.218	103.51	25.986	0.207	0.051	0.00009	0.00010
84.2	---	---	---	---	---	---	---	---
94.9	---	---	---	---	---	---	---	---

Table 57. (Continued)

% Chord	Perry-Schofield Similarity	
	B (mm)	U _s (m/s)
2.6	2.665	49.23
7.6	3.458	24.78
12.7	4.713	19.68
23.0	6.091	18.37
33.2	7.783	23.04
43.3	8.944	24.72
53.6	11.917	28.38
63.2	14.993	33.68
74.0	21.768	38.76
84.2	30.988	41.76
94.9	46.494	41.01

Table 58. Perry-Schofield Similarity Variables for the Suction Surface Boundary Layers

<i>y</i> (mm)	<i>u</i> (m/s)	Turbulence Intensity
-63.500	28.98	0.019
-62.230	29.00	0.019
-60.960	29.02	0.021
-59.690	29.11	0.020
-58.420	29.07	0.021
-57.150	29.01	0.020
-55.880	29.08	0.020
-54.610	29.11	0.021
-53.340	29.13	0.020
-52.070	29.16	0.022
-50.800	29.13	0.022
-49.530	29.27	0.023
-48.260	29.19	0.027
-46.990	29.26	0.027
-45.720	29.22	0.033
-44.450	29.28	0.036
-43.180	29.21	0.038
-41.910	29.05	0.051
-40.640	28.66	0.068
-39.370	28.05	0.082
-38.100	26.84	0.105
-37.465	26.16	0.117
-36.830	25.24	0.131
-36.195	24.32	0.140
-35.560	23.29	0.147
-34.925	22.06	0.151
-34.290	21.09	0.162
-33.655	20.05	0.167
-33.020	18.87	0.173
-32.385	17.84	0.169
-31.750	17.15	0.164
-31.115	16.07	0.168
-30.480	15.07	0.170
-29.845	13.97	0.167
-29.210	13.30	0.165
-28.575	12.37	0.163
-27.940	11.51	0.166
-27.305	10.56	0.166
-26.670	9.53	0.168
-26.035	8.92	0.166
-25.400	8.32	0.165
-24.765	7.57	0.165
-24.130	6.87	0.167
-23.495	6.35	0.164
-22.860	5.54	0.165
-22.225	4.99	0.168
-21.590	4.33	0.167
-20.955	3.96	0.167
-20.320	3.37	0.168
-19.685	2.83	0.165
-19.050	2.22	0.161
-18.415	1.90	0.162
-17.780	1.51	0.159
-17.145	1.08	0.165
-16.510	0.65	0.177
-15.875	0.40	-0.217
-15.240	0.11	-0.072
-14.605	-0.14	0.248
-13.970	-0.37	0.164
-13.335	-0.63	0.187

Table 59. Wake at 105.4% Chord

-12.700	-0.94	0.134
-12.065	-1.29	0.148
-11.430	-1.26	0.123
-10.795	-1.45	0.119
-10.160	-1.71	0.110
-9.525	-1.93	0.108
-8.890	-2.02	0.104
-8.255	-2.08	0.101
-7.620	-2.21	0.094
-6.985	-2.19	0.093
-6.350	-2.24	0.089
-5.715	-1.88	0.088
-5.080	-0.98	0.102
-4.445	1.17	0.146
-3.810	4.50	0.136
-3.175	8.65	0.159
-2.540	14.29	0.183
-1.905	20.46	0.166
-1.270	25.01	0.118
-0.635	27.55	0.078
0.000	28.63	0.062
1.270	29.53	0.039
2.540	29.62	0.031
3.810	29.48	0.030
5.080	29.44	0.025
6.350	29.25	0.021
7.620	29.19	0.020
8.890	29.11	0.021
10.160	29.05	0.021
11.430	28.93	0.022
12.700	28.93	0.022
13.970	28.80	0.021
15.240	28.75	0.021
16.510	28.64	0.022
17.780	28.56	0.021
19.050	28.53	0.021
20.320	28.54	0.021
21.590	28.46	0.021
22.860	28.49	0.020
24.130	28.43	0.021
25.400	28.37	0.020
26.670	28.33	0.021
27.940	28.28	0.021
29.210	28.36	0.022
30.480	28.22	0.021
31.750	28.26	0.023
33.020	28.25	0.022
34.290	28.24	0.022

Table 59. (Continued)

y (mm)	u (m/s)	Turbulence Intensity
-66.040	28.78	0.023
-64.770	28.82	0.023
-63.500	28.90	0.023
-62.230	28.88	0.024
-60.960	28.90	0.024
-59.690	28.90	0.023
-58.420	28.87	0.025
-57.150	28.91	0.026
-55.880	28.98	0.026
-54.610	29.01	0.026
-53.340	29.08	0.028
-52.070	28.95	0.027
-50.800	28.95	0.039
-49.530	28.94	0.042
-48.260	28.91	0.044
-46.990	28.79	0.053
-45.720	28.30	0.071
-44.450	27.43	0.098
-43.815	27.39	0.098
-43.180	26.65	0.110
-42.545	25.87	0.127
-41.910	25.42	0.129
-41.275	24.41	0.143
-40.640	23.87	0.152
-40.005	22.62	0.159
-39.370	21.47	0.169
-38.735	20.80	0.175
-38.100	19.53	0.176
-37.465	18.90	0.175
-36.830	17.85	0.183
-36.195	16.84	0.183
-35.560	16.11	0.187
-34.925	14.90	0.191
-34.290	13.85	0.195
-33.655	13.39	0.186
-33.020	12.33	0.195
-32.385	11.51	0.190
-31.750	10.57	0.197
-31.115	9.94	0.188
-30.480	8.91	0.191
-29.845	7.98	0.187
-29.210	7.52	0.187
-28.575	6.65	0.191
-27.940	6.34	0.190
-27.305	5.46	0.189
-26.670	5.26	0.186
-26.035	4.24	0.190
-25.400	3.86	0.193
-24.765	3.05	0.185
-24.130	2.81	0.185
-23.495	2.15	0.188
-22.860	1.57	0.179
-22.225	1.25	0.187
-21.590	0.81	0.207
-20.955	0.54	0.266
-20.320	-0.20	0.174
-19.685	-0.52	-0.359
-19.050	-0.59	0.241
-18.415	-0.79	0.173
-17.780	-1.28	0.145

Table 60. Wake at 109.6% Chord

-17.145	-1.52	0.140
-16.510	-1.86	0.137
-15.875	-1.86	0.134
-15.240	-2.10	0.126
-14.605	-2.36	0.121
-13.970	-2.44	0.111
-13.335	-2.36	0.110
-12.700	-2.46	0.109
-12.065	-2.41	0.107
-11.430	-2.31	0.102
-10.795	-2.03	0.103
-10.160	-1.39	0.105
-9.525	-0.62	0.123
-8.890	0.56	0.442
-8.255	2.14	0.137
-7.620	4.23	0.141
-6.985	6.61	0.150
-6.350	9.14	0.162
-5.715	12.56	0.174
-5.080	16.37	0.178
-4.445	20.54	0.169
-3.810	23.97	0.142
-3.175	26.46	0.108
-2.540	27.91	0.081
-1.270	29.24	0.048
0.000	29.41	0.043
1.270	29.45	0.031
2.540	29.44	0.024
3.810	29.31	0.024
5.080	29.22	0.022
6.350	29.20	0.024
7.620	29.17	0.024
8.890	29.11	0.023
10.160	29.04	0.023
11.430	28.93	0.023
12.700	28.93	0.022
13.970	28.90	0.023
15.240	28.75	0.023
16.510	28.79	0.024
17.780	28.73	0.023
19.050	28.71	0.023
20.320	28.71	0.024
21.590	28.61	0.024
22.860	28.65	0.023
24.130	28.59	0.023

Table 60. (Continued)

<i>y</i> (mm)	<i>u</i> (m/s)	Turbulence Intensity
-134.137	26.26	-----
-130.962	26.25	-----
-127.787	26.15	-----
-124.612	26.04	-----
-121.437	25.79	-----
-118.262	25.38	-----
-115.087	25.02	-----
-111.912	24.60	-----
-108.737	23.77	-----
-105.562	22.64	-----
-102.387	22.12	-----
-99.212	20.81	-----
-96.037	19.32	-----
-92.862	18.04	-----
-89.687	16.33	-----
-86.512	14.69	-----
-83.337	13.17	-----
-80.162	11.84	-----
-76.987	10.74	-----
-73.812	9.69	-----
-70.637	9.32	-----
-67.462	9.16	-----
-64.287	9.58	-----
-61.112	10.60	-----
-57.937	12.26	-----
-54.762	14.20	-----
-51.587	16.11	-----
-48.412	18.33	-----
-45.237	20.22	-----
-42.062	22.08	-----
-38.887	23.55	-----
-35.712	24.78	-----
-32.537	25.43	-----
-29.362	25.90	-----
-26.187	26.05	-----
-23.012	26.16	-----
-19.837	26.15	-----
-16.662	26.17	-----
-13.487	26.14	-----

Table 61. Wake at 152.6% Chord

		Pressure Side of Wake Centerline						
% Chord	U_e (m/s)	L_p (mm)	δ^* (mm)	θ (mm)	δ_3 (mm)	H_{12}	H_{32}	Re_θ
105.4	29.09	3.7	3.917	0.578	0.922	6.78	1.60	1120
109.6	29.15	7.1	7.420	0.769	1.268	9.65	1.65	1494
152.6	26.18	18.1	12.092	6.420	10.182	1.88	1.59	11204

Table 62. Wake Parameters on the Pressure Side of the Wake Centerline Determined from a Parametric Cubic Spline Fit of the Data

Suction Side of Wake Centerline								
% Chord	U_e (m/s)	L_S (mm)	δ^* (mm)	θ (mm)	δ_3 (mm)	H_{12}	H_{32}	Re_θ
105.4	29.09	22.8	23.321	3.307	5.058	7.05	1.53	6414
109.6	29.15	20.9	21.886	3.576	5.597	6.12	1.57	6950
152.6	26.18	24.7	16.958	9.030	14.367	1.88	1.59	15759

Table 63. Wake Parameters on the Suction Side of the Wake Centerline Determined from a Parametric Cubic Spline Fit of the Data

1. Report No. NASA CR-179492	2. Government Accession No.	3. Recipient's Catalog No.	
4. Title and Subtitle The Measurement of Boundary Layers on a Compressor Blade in Cascade at High Positive Incidence Angle II - Data Report		5. Report Date August 1986	
7. Author(s) Steve Deutsch and William C. Zierke		6. Performing Organization Code	
9. Performing Organization Name and Address Pennsylvania State University P.O. Box 30 State College, Pennsylvania 16801		8. Performing Organization Report No. None	
12. Sponsoring Agency Name and Address National Aeronautics and Space Administration Washington, D.C. 20546		10. Work Unit No.	
		11. Contract or Grant No. NSG-3264	
		13. Type of Report and Period Covered Contractor Report	
		14. Sponsoring Agency Code 505-62-21	
15. Supplementary Notes Interim report. Project Manager, Nelson L. Sanger, Internal Fluid Mechanics Division, NASA Lewis Research Center, Cleveland, Ohio 44135.			
16. Abstract Detailed boundary layer and near-wake velocity measurements have been made in the well documented flow field about a double circular arc compressor blade in cascade, at an incidence angle of 5° and a chord Reynolds number of 500,000. In Part I of this report these measurements were analyzed and presented in standard graphical format. The flow geometry, measurement techniques, and physics of the flow field were also discussed. In this, part II of the report, we present raw and analyzed data in tabulated form in an attempt to make this data more accessible to computational comparison. The potential usefulness of this data for computational comparison was the prime motivation for the research. Also included in part II is a description of the data analysis we employed. A computer tape containing the data is available.			
17. Key Words (Suggested by Author(s)) Boundary layer; Cascade; Compressor blades; Laser velocimetry		18. Distribution Statement Unclassified - unlimited STAR Category 07	
19. Security Classif. (of this report) Unclassified	20. Security Classif. (of this page) Unclassified	21. No. of pages 113	22. Price* A06